

THE UNIVERSITY OF MANCHESTER

FACULTY OF TECHNOLOGY

**"THE FATIGUE BEHAVIOUR
OF FILLET WELDED JOINTS
OF PLATES AND SQUARE HOLLOW SECTIONS"**

A Thesis Submitted for
The Degree of
Doctor of Philosophy

by

HASSAN KHALIL SAKET, B.Sc., M.Sc.

Department of Civil and Structural
Engineering, University of Manchester
Institute of Science and Technology

October 1988

TO MY PARENTS AND FAMILY

SUMMARY

The research described in this thesis is generally concerned with the fatigue behaviour of fillet welded joints of plates and square hollow section members.

Finite element of stress analysis was employed in the theoretical study to calculate the stress intensity factors at the fillet weld root position. Emphasis in this thesis has been placed on two major aspects. The influence of various geometrical parameters of the joints studied on the stress intensity factors at the fillet weld root position, and the confirmation that a geometric thickness/size effect existed for fatigue failure in fillet welds just as it does for fatigue cracks growing in plate from the toe of fillet welds.

The stress intensity factors and the fatigue strengths of the joints analysed theoretically were presented by parametric formulae.

Experimental programme was conducted on fillet welded plate and SHS members to investigate their fatigue behaviour.

DECLARATION

No portion of the work referred to in the thesis has been submitted in support of an application for another degree or qualification of this or any other University or other institution of learning.

H. K. Saket

ACKNOWLEDGEMENTS

The author wishes to express his sincere gratitude and appreciation to his supervisor, Professor F.M. Burdekin, for his help and guidance and above all for his encouragement at the various stages of this project.

The author wishes to thank Mr. A. Kirk for the help received during the execution of the experimental work carried out in the structural laboratory at UMIST.

Thanks are also due to Mr. R. A. Heywood, Mr. D. Walls, of the Departmental Computer Link, and Miss A. J. Howse, Secretary to Professor F. M. Burdekin, all assisted in speeding up the work.

The author also wishes to thank members of the Structural Assessment Group at UMIST for their help and advice, the Workshop Staff for their contribution to the completion of the experimental work.

Thanks are also due to Mrs Sandie Pletan, for her patience in typing my thesis.

The author also gratefully thanks Robert Watsons for fabrication of plates and SHS joints and supplying material for the SHS programme. The University of Jordan, Institute of Science and Technology for financial support received during the author's post-graduate study at UMIST.

CONTENTS

	<u>Page</u>
Summary	i
Declaration	ii
Acknowledgement	iii
Contents	iv
Notation	vii
 <u>INTRODUCTION</u>	 1
 <u>CHAPTER ONE</u>	
<u>STATIC AND FATIGUE DESIGN</u>	
<u>RECOMMENDATIONS OF FILLET WELDS</u>	
<u>AND SHS MEMBERS</u>	
1.0. Introduction	6
1.1. Static Design of Fillet Welds (Strength Formulae)	7
1.2. Static Design of SHS Welded Joints	9
1.3. General Approach to Fatigue Design of Fillet Welds.	16
1.4. Fatigue of SHS Joints (Joint Design Recommendations).	17
1.5. Methods of Analysis and Recommendations to Fatigue Design.	20
 <u>CHAPTER TWO</u>	
<u>FRACTURE MECHANICS APPROACH</u>	
2.0. Introduction.	35
2.1. Crack Tip Stress Field Equations	35
2.2. Modes of Crack Growth and Stress Intensity Factor Concept.	37
2.3. Conventional Approach to Design Against Fatigue.	37
2.4. Fracture Mechanics Approach to Design Against Fatigue.	38
 <u>CHAPTER THREE</u>	
<u>THE FINITE ELEMENT METHOD</u>	
3.0. Introduction	44
3.1. Formulation of Displacement Method.	45
3.2. Finite Element Package ABAQUS.	47
3.3. Structural Modelling.	48

3.4.	Mesh Generation and the Phases of ABAQUS Calculation.	49
3.5.	The Special Use of Crack Tip Elements.	51
3.6.	Calculation of Stress Intensity Factors from F.E. Analysis.	53

CHAPTER FOUR**THEORETICAL STUDY PHASE ONE**

4.0.	Introduction	59
4.1.	Review of Research Into the Fatigue Behaviour of Transversally Loaded Fillet Welded Connections.	60
4.2.	J. Integral Technique.	63
4.3.	Assumptions Made in the Finite Element Analysis of Fillet Welded Cruciform Joint.	64
4.4.	Modelling the Cruciform Fillet Welded Joint.	65
4.5.	Results of the Finite Element Analyses.	67
4.6.	Fatigue Life Estimation.	69
4.7.	Evaluation of the Integral I and the Construction of the S-N Family of Curves for Fatigue Design.	
4.8.	Comparison of Theoretical Findings with Frank & Fisher Life Predictions and Code of practice BS5400.	74
4.9.	Finite Element Investigation of the Influence of Misalignment on the Stress Intensity Factors.	75
4.10.	Finite Element Modelling of Misalignment.	76
4.11.	Results of the Finite Element Study.	78
4.12.	The Use of Interface Elements to Check Surface Contact.	79

CHAPTER FIVE**THEORETICAL STUDY PHASE 2
(SHS JOINTS)**

5.0.	Introduction.	112
5.1.	Summary of the Research into the Fatigue Behaviour of Structural Hollow Section Joints.	113
5.2.	Finite Element Model.	
5.3.	Results of the Finite Element Analysis.	119
5.4.	Fatigue Life Estimation.	121

CHAPTER SIX**THEORETICAL STUDY PHASE 3**

6.0.	Crack at the Weld Toe in SHS Connection.	145
6.1.	Finite Element Model and Results.	145

CHAPTER SEVEN**EXPERIMENTAL PROGRAMME**

7.0.	General.	152
7.1.	Experimental Programme Part A.	154
7.1.1.	Cruciform Fillet Weld.	154
7.1.2.	Welding.	155
7.1.3.	Instrumentation and Test Procedure.	156
7.1.4.	Failure Mode and Test Results.	157
7.1.5.	Comparison of Test Results with With Behaviour Predicted by Fracture Mechanics Analysis.	158
7.2.	Experimental Programme Part B.	
7.2.1.	Fillet Welded Joints (SHS Members)	160
7.2.2.	Welding and Instrumentation.	160
7.2.3.	Test Procedure and Results.	161
7.2.4.	Mode of Failure for Tests HSK1, HKS2, and HKS3.	162
7.2.5.	Mode of Failure for Tests HSK4 to HSK7.	162
7.2.6.	Comparison of Test Results With Behaviour Predicted By Fracture Mechanics Analysis.	163
7.3.	SPATE	164

CHAPTER EIGHT

8.0.	Discussion	180
8.1.	Conclusions	185

APPENDIX

A	Photographs of the Tests and Equipment.	188
---	--------------------------------------------	-----

REFERENCES

LIST OF SYMBOLS

The following symbols are used are used in this thesis. They are defined briefly, and some of the symbols which are omitted are explained at the appropriate point in the thesis.

b_i	Nominal width of member i .
b_{eoi}	Effective width of outer crosswall of web member i , for gap or overlap joints with less than 100% overlap, for the "effective width" failure mode.
$b_{eo(p)}$	Effective width of outer crosswall of web member in a gap joint for the "punching shear" failure mode.
F_k	Chord sidewall buckling stress.
F_{yi}	Yield stress of member i .
h_i	Nominal depth of member i .
K	Effective length factor for a compression member.
L	Length of member i .
N_{ui}	Ultimate joint strength expressed as a force in member i .
r	Radius of gyration of a member (r_c for bending about x axis, r_y for bending about y axis).
t_i	Wall thickness of member i .
β	Average web to chord width ratio.
θ_{iPv}	Acute angle between web member i and chord member.

INTRODUCTION

INTRODUCTION

In the design of dynamically loaded welded structures it is necessary to consider the fatigue performance of the structural details. As fatigue cracks form at stress concentration sites, consequently the stress distribution in and around areas of stress concentration provides important information to be used for the design of safe cyclically loaded welded joints.

Fillet welds are used extensively as a method of joining various types of structural members together. Fillet welded plate joints are a typical example and the fatigue design of these joints is based on the use of experimentally determined fatigue classifications for different types of joints [1,2].

In tubular joints, high stress concentrations can occur due to local bending of the walls of the members. Extensive research has been carried out on circular tubes for offshore construction to determine fatigue behaviour [3,4,5 & 6] and in RHS/SHS joints to determine static strength [7,8,9,10,11 & 12].

Stress analysis of welded joints between SHS members is also important in understanding the behaviour of these joints under both static and fatigue loading. SHS members are generally used in two-dimensional lattice girders.

Fracture mechanics is now being more widely applied as a rational method of providing quantitative relationships which can be used for the fatigue design of fillet welded joints. If the time taken for a crack to propagate to failure can be calculated it can be determined whether a crack will grow to catastrophic size within the life of the structure given its design loadings.

The purpose of this research programme into the fatigue of fillet welded connections of plates and SHS members is to investigate the use of fracture mechanics methods to calculate the behaviour of fatigue cracks so that the validity of existing methods may be checked more comprehensively, and confidence established in design methods for geometries outside the range of those included in the major experimental test programmes. Further particularly in the case of SHS welded joints no unified in depth recommendations which cover a wide range of parameters exist. Recommendations are generally based on results obtained from tests on a limited range of joints.

As a result a decision was taken to approach this problem by use of numerical methods. Aspects of the behaviour of fillet welded joints comprising plates and SHS members are investigated using the finite element analysis.

In this thesis three pieces of theoretical work and two pieces of experimental study are conducted.

In the first phase of the theoretical study, fillet welded joints of plates in which the welds are stressed transversely to the weld line are analysed using the finite element method to study the geometrical effects on these stress intensity factors at the fillet weld root. In the second phase SHS fillet welded joints subjected to fatigue loading were analysed again using the finite element method. Phase 3 of the theoretical study involved the incorporation of a semi-elliptical crack in the three-dimensional model of SHS fillet welded joint at the weld toe. Parametric equations were derived which relate the stress intensity factors at weld root in phase (1) and in phase (2) where the bending stresses magnify the stress state in the fillet welds.

The theoretical study was followed by a two part experimental programme. Firstly cruciform fillet welded joints made from different attachment plate thicknesses and different weld sizes were tested dynamically in an Instron tensile testing machine and the results compared with theoretical findings. The second part involved the testing of two groups of SHS fillet welded joints to confirm the theoretical work.

The first three chapters in this thesis include an outline of the conventional recommendations and guidance for the static and fatigue design of fillet welds and SHS members, a brief description of the fracture mechanics approach, and in Chapter 3, the finite element tool of stress analysis is described.

CHAPTER ONE

1.0. Introduction

1.1. Static design of fillet welds (strength formulae)

1.2 Approach to fatigue design of fillet welds

1.3 Fatigue of SHS joints

CHAPTER ONE

1.0. INTRODUCTION

Fillet welds are used to transmit forces from one part of a structure to another. Despite the fact that fillet welds are in concept simple, the manner by which forces are transmitted and the internal stress system are highly complex. Valuable quantitative strength results of fillet welds can be obtained by approximate solutions based on elastic theory, whereas a rigorous solution for the stress distribution in fillet welds cannot be obtained without resort to numerical methods.

Structural hollow sections enjoy an efficient distribution of their material, particularly in regard to beam bending or column buckling about multiple axes. Added to that, the closed sections are aesthetically pleasing. Square and rectangular hollow sections in particular are often favoured over circular hollow sections because of the fabrication, and preparation and welding complexity associated with joining CHS individual members directly to each other. The application for SHS and RHS members is mainly in welded trusses or Lattice Girders. As a result of their popular use, the strength and stiffness of the welded joints of these members have been the subject of extensive research.

In this chapter the general approaches to static and fatigue design of fillet welds and SHS members are reviewed. The

recommendations and guidance to design are outlined with a brief description of the research carried out in this area.

1.1. STATIC DESIGN OF FILLET WELDS (STRENGTH FORMULAE)

Using conventional analytical methods, weld stresses calculated as resulting from design actions are simply added vectorially to obtain a fictitious resultant stress over the throat area.

Generally the method used by the codes of practice for the static design of fillet welds is to find the forces acting on and perpendicular to the plane of the weld throat. Stresses are then calculated on the throat area assuming a uniform stress distribution prevails along the length of weld. Calculated stresses are then combined in a prescribed manner and made to satisfy some design criterion.

Bodies like the International Institute of Welding provide direct guidance to design through its sub-commissions. In the case of fillet welds guidance and rules for their static design have been worked out by the IIW Sub-commission YXV-A[13]. These rules are based on research carried out in many countries.

According to the IIW method, if the fillet welds are loaded in an arbitrary direction, the loading and stresses can be resolved into three components acting on the throat area.

These are the normal stress perpendicular to the throat section (σ_1), shear stress on the throat parallel to the weld axis ($\tau_{//}$), and Shear stress transverse to the axis of the weld (τ_1). These stresses are combined and checked that they comply with the condition:

$$\beta[(\sigma_1^2 + 3(\tau_1^2 + \tau_{//}^2)]^{1/2} \leq \sigma_c$$

and $\sigma_1 \leq \sigma_c$ (1.1)

σ_c is equal to the permissible tensile stress in the base material

$$\beta = .7 \text{ For Fe 360} \quad (F_y = 235 \text{ N/mm}^2)$$

$$= .85 \text{ for Fe 510} \quad (F_y = 355 \text{ N/mm}^2)$$

F_y is the yield stress.

According to BS5950 [14], which is based on the Limit State design approach, the design strength of fillet welds made using covered electrodes complying with BS639 [15] on steel complying with BS4360 [16] should be limited to 215 N/mm².

In BS5400, [1] the limit state design for bridges, the shear resistance τ_D of fillet welds is given by:

$$\tau_D = K(F_y + 455) / (\gamma_m \gamma_f \sqrt{3}) \quad (1.2)$$

where F_y = the nominal yield stress of the weaker part joined

$K = 0.9$ for side fillets, or
 $= 1.4$ for end fillets in end connections
 $= 1.0$ for all other welds.

The applied stresses in a fillet weld, based on the resultant of all shear forces acting on any part of it should not exceed τ_D . An alternative method in BS5400 is that:

$$[\sigma^2 + 3(\tau_{\perp} + \tau_{//})]^2 \leq K (\sigma_y + 455)^2 / (2\gamma_m \gamma_{f3}) \quad (1.3)$$

where σ = stress normal to a section through the throat of the weld.

τ_{\perp} = The shear stress perpendicular to the length of weld on the throat section.

$\tau_{//}$ = The shear stress acting parallel to the length of the weld on the throat section.

σ_y , and K are as defined above.

γ_m = material factor

γ_{f3} = load factor.

1.2. STATIC DESIGN OF SHS WELDED JOINTS

Research into the behaviour of SHS welded joints carried out by researchers has shown the complexity of design of such

joints and the large number of factors involved. Ultimately the prime aim is to derive simple design rules to be followed when designing these joints. The research on welded SHS joints has taken place principally in England at Sheffield University, Nottingham University and British Steel Corporation Tubes Division, in the Netherlands at Delft University of Technology, in West Germany at Karlsruhe University and the Mannesmann Research Institute, in Italy at Pisa University and in Canada at McMaster University. These have been summarised by Wardenier (1982)[9]. The main interest has focused on K type Y, T, and X type Lattice girder joints.

R. Haleem, 1977[7] presented in his paper some suggestions for approaching the static design of SHS welded joints. He proposed, based on experimental results, that for gap joints of SHS members the most common mode of failure is the shearing of the face of the chord at the weld toe of tension bracing initially at the toe and spreading round the circumference. He added that for certain combinations of parameters, large deformation of the chord face precedes the shearing of the chord face in the case of small β ratio and large gaps. In his approach he proposed that the shear area (S.A) is a function of β , chord width and chord thickness.

Shear area assumed to have a minimum value of $d.T$ for small β ratio and will then spread round the circumference of the tension bracing as β increases. The reason suggested by

Haleem for this assumption is that in the case of small ratio of β a high proportion of the load in the bracing passes through its side facing the gap, on the other hand for joints with high β a proportion of the load is transferred across the side walls of the bracing to the chord side walls which increases the proportion of the perimeter of the tension bracing effective in transferring the load to the chord than in the case of small β ratios. He supported his assumption by strain gauge measurements. The assumed shape of the curve for variation of shear area with β ratio is shown in Fig (1.1). Also the function assumed is:

$$SA = T. C. \left(\frac{d}{c} \cdot e^{140/D'(d/D)} \right) \quad [1.3]$$

where

$$D' = D - 3T$$

D is the chord size

T chord wall thickness

c brace perimeter

and d is brace size

He also suggested that the second mode of failure for gap joints of SHS members is the local buckling of the compression bracing. Haleem also considered the overlap joints of SHS members and suggested that the most common type of failure for these joints is the local buckling of the compression bracing based on the assumption that a member will buckle when the stresses in the extreme fibres reach the yield strength of the material of that member.

Eastwood and Wood [12] at Sheffield University carried out a small number of tests on a narrow range of RHS section sizes and developed several empirical design rules. After that CIDECT sponsored and co-ordinated a large research investigation into Structural Hollow Joints strengths, principally undertaken at different research centres mentioned earlier in the Chapter. The results of the research ~~are~~ contained in Monograph No. 6 - a [17] 'state-of-the-art' document giving design guidelines. A summary of design guidelines for static case of X, Y and T joints ~~is~~ chosen to be outlined here.

For plastic deformation of the chord face, the joint strength is based upon a yield line mechanism such that:

$$N_{ui} = F_{yo} t_o^2 [2h_i/b_o \sin\theta_i + 4 (1-\beta)^{0.5}]^{1/(1-\beta)} \cdot 1/\sin\theta_i$$

$$, \text{ For } \beta \leq .85 \quad (1.4)$$

A comparison of test results of T and X joints loaded in compression with equation (1.4) is shown in Fig (1.2). It is shown that the calculated strength is generally lower than the actual strength due to membrane action which will be particularly strong for joints with a high (b_o/t_o) and a low β ratio.

In the case of width ratios between brace and chord members approaching unity, failure (and hence joint strength) is

dominated by web bearing or buckling of the chord side walls, such that:

$$N_{ui} = F_k t_o [2h_i / \sin \theta_i + 10t_o] / \sin \theta_i, \text{ for } \beta = 1.0 \quad (1.5)$$

For values of $.85 < \beta < 1.0$ the strength at the joint is evaluated by interpolation between the two equations above. It is important to note that F_k is equal to the yield stress if the brace member is in tension. For compression load in the brace member, F_k is a buckling stress computed using chord slenderness ratio:

$$Kl/r = 3.46 [(h_o/t_o) - 2] \sqrt{\sin \theta_i} \quad (1.6)$$

In IIW DOC XV-492-81 [8], F_k is computed using European buckling Curve "a" for hot formed SHS members. The chord side wall slenderness ratio above assumes a pin-ended column of length $(h_o - 2t_o)$ and radius of gyration (r) of $(t_o/3.46)$. ($I = \text{effective column width} \times t_o^3/12 = \text{effective column width} \times t_o \times r^2$).

Equation (1.5) given above is compared with the test results for cross joints $\theta=90^\circ$ Fig. (1.3) reported by Wardenier [9].

Further the effective width and punching shear strength failure mode checks have been stipulated. These are in the

form of analytical lower bound equations to be applied only when $\beta > 0.85$ (IIW 1981).

For the effective width failure criterion, the joint strength is given as:

$$N_{ui} = F_{yi} t_i [2h_i - 4t_i + 2b_{eoi}], \text{ where } i=1 \text{ or } 2 \quad (1.7)$$

For the punching shear failure criterion, the joint strength is given as:

$$N_{ui} = F_{yo} t_o / \sqrt{3} \sin \theta_i [2h_i / \sin \theta_i + 2b_{eo(p)}], \quad (1.8)$$

where $i = 1 \text{ or } 2$

An example of comparison between the available test results for T - and X - joints in tension and the equations for effective bracing width and chord punching shear [10] is given in Fig (1.4).

The limits of validity of the equations covering the strength of X, Y and T joints described in this section are listed in Table (1.1). Some of these limits represent bounds for which supporting test evidence is available and others are theoretically estimated to ensure adequate joint performance. The main factors are local joint deflections at the service load level, sufficient moment redistribution capacity and prevention of premature local buckling.

With regard to determination of design strength IIW [8] gives the design strength for the effects of factored loading given by:

$$N = N_k / Y_m Y_c \quad (1.9)$$

where N_k : characteristic joint strength (95% confidence).

The factor $Y_m Y_c$ depends on the mode of failure and the way in which the strength functions are determined. If this is based on the theoretical model based on the yield and justified by tests which show sufficient ductility $Y_m Y_c = 1.0$ can be chosen. If the ultimate strength is derived from the ultimate load capacity based on experimental evidence, the $Y_m Y_c \geq 1.0$ due to the greater uncertainties.

T - Y - X joints with a width ratio $\beta \leq .85$ can be designed on the basis of the chord face yield criterion mentioned earlier with an adopted $Y_m Y_c = 1.0$, because it is based on an analytical model giving a lower bound for the test results.

T - Y, X joints with $\beta = 1.0$ have to be designed on the strength of the chord side walls, $Y_m Y_c = 1.0$ for T-joints and $Y_m Y_c = 1.25$ for X-joints because T-joints are taken to have a better chord side wall buckling resistance than X - joints. For $.85 < \beta < 1.0$, $Y_m Y_c = 1.25$ is recommended due to the lower ductility.

Lastly recommendations for fillet weld sizes are that they should satisfy the following conditions:

Fe 360}	$a \geq t$
Fe 430}	
Fe 510}	$a \geq 1.2 t$

where

a = throat thickness of the fillet weld

t = wall thickness of the SHS Section to be connected.

1.3. GENERAL APPROACH TO FATIGUE DESIGN OF FILLET WELDS

The general approach to fatigue design of fillet welds depicted by the different codes of practice [1, 2] is to divide the various types of joints into classes depending on their stress concentration effect and with allowable stress ranges on parent material near to the weld toe or on the weld throat. For example, the design curves in BS 5400 Pt10 are based on mean minus two standard deviations, for seven different classes of geometric detail. The classical S-N curves were arrived at by considering the results of a large number of experiments where welded joints were subjected to cyclic stresses to give the necessary base for statistical analysis, however most of the joints studied were of a restricted range of plate thicknesses.

Empirically derived rules in general have the disadvantage of being limited to a given range of applicability.

1.4. FATIGUE OF SHS JOINTS (JOINT DESIGN RECOMMENDATIONS)

The fatigue design of welded connections of Hollow Structural sections found in lattice constructions requires much more understanding and is far more complex than the general fatigue design of steel structures made of plates and open sections.

The stress distribution in the welds between the main and bracing members must be studied together with the rigidity associated with the geometries of the sections and the joint.

The research work carried out to study the behaviour of SHS joints had been very little until in 1975 a programme of work was launched and sponsored by the European Coal and Steel Community [ECSC], CIDECT, and the Studiengesellschaft für Anwendungstechnik which yielded results on which the design rules and recommendations described in this section are based on.

Firstly, the influencing factors on which the fatigue behaviour of SHS joint depend are:

a) Loading

Fatigue behaviour is usually determined on the basis of constant amplitude loading. This type of loading is characterised by:

stress ratio $R = \sigma_{\min} / \sigma_{\max}$,

and stress range $S_r = \sigma_{\max} - \sigma_{\min}$

The stress range being the most important parameter.

When the loading fluctuations are not constant, the stress spectra have to be considered. The shape of the spectrum has an influence on the endurance. An example of the influence of load spectrum on the fatigue behaviour for a welded joint is shown in Fig (1.5) (Wardenier, 1982).

b) **The Joint Detail**

Under predominantly static loading, local stress or strain concentrations are of minor importance because of the redistribution of stresses by local yielding. In the case of fatigue loading, the stress and strain concentrations play a dominant role and influence the fatigue behaviour.

Localised stress concentrations in welded Hollow Structural Sections arise from weld shape, weld angle and the weld defects, also from the variation in stiffness and local bending of the walls along the intersection of the connected members.

One common method of taking account of geometrical influence is to determine the relationship between the hot spot stress or strain range and the number of cycles

to failure for a specific joint detail either by experimental strain gauging or finite element analysis. This method again has the disadvantage of generally being limited to a certain range of parameters only.

c) **Environment**

In a corrosive environment e.g. sea water, a deterioration in fatigue performance of steel structures is observed. Corrosion in fatigue loaded components leads to an increased crack growth rate. The formula listed below applies if the corrosion effect is considered in addition to fatigue loading, whereby crack initiation and growth are both taken into account [18] as reported in monograph 7, CIDECT [19].

$$da/dN = \Delta k^2 / (4\pi \sigma_e^2 E) \left((\Delta k - \Delta k_{th}) / (k_{Ic} - \Delta k / (1-R)) \right)^{0.5} \quad (1.10)$$

where

Δk = stress intensity factor level

Δk_{th} = threshold value ΔK for fatigue crack growth

Δk_{Ic} = fracture toughness of the material

Δk_{th} = can be calculated in relation to the stress ratio

$$\Delta k_{th} = k_{th}^0 (1-R)^m$$

k_{th}^0 is the threshold stress intensity factor level for fatigue crack growth at $R = 0$ and m is the exponent.

The time dependence of corrosion implies that the test results depend on the frequency used as shown in Fig (1.6).

1.5. METHODS OF ANALYSIS AND RECOMMENDATIONS TO FATIGUE

DESIGN

Several methods are employed to study the fatigue behaviour of SHS joints. These methods are:

a) Hot spot stress method:

Due to the fact that stress concentrations in structural hollow sections affects their fatigue behaviour, the test results analysis is done by plotting the number of cycles against the measured hot spot strain or hot spot stress ranges. Hot spot stress or strain ranges are determined in such a way that the local weld defects are not included, only the geometrical effects are included.

In SHS joints the maximum hot spot stress range at a weld toe is defined as:

$$SCF = \frac{\text{maximum hot spot stress somewhere at the weld toe}}{\text{nominal stress in the bracing at the intersection}}$$

while the hot spot method is the one most commonly used for circular hollow sections, for square hollow sections, however, only a limited information on the stress concentration factors is available. Wardenier (1982) reported some orientational investigation in this field [20] which was carried out on N-type square hollow section joints. The results are summarised in Table

(1.2). Fig (1.7] also shows a comparison made with test results.

At present no parametric formulae are available for the determination of SCF values for SHS joints.

b) Classification Method:

This method is proposed for the design of SHS joints under fatigue loading due to the limited number of tests available at present for these joints.

The basis of this method [21] reported in [9] is to divide the fatigue test results for similar joints into categories and analyse them separately. The stress concentration factors are taken indirectly into consideration. Various experimental stress ranges S_r . nom. braces. vs. N curves are related to specific type of joint. These curves have been classified according to groups of joints having similar geometrical ratios and similar loads.

Wardenier, Noordhoe and Dutta (1981) [21] describe a method of analyses of joints with square hollow sections and only limited to K , N joints with a defined gap or fixed overlap. They reduced the number of S-N lines based on experimental results by plotting on the vertical axis of the S-N graphs the value S_{rx} , which has to be multiplied by functions representing the main influencing

geometrical parameters to obtain the allowable stress range. These design guidances are represented in Fig. (1.8). Further it should be concluded that the assessed test results are only valid over the tested parameter range. To extend the application of test results beyond that range, more tests are necessary.

c) Failure criterion method:

In this method which is being developed at the University of Karlsruhe [22,23] for square hollow section joints and also for SHS joints, the stress concentration factors are indirectly taken into account by giving an allowable nominal stress or stress range at a fixed number of cycles e.g. 2×10^6 . This stress is given in diagrams for $R = -1$ as a function of the joint parameters. The S-N curve is then described by the stress for $N = 2 \times 10^6$ cycles, a slope for the S-N curve and an influence function for the R ratio.

The design charts for SHS joints derived from the available test results are restricted to limited parameter ranges and joint types. Examples are given in Fig. (1.9). These curves correspond to a statistical survival probability of 50% due to the low number of tests.

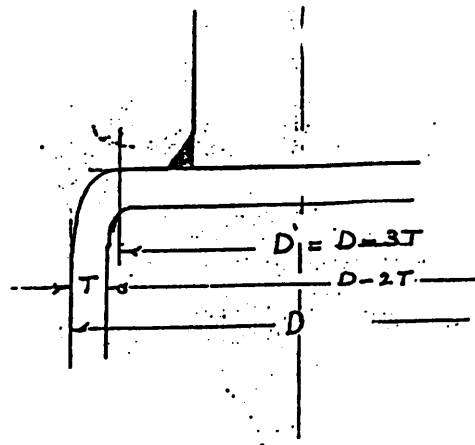
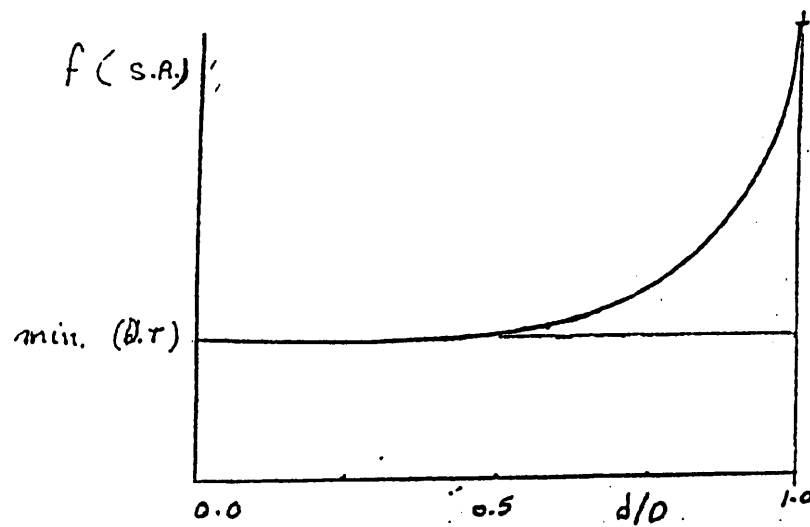


Fig. (1.1) Variation of Shear Area (Face of Chord Shearing Failure) with Ratio for SHS Welded Joints. [7]

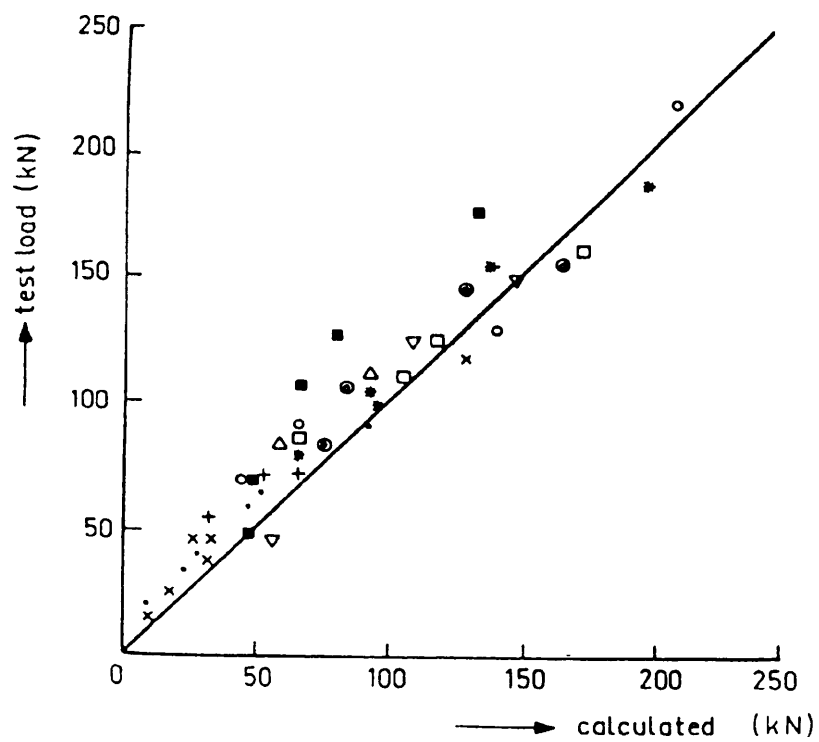


Fig. (1.2). Comparison of Test Results of T and X Joints Loaded in Compression. [17].

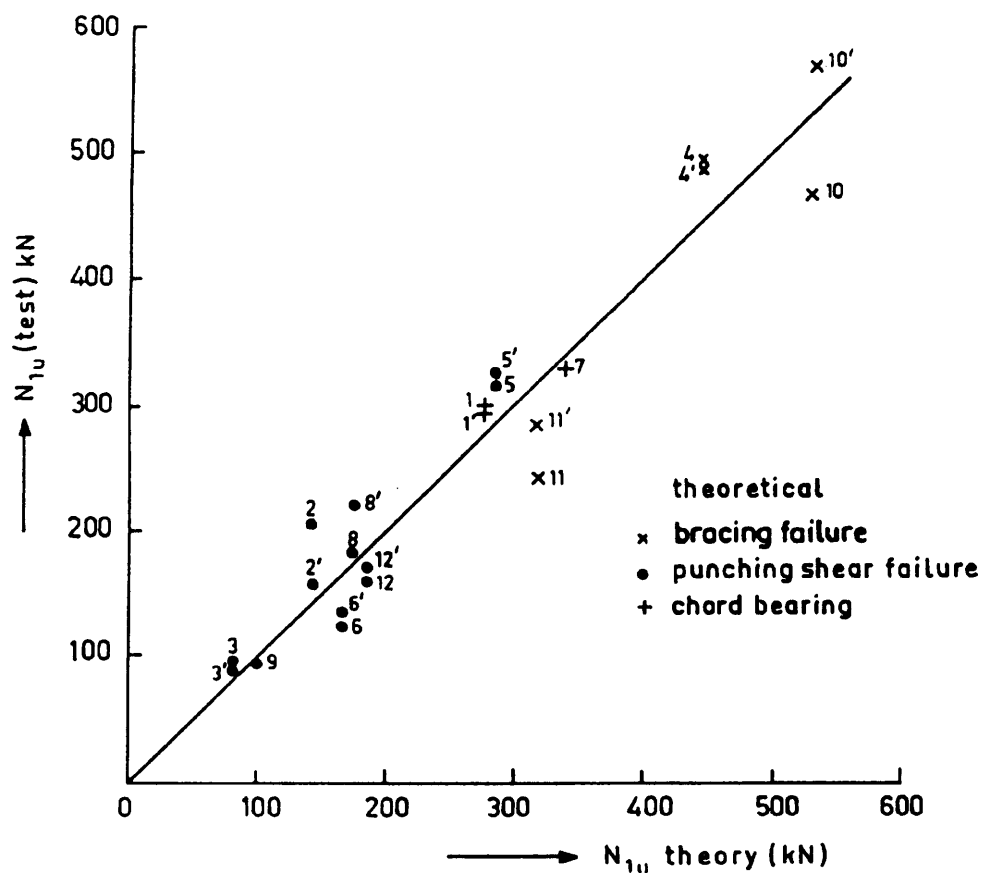


Fig. (1.3). Test Results for Wall Bearing and Wall Buckling. [9]

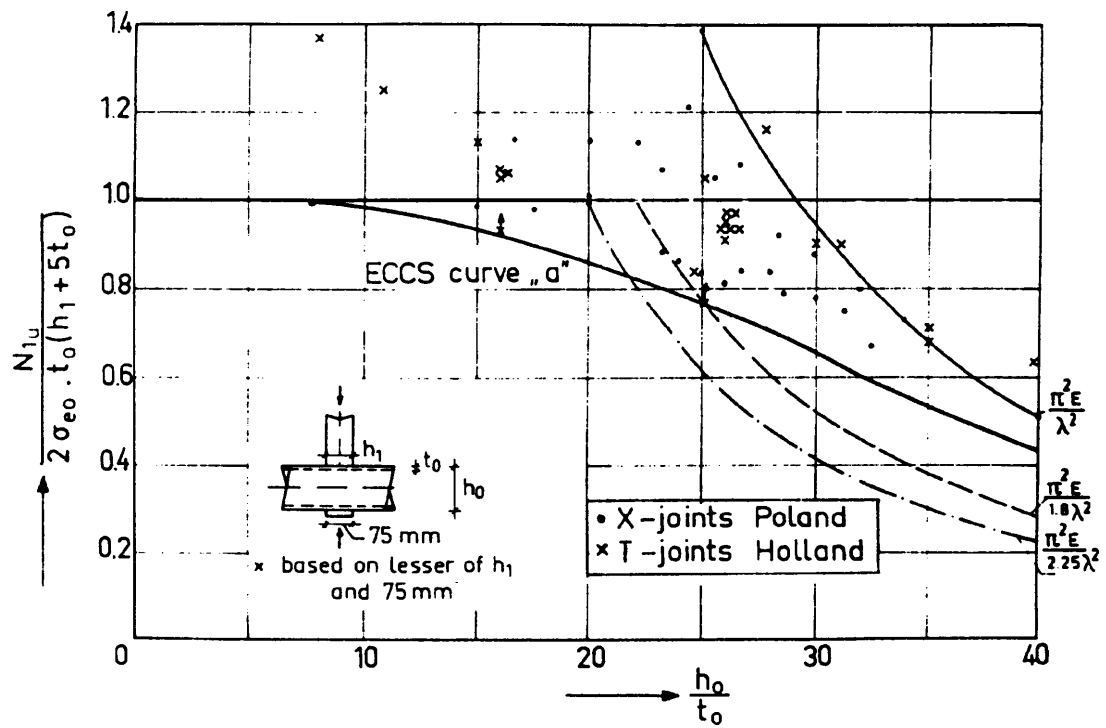


Fig. (1.4). Comparison Between Test Results for T and X Joints. [10]

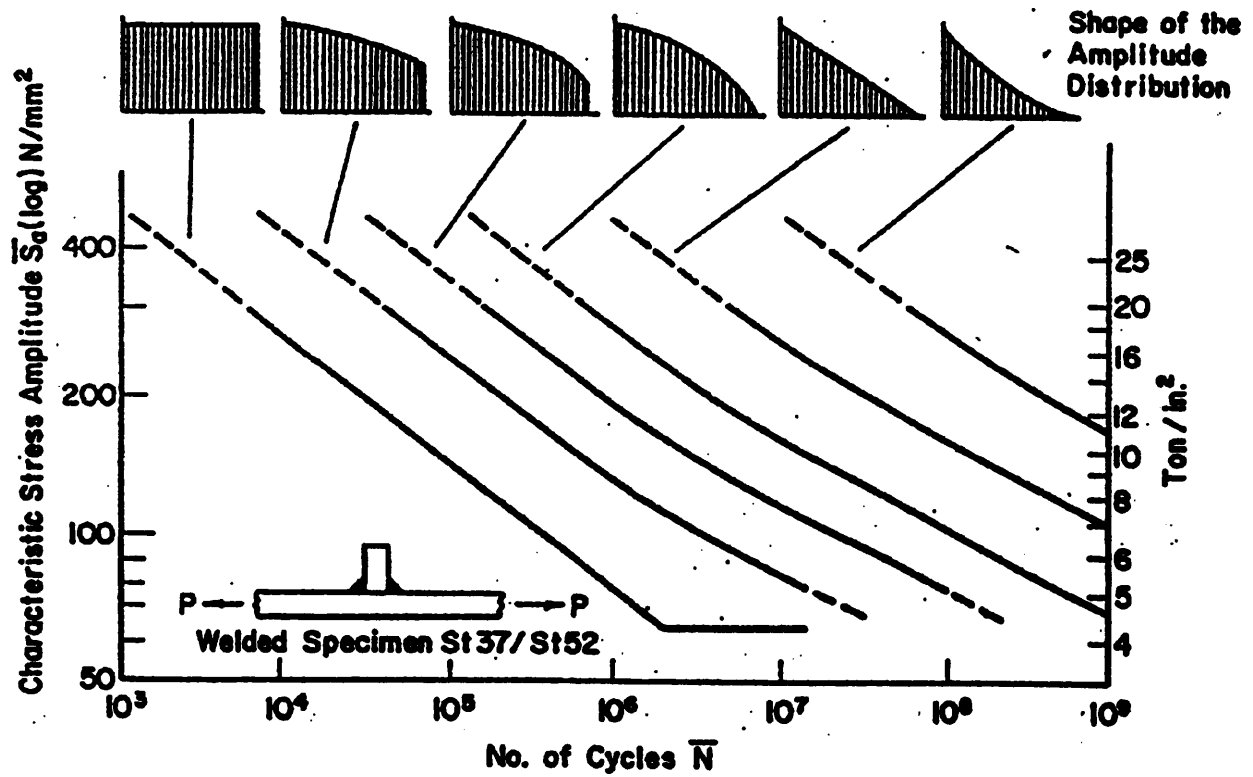


Fig. (1.5). Effective of Shape of Amplitude Distribution on Cycles to Failure.

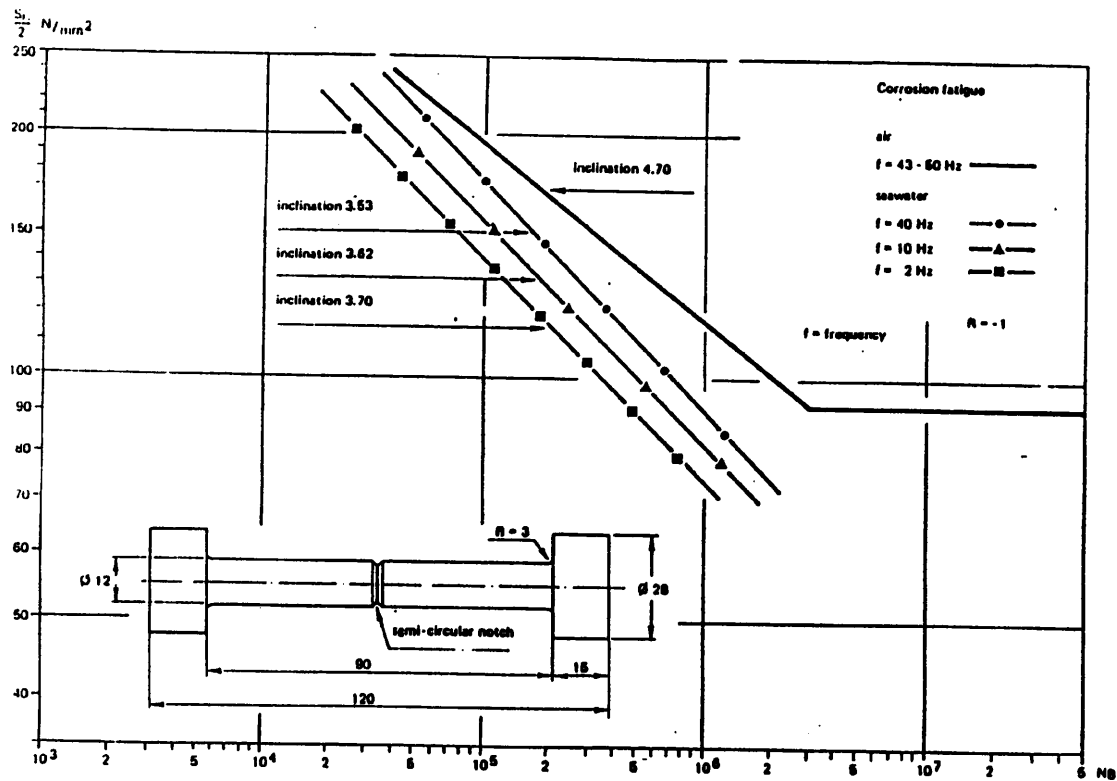


Fig. (1.6). Curves for Structural Components in Air and Seawater. Influence of load frequency f on stress amplitude. [19]

For Lap Joints and X, Y and T Joints
$b_i/b_0, h_i/b_0 \geq 0.25$ b_0/t_0 and $h_0/t_0 \leq 35$ b_1/t_1^* and $h_1/t_1^* \leq 412/\sqrt{F_{y1}}$ b_2/t_2 and $h_2/t_2 \leq 35$ $0.5 \leq h_i/b_i \leq 2.0$ $-0.55 h_0 \leq e \leq 0.25 h_0$ $\theta_i \geq 30^\circ$ $F_{yi} \leq 360 \text{ MPa}$ $F_{yi}/F_{ui} \leq 0.8$ $b_i/b_{ov} \geq 0.75$ $q/p \geq 0.3, \text{ for Lap Joints}$ $d_1/t_1^* \leq 550/\sqrt{F_{y1}}$ $d_2/t_2 \leq 50$ $0.4 \leq d_i/b_0 \leq 0.8$

Table (1.1). Joint Parameter Range of Validity for Equations Recommended by I.I.W. (1981). [9].

Joint type	θ_1/θ_2	Chord mm	Bracing 1 2 mm	$S_{r,axial} : S_{r,bend}$ 1 2 aug	Gap $\frac{g}{b_2}$	Overlap	Determined by	Location SNCF
N (Elastic model)	90° 45°	100x100x4	60x60x4 60x60x4	1 : 1,9 1 : 1,4	0,4	-	Finite element calculation + Strain gauge measurements	on chord at end of bracing -6,0
N (Elastic model)	90° 45°	100x100x4	60x60x4 60x60x4	1 : 2,5 1 : 1,0		48 %	Finite element calculation + Strain gauge measurements	on chord at end of bracing -2,6
N (Steel specimens)	90° 45°	100x100x6,3	60x60x3,2 60x60x3,2	1 : 0,5 1 : 0,1		100 %	Strain gauge string	on bracing member a weld connection in overlap -2,0 zone with vertical member
							Strain gauge string	at the weld -1,95 on vertical member
N (Steel specimens)	90° 45°	100x100x6	60x60x3,2 60x60x5	1 : 0,9 1 : 0,6	0,4	-	Strain gauge string	at base of the weld on bracing member -3,75
							Strain gauge string	at the weld on vertical member -3,0

Table (1.2). Summary of Tests Carried Out on Square Hollow Section Joints to Determine SNCF.

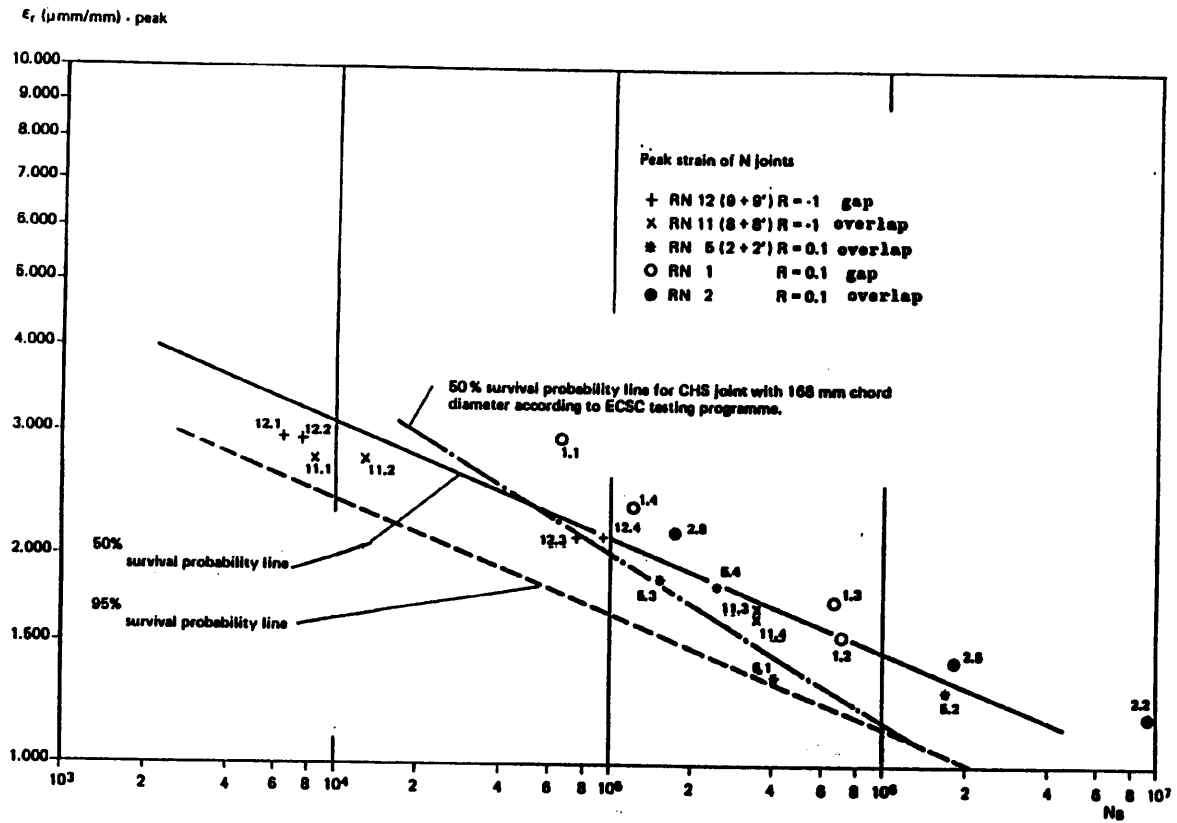


Fig. (1.7). Peak Strain Ranges for RHS N Joint Failure.

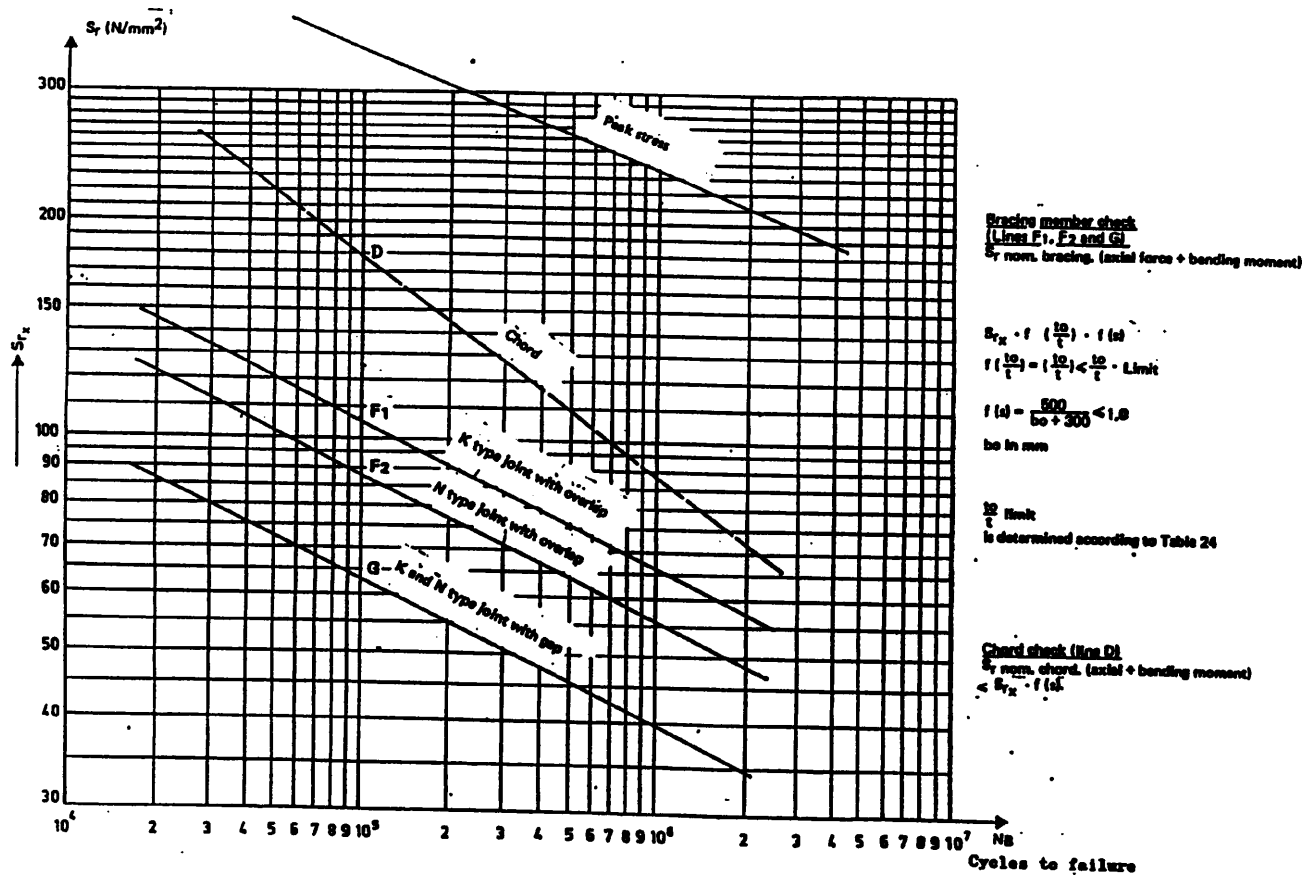


Fig. (1.8). Recommended 95% Survival Probability Line S_{rx} vs. NB for K and N type RHS Joints ($-1 < R < +0.2$). [21]

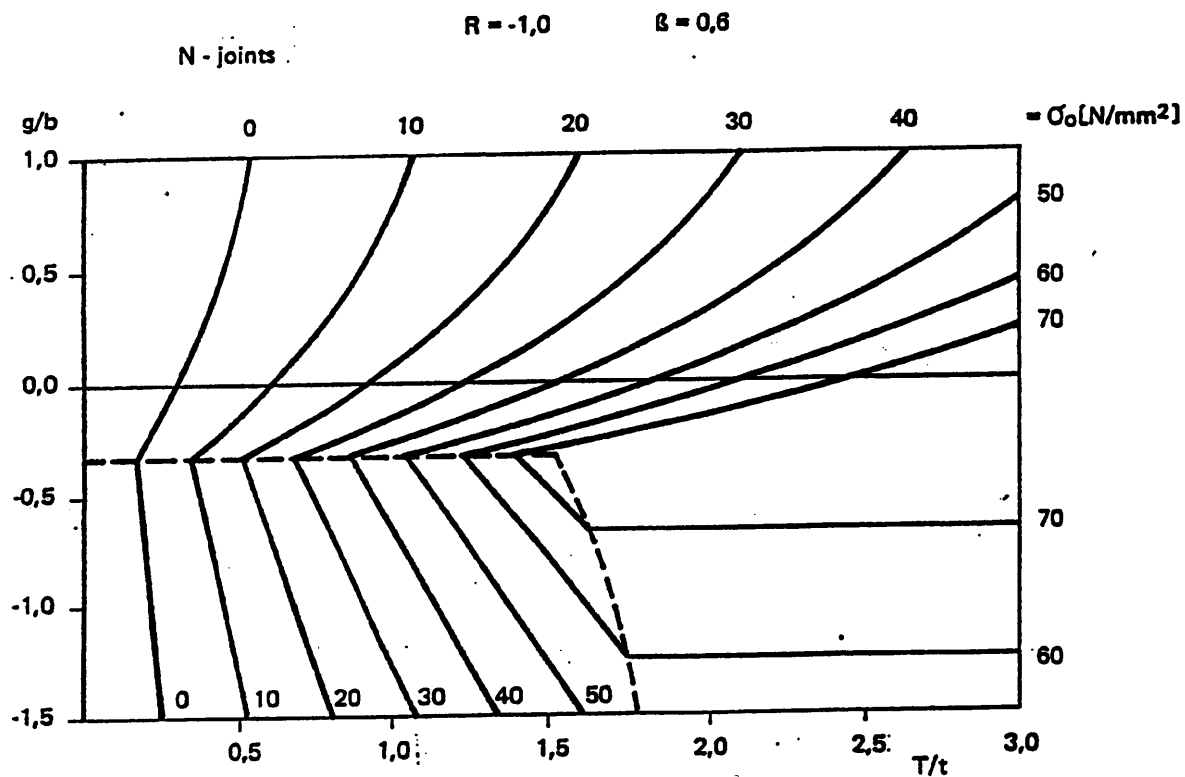


Fig. 1.9 Design chart for N type RHS joints with chord width $\leq 200\text{mm}$. ($b/b_o=0.6$; $\theta = 45^\circ$; $R = -1$; St37 and St 52). [22,23]

CHAPTER TWO
FRACTURE MECHANICS APPROACH

2.0. Introduction

2.1. Crack Tip Stress Field Equations

**2.2. Modes of Crack Growth and Stress Intensity Factor
Concept**

2.3. Conventional Approach to Design Against Fatigue

2.4. Fracture Mechanics Approach to Design Against Fatigue

CHAPTER TWO

FRACTURE MECHANICS APPROACH

2.0. INTRODUCTION

In the early 1920s Griffith [24] has laid the foundations of fracture mechanics. The theory of fracture proposed by Griffith was only strictly true for wholly brittle material. Extension of Griffith's theory to make it applicable to materials which were not completely brittle was proposed by Irwin and Orowan. Since then the approach has been broadened and fracture mechanics can now be applied to the study of any mode of failure which involves the extension of cracks including fatigue.

Fracture mechanics provide a quantitative relationship which can be used to determine limiting sizes of crack-like defects when the applied stresses and fracture toughness are known.

In this chapter the elastic stress field developed in the region of a crack tip is first considered. Conventional approaches to design against fatigue and the fracture mechanics approach are described in sections 2.3 and 2.4.

2.1. CRACK TIP STRESS FIELD EQUATIONS

Westergaard's equation for the elastic stresses (σ_x , σ_y , and τ_{xy}) in the vicinity of a crack tip ($r \ll a$) either under opening or sliding modes [25,26] is:

$$\begin{Bmatrix} \sigma_x \\ \sigma_y \\ \tau_{xy} \end{Bmatrix} = \frac{1}{\sqrt{2\pi r}} \begin{Bmatrix} \cos\theta/2[1-\sin\theta/2\sin 3\theta/2] - \sin\theta/2[2+\cos\theta/2\cos 3\theta/2] \\ \cos\theta/2[1+\sin\theta/2\sin 3\theta/2] \quad \sin\theta/2 \cdot \cos\theta/2 \cos 3\theta/2 \\ \sin\theta/2 \cos\theta/2 \cos 3\theta/2 \quad \sin\theta/2 \cos\theta/2 \cos 3\theta/2 \end{Bmatrix} \begin{Bmatrix} K_I \\ K_{II} \end{Bmatrix} \quad (2.1)$$

where

K_I and K_{II} are the mode I and mode II stress intensity factors.

r, θ are polar co-ordinates measured from the crack tip.

Figs (2.1a). K_I represents the contribution of a symmetric and K_{II} an antisymmetric stress distribution with respect to the crack plane on the crack tip stress field.

In general, for idealised elastic material, provided the co-ordinate point (r, θ) is in the immediate vicinity of the crack tip but is not affected by the proximity of edges, the omitted terms in equation (2.1) are negligible and the stress state is adequately described in terms of the two terms given above containing K and K_I . For real materials showing elastic plastic behaviour if the point (r, θ) is close to the crack tip then the effect of local, yielding in the high stress region renders equation (2.1) invalid. In practice also as the co-ordinate point moves further away from the crack tip region, further terms must be included in equation (2.1) to allow for the finite dimensions of the cracked body. Provided the size of any yielded zone is small compared to the crack and ligament dimensions, the overall stress field surrounding the crack remains elastic and dominated by the stress intensity factor.

2.2. MODES OF CRACK GROWTH AND STRESS INTENSITY FACTOR

CONCEPT

There are three basic modes of crack surface displacement which can cause crack growth. The opening mode, where crack surfaces move directly apart is known as mode I opening displacement, the edge sliding mode where the crack surfaces move normal to the crack front and remain in the crack plane is known as Mode II displacement, and the shear mode where the crack surfaces move parallel to the crack front, known as mode III. The three modes of crack growth are shown diagrammatically in Fig. (2.1b).

This form of stress analysis of cracks led to the concept of using stress intensity factors which describe the elastic crack tip stress field as a means of characterising cracks. For some materials the crack propagates catastrophically at a critical value of this factor, and this value is taken as a measure of fracture toughness.

The stress intensity factor is a function of specimen dimensions, loading conditions and crack size.

2.3. CONVENTIONAL APPROACH TO DESIGN AGAINST FATIGUE

The importance of the stress concentration effect of structural details is recognised in the various structural steel design codes.

Design rules have been published [1,2] which give the fatigue performance of various types of welded details. These design rules were arrived at by considering the results of a large number of experiments where welded joints were subjected to cyclic stresses.

The welded joints have been categorised by codes of practice into various classes of permitted stress range.

2.4. FRACTURE MECHANICS APPROACH TO DESIGN AGAINST FATIGUE

An alternative approach to design against fatigue to the empirical approaches described in the previous section is the fracture mechanics approach.

The fracture mechanics approach enables the prediction of fatigue crack growth rates for any cracked body configuration in terms of elastic stress field parameters. Apart from locally at the crack tip, the fatigue crack propagates under essentially elastic loading conditions so that the propagation of such cracks is governed by the elastic stress intensity factor associated with the crack and accordingly can be studied by linear elastic fracture mechanics (LEFM).

The fracture mechanics approach is particularly relevant to welds owing to the inherent stress concentrations due to geometrical discontinuities such as those associated with weld profiles, weld toe and the unwelded length of fillet welds.

Apart from the calculation of rate of fatigue crack growth, the fracture mechanics approach also enables the determination of the threshold stress intensity K_{th} below which a fatigue crack will not propagate. This fracture mechanics approach has been endorsed in BS: PD 6493 [27].

In order to apply the linear elastic fracture mechanics approach, it is necessary to know the initial flaw size, the load history and the stress intensity factor which describes the stress field around the crack tip. The growth rate of the flaw can then be determined from the knowledge of the range of stress intensity factor using the Paris law [28].

Paris proposed the following relationship:

$$da/dN = C (\Delta K)^m \quad (2.2)$$

This relationship is a semi-empirical attempt to fit experimental data with the stress intensity factor.

where:

da/dN is the crack growth rate (e.g. mm/cycle).

ΔK is the range of stress intensity factor occurring at the crack tip.

C , m are constants for a particular material and loading conditions and their values are determined experimentally.

For steel weld m is usually between 2.5 and 3.5 with a typical value being 3.

Values of C may be calculated from a relationship proposed by Gurney for behaviour of steel in air [29]:

$$C = 1.315 \times 10^{-4} (1/895)^m \quad (2.3)$$

The stress intensity factor range can be generally expressed as:

$$\Delta K = S f(a, g) \quad (2.4)$$

where S = nominal stress range

a = crack length

g = geometric related constants for the body.

substituting equation (2.4) into equation (2.2) yields:

$$f(a, g)^{-m} da = C (S)^m dN \quad (2.5)$$

Integrating this equation between the limits of the initial crack size a_i and the limiting crack size of a_f then:

$$N(S)^m C = \int_{a_i}^{a_f} f(a, g)^{-m} da \quad (2.6)$$

This equation provides a means to estimate the fatigue life of components if the S , a_i , a_f , C , m and the function (f) are known. It is also assumed that the fatigue behaviour of the component is totally a function of crack growth. Crack initiation is not considered here.

Further simplification of the above equation is done by expressing:

$$\int_{a_i}^{a_f} f(a, g)^{-m} da = I \quad (2.7)$$

Hence substituting back in equation (2.6) and rearranging to give the general expression

$$N = (S)^{-m} I / C \quad (2.8)$$

This equation is explored further and its application analysed for fillet welded joints of plates phase 1 and SHS members phase 2, 3.

S. J. Maddox [30,31] is one of the first investigators who carried out finite element analysis to model the non-load carrying transverse fillet welds in two dimensions to investigate the geometrical parameters effect on the stress intensity factors at the fillet weld toe position and the fatigue performance of these joints. Maddox postulated that the stress intensity factor for a crack at the toe of a welded joint could be derived from that for the corresponding crack in flat plate by multiplying the factor M_k , which takes into account the stress concentration effect of the weld.

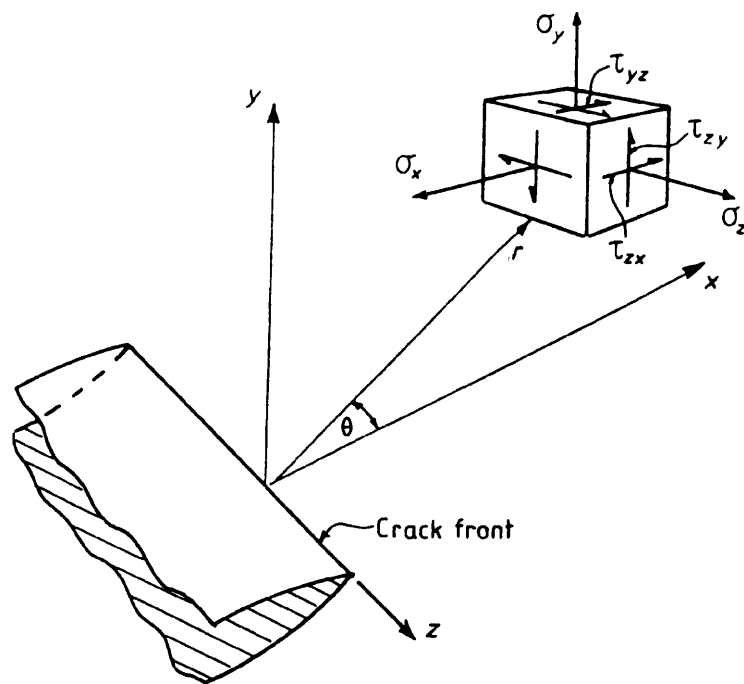
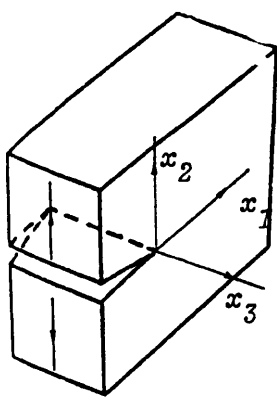
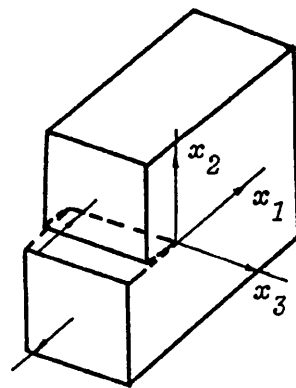


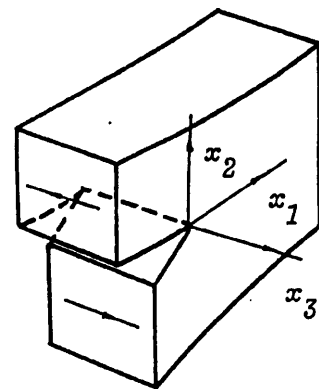
Fig. (2.1a). Crack Tip Stress Field Coordinates.



Mode I



Mode II



Mode III

Fig. (2.1b). Modes of Crack Growth.

CHAPTER THREE
THE FINITE ELEMENT METHOD

- 3.0. Introduction**
- 3.1. Formulation of Displacement Method**
- 3.2. Finite Element Package ABAQUS**
- 3.3. Structural Modelling**
- 3.4. Mesh Generation and the Phases of ABAQUS Calculation**
- 3.5. The Special Use of Crack Tip Elements**
- 3.6. Calculation of Stress Intensity Factors from F.E.
Analysis.**

CHAPTER THREE
THE FINITE ELEMENT METHOD

3.0. INTRODUCTION

The finite element method has in recent years emerged as a very powerful technique for general structural analysis. The method provides engineers with a versatile tool which has a very wide applicability. As a result the finite element method is now firmly established as a general numerical method to be used for obtaining solutions for complicated structures.

Developments in the field of computational hardware and the recent development of supercomputers have meant that problems which were previously not feasible because of large run times and large computational capacity requirements can now be contemplated.

Popularity of the finite element technique stems from the fact that complicated configurations can be handled through the discretization process of this method. Moreover, the technique can handle complex boundary conditions in homogeneity in material composition and mixed structures with relative ease. The basis of the method is to replace the continuum geometry by an assembly of structural elements, with each element connected at nodal points to adjacent

elements. Conditions of compatibility are satisfied at nodal points, and those of equilibrium by an energy minimisation procedure.

In this chapter a description of the finite element package ABAQUS which is used in this research is given and the phases of ABAQUS calculation are also outlined. The important aspect of applicability of the finite element method to fracture mechanics studies is discussed, together with the crack tip element used and the evaluation of stress intensity factors from the F.E. analysis.

3.1. FORMULATION OF DISPLACEMENT METHOD

The displacement method is used for the solution in the finite element package ABAQUS. A brief description of the formulation is described here.

The displacement of any point in an element is defined with respect to the displacement of the element nodes by:

$$U_i = [N] \{U\} \quad (3.1)$$

where $[N]$ represents the interpolation functions or shape functions.

The strains at an arbitrary point in the element can be obtained by taking the proper derivative of the displacement

field with respect to any chosen co-ordinate system. As a result the strain displacement relationship can be expressed in matrix form as:

$$\{\epsilon\} = [B] \{U\} \quad (3.2)$$

where $[B]$ is nodal co-ordinate dependent. Then the constitutive relation is formulated using the uniaxial stress strain curve of the material. For the elastic case it is defined as:

$$\{\sigma\} = [D] \{\epsilon\} \quad (3.3)$$

where $[D]$ is the matrix which defines the material property.

For a surface traction $\{T\}$ and a body force $\{F\}$, the work equivalent nodal Load P is:

$$P = \int_V [N]^T \{F\} dv - \int_S [N]^T \{T\} ds \quad (3.4)$$

Satisfying the equilibrium of the system and utilising the principle of virtual work, it can be shown that:

$$[K] \{U\} = \{P\} \quad (3.5)$$

where $[K]$ is the element stiffness matrix and is defined as:

$$[K] = \int [B]^T [D] [B] dv \quad (3.6)$$

Hence to summarise the solution, the stiffness, matrix of each individual element is first determined. This matrix relates each nodal force (a vector) to the nodal displacement (also a vector) via the element stiffness matrix defined above. Then at the structure level, all the element stiffness matrices and the equivalent nodal loads for those elements are combined into an overall assemblage stiffness matrix by proper superposition. Finally, the solution of the problem is by using the assemblage stiffness matrix with proper values of known boundary displacements and equivalent nodal loads to obtain unknown forces and displacements of active nodes.

If further one desires to evaluate stresses and strains at certain points within an element, the nodal displacements are then applied at the element level to find those stresses and strains.

3.2. FINITE ELEMENT PACKAGE ABAQUS

Finite element packages which handle elastic and elastic-plastic analysis are available. One of these, ABAQUS [50] has been used in this programme. The finite element package ABAQUS is a general purpose finite element program. The theoretical formulation is based on the finite element stiffness method. The program can handle one-two and three dimensional continuum models. The program is designed so that any combination of elements can be used in the same model, thus allowing very general modelling. This area of combining different element types involves careful consideration at the

boundaries of the different elements to ensure compatibility and maintain continuity. An example of combining shell elements with brick (solid) elements using transition elements is given, [51] also at UMIST.

Many material types can be used in ABAQUS and static and dynamic responses can be considered. The program also most importantly provides a fracture mechanics design evaluation capability including "Line spring" elements for modelling part-through cracks in shell and J-integral calculation by the differential stiffness method. The latter fracture mechanics facility is used in this research and the technique for J-integral evaluation is described in Chapter 4. Details of theoretical formulations are found in ref. [32].

3.3. STRUCTURAL MODELLING

The important parameters which influence the decisions on the manner of structural modelling are desirable accuracy and computational cost. The optimum level of combination of these parameters is achieved through understanding of the behaviour of selected elements, the manner of loading and the constraints applied.

An important aspect contributing to the accuracy of the finite element technique is the selection of the right type of element. A proper selection of element depends upon the expected behaviour of the structure in a given area under a prescribed load, one having the desired behavioural characteristics.

Efficiency in the use of the finite element method is achieved by using an optimum size of mesh with proper degrees of freedom at the nodes depending upon the behaviour of the structural response under consideration. It is desirable to have a finer mesh for accuracy, but there is the associated disadvantage of generating a larger number of nodes and degrees of freedom which results in higher computational costs. Ideally one should refine the mesh in areas where the stress gradient is sharp, like the regions surrounding a sudden discontinuity in the stress field. Hence careful modelling achieves more accurate results and makes the analysis more efficient.

3.4. MESH GENERATION AND THE PHASES OF ABAQUS CALCULATION

It is well recognised that in using finite element analysis considerable time is taken up by mesh generation and input data preparation. Preparation of input data consists of discretization of the given structure into a suitable mesh using well defined elements connected at node points. The node and element numbering and the tabulations of co-ordinates and incidences are the major portions of data preparation.

In the case of two dimensional structures the task of discretization is easier than that for three dimensional structures, as it is possible to draw an exact diagrammatic representation of the structure and retrieve the co-ordinates at the node points. However, when the structure is not only

three dimensional, but at the same time has the added complexity of curved surfaces as in the case of modelling fillet welded joints between SHS members which is the piece of work discussed in Chapter 5, discretization poses a formidable task. A manual attempt to achieve a solution would not only consume a long time, but also would be highly prone to error.

For the two-dimensional structure analysed in the first theoretical piece of work (phase 1) meshes were prepared manually. The meshes were designed to have a core, which embodied the weld root area, common to the wide range of meshes analysed and changing the surroundings of the core area to achieve the desired geometrical changes. Details of the 2-D modelling are found in Chapter 4.

For the second and third pieces of theoretical work which are aimed at modelling fillet welded connections between SHS members, access to FEMGEN (Finite Element Generator) and PREABAQUS (for data preparation in ABAQUS format) on the SERC PRIME at UMIST has enabled the otherwise formidable task of data preparation for the 3-D models designed to be speeded up considerably.

The full finite element analysis conducted using ABAQUS involved the execution of the ABAQUSP/ABAQUSM procedure pair. The phase in ABAQUS calculation are outlined in the Table (3.1).

3.5. THE SPECIAL USE OF CRACK TIP ELEMENTS

Crack tip stress field equations given in Chapter 2 show that at the crack tip a stress singularity of the form $1/\sqrt{r}$ exist for elastic materials. Consequently a displacement field of the form $r^{1/2}$ exists in the region of the crack tip. In second order elements (eight nodes quadrilaterals or twenty node bricks) used in the modelling of the joints analysed in phases 1, 2 and 3 a very appealing aspect can be used for crack problems, which is the $1/4$ point concept. These elements can have the elastic strain of the order $1/\sqrt{r}$ as the crack tip is approached, built into their formulation. The elements have to be focused on the crack tip, and the mid-side nodes on the edges radiating out from the crack tip are moved to one quarter of the distance from the crack tip to the other node on that edge, Fig. (3.1).

The use of these special elements is a method of handling the singularity present at the crack tip, in crack problems. However, despite the fact that stress intensity factor evaluation using J-integrated technique does not necessarily require crack tip elements, the use of those elements is recommended to be able to model the stress state at or near the crack tips more accurately for linear elastic materials.

Table 3.1 The Phases in ABAQUS Calculations

Procedure	Short Description	Detailed Description
Pre-	Read	All input scanned and interpreted for consistency in the preprocessor program.
ABAQUS	Data check.	Extensive input data checking and default values are inserted.
	Incremental generation	Applied to nodes and elements. The full co-ordinates and topological description of the complete mesh of elements are constructed.
	Pre-solution	The constraints on the House keeping problem are considered.
	Pre plotting*	Full or partial nodal plots with arbitrary view points.
	Element	The stiffness matrices of all elements are found and stored.
ABAQUS -M	Solution	The system equations are solved for displacements, temperatures or whatever happens to be the primary unknown in the problem tackled. The loading histories being divided into 'steps'. Each step subdivided into increments either by user control or automatically.
	by wave front solution algorithm	
	Stress	The stresses are found at node position and/or integration points.
	External File (Restart)*	Element or nodal results are written to a file to be used for post processing or segmental solution.
	Analysis* Plotting	Plotting of deformed geometry, contour plots of element quantities, etc.

*Optional

3.6. CALCULATION OF STRESS INTENSITY FACTORS FROM F.E.

ANALYSIS

The stress intensity factor is of fundamental importance in describing the severity of stresses at crack tips. Determining the stress intensity factors enables the study of fracture and fatigue behaviour of structures using linear elastic fracture mechanics principles.

The finite element technique is a powerful tool which can be used to determine the stress intensity factors. The techniques used for estimating stress intensity factors by the finite element method may be classified under two main headings.

a) Non-singular crack tip representation. This technique involves the use of a very high density of conventional elements around the crack tip. Stress intensity factors are then derived using equations described in chapter 2. For example the first mode stress intensity factor can be evaluated if the stress (σ_y) or displacement (v) at some small distance r from the crack tip are known hence:

$$\begin{aligned} K_I &= (2\pi r)^{1/2} \lim_{r \rightarrow 0} \sigma_y \\ K_I &= \lim_{r \rightarrow 0} E v / 4(1-\nu^2) (2\pi/r)^{1/2} \end{aligned} \quad (3.7)$$

Attempts aimed at reducing the requirement for large numbers of very small elements near the tip of cracks and consequently obviating the need to approach the crack include:

1) Employing the expression for strain energy release rate per unit thickness:

$$G = dU/da \quad (3.8)$$

by solving for a strain energy of the system, U , at a given crack length a and at a crack size $a + da$, the change in strain energy may be calculated. The stress intensity factor is then calculated using the expressions:

$$K_I = \begin{cases} (GE)^{1/2}, & \text{plane stress} \\ (GE/1-\nu^2)^{1/2}, & \text{plane strain} \end{cases} \quad (3.9)$$

2) Employing the concept of compliance, C . This technique is used by Frank [33] in his work using finite elements to study the fatigue behaviour of fillet welded cruciform joints. His work will be reviewed in detail in Chapter 4. The derivation of K based on compliance method can be reviewed briefly here.

For a cracked body having a crack of length a and acted upon by loads say for simplicity P_1 and P_2 , the displacement of the loading points is given by:

$$\begin{aligned} u_1 &= C_{11}P_1 + C_{12}P_2 = u_1^1 + u_1^2 \\ u_2 &= C_{22}P_2 + C_{21}P_1 = u_2^2 + u_2^1 \end{aligned} \quad (3.10)$$

where u_i is the displacement of P_i , u_i^j is the component of u_i caused by P_j , The term C_{ij} is the displacement coefficient (a function of crack length) which gives the displacement at i caused by a unit load at j . The reciprocal theorem gives:

$$C_{ij} = C_{ji} \quad (3.11)$$

Then the strain energy can be calculated from forces and displacements:

$$U|P_1 = 1/2 P_1 U_1 = 1/2 P_1 (C_{11}P_1 + C_{12}P_2) \quad (3.12)$$

$$U|P_2 = 1/2 P_2 U_2 = 1/2 P_2 (C_{22}P_2 + C_{21}P_1)$$

Then $G = dU/da|_{\text{fixed loads}}$

where U is the total strain energy, and hence using expressions equation 3.9 the stress intensity factor K_i can be calculated.

3. J-integrals based evaluation of stress intensity factor [34] involve the use of the equation:

$$J = \int_{\Gamma} (U dy - T \cdot du/dx ds) \quad (3.13)$$

where J is constant for any contour Γ surrounding the crack tip, U is the strain energy density, T the traction vector defined according to the outward normal along Γ , u is the

displacement vector and ds the arc length along Γ For linear elasticity K can be calculated by:

$$K = \begin{cases} (JE)^{1/2}, & \text{plane stress} \\ (JE/(1-\nu^2))^{1/2}, & \text{plane strain} \end{cases} \quad (3.14)$$

A procedure for evaluation of J-integral based on virtual crack extension method by Parks [35] is encoded in the finite element package - ABAQUS and will be discussed in Chapter 4.

b) Singular elements

The non-singular techniques described in a) above infer the crack tip singularity from information obtained remote from the tip. An alternative route is to try to model the singularity at the tip of the cracks.

Byskov [36] developed an element based on the Muskhelishvili [37] stress functions. Stress functions are built into the elements. The other technique is to modify a conventional eight-noded quadrilateral element or 20 node brick element to introduce a singularity of order $r^{-1/2}$. The latter technique which uses crack tip elements has been discussed earlier in Chapter 2.

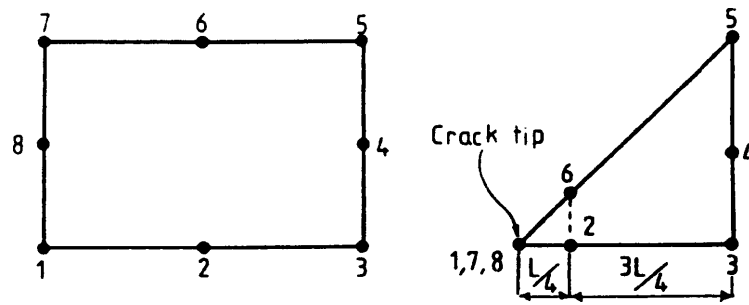


Fig. (3.1). Conventional Quadrilateral Isoparametric Element, and the Modified Element with $r^{-1/2}$ singularity.

CHAPTER FOUR

- 4.0. Introduction.**
- 4.1. Review of Research Into the Fatigue Behaviour of Transversally Loaded Fillet Welded Connections.**
- 4.2. J. Integral Technique.**
- 4.3. Assumptions Made in the Finite Element Analysis of Fillet Welded Curciform Joint.**
- 4.4. Modelling the Cruciform Fillet Welded Joint.**
- 4.5. Results of the Finite Element Analyses.**
- 4.6. Fatigue Life Estimation.**
- 4.7. Evaluation of the Integral I and the Construction of the S-N Family of Curves for Fatigue Design.**
- 4.8. Comparison of Theoretical Findings with Frank & Fisher Life Predictions and Code of Practice BS5400.**
- 4.9. Finite Element Investigation of the Influence of Misalignment on the Stress Intensity Factors.**
- 4.10. Finite Element Modelling of Misalignment.**
- 4.11. Results of the Finite Element Study.**
- 4.12. The Use of Interface Elements to Check Surface Contact.**

CHAPTER FOUR

THEORETICAL STUDY PHASE ONE

4.0. INTRODUCTION

The design rules which give the fatigue performance of various types of welded detail have been published and adopted for code usage. [1, 2]. These rules were arrived at by studying the results of a large number of experiments where welded joints were subjected to cyclic loads. Most of the welded joints were subjected to cyclic loads. Most of the welded joints studied were of a restricted range of plate thicknesses. Until recently, those classical S-N curves were the only design tool for predicting the fatigue life of welded joints. Since the early 1970s the discipline of linear elastic fracture mechanics has been applied to welded joints and has provided a more general method of life prediction [e.g. 30,31]. In the case of fillet welded joints where the welds are loaded perpendicular to the weld line and are regarded as load carrying, the code of practice [1] places them in class W where for a fatigue life of 2×10^6 cycles the stress range on the weld throat is limited to 43N/mm^2 for a 2.3% probability of failure.

In this chapter, the first phase of the theoretical investigations conducted in this research is reported. The piece of work described here, involved numerical studies of models of fillet welded cruciform joints Fig (4.1). The finite element method is used to study the effect of changes

in geometry of the fillet welded connection on the stress intensity factors at the fillet weld root and obtain the relationship between stress intensity factor, the size of the unpenetrated depth between the fillet welds, and the weld size and plate thicknesses.

The description of the J-Integral technique used to evaluate the stress intensity factors together with the outcome of the numerical study are preceded by a review of the previous work carried out in this area.

4.1. Review of Research into the Fatigue Behaviour of Transversally Loaded Fillet Welded Connections

Transverse load carrying fillet welded connections were investigated by Frank & Fisher [33]. They carried out a study into the fatigue behaviour of fillet welded cruciform joints stressed transversely to the weld line. The finite element method was used to determine a solution for stress intensity factors specifically for a crack at the root of fillet welds. They analysed the cruciform joint as a two dimensional stress problem using constant strain triangle (CST) elements. They solved the joint geometry for several cracks of slightly varying length and were able to obtain the compliance as a function of crack length. Numerical differentiation of this relationship with respect to crack length was related to the strain energy G :

$$G = P^2/2 \, dC/dA \quad (4.1)$$

where P is the applied load

dC/dA is the rate of change of compliance with crack area, where the compliance is defined as

$$C = \Delta/P \quad (4.2)$$

where Δ is the displacement of the loaded point.

For the predominantly mode I crack displacement assumed they then calculated the stress intensity factors using Irwin's expression [25].

$$\begin{aligned} G &= K_I^2/E, \text{ for plane stress} \\ &= K_I^2/E [1-\nu^2], \text{ for plane strain} \end{aligned} \quad (4.3)$$

The expression for the stress intensity factor for roots cracks calculated by Frank & Fisher [33] is:

$$K = \sigma_p / [1 + (2L/t_p) \{C_1 + C_2(a/W)\} \{\pi a \sec(\pi a/2W)\}]^{1/2} \quad (4.4)$$

where a , W , t_p are shown in Fig (4.2).

σ_p is the nominal stress in the loaded attachment plate.

The values of C1 and C2 for equal leg length fillet welds and main plate to attachment plate thickness ratio equal to unity were fitted by least squares to polynomials of L/tp. This yielded the following expressions:

$$\begin{aligned}
 C1 &= 0.05281 + 3.2872 (L/tp) - 4.3610 (L/tp)^2 + \\
 &\quad 3.6958 (L/tp)^3 - 1.8745 (L/tp)^4 + 0.4149 (L/tp)^5, \\
 C2 &= 0.2180 + 2.7173 (L/tp) - 10.171 (L/tp)^2 + \\
 &\quad 13.122 (L/tp)^3 - 7.7546(L/tp)^4 + 1.7827(L/tp)^5
 \end{aligned}
 \tag{4.5}$$

The expression for C1 and C2 are valid for values of L/tp between 0.20 and 1.20.

The Paris law was then used to estimate the fatigue life:

$$N = \sigma_p / c \int_{a_i}^{a_f} [(1+2L/tp)/(C1 + C2 a/W) (\pi a \sec \pi a / 2W)^{1/2}]^3 da
 \tag{4.6}$$

where ai and af are the initial and final crack sizes respectively.

The value of the numerical integration is plotted in Fig. (4.3).

Frank assumed that fatigue cracks of equal length would propagate from the root of each weld of the cruciform joint and that these cracks would grow parallel to the transverse main plate.

P.R. Ford [49] studied the fatigue strength of transverse load carrying fillet welds as a function of weld metal strength and flux type. He determined the S/N curves for the different weld metals. The crack growth rates were determined by sectioning a number of specimens at various stages of their cyclic life and also by measurement of the fatigue striation spacing in the transmission electron microscope.

From his study Ford concluded that fatigue strength of fillet welds is independent of weld metal strength level at cyclic lives approaching 2×10^6 cycles for root failure. Fig (4.4) shows a comparison of S/N curves for different strength weld metals with stresses permitted under different standards.

4.2. J - Integral Technique

Two basic approaches exist in general for the determination of stress intensity factors using the finite element method. One involves the use of conventional finite elements in the crack tip region, then because of the characteristic elastic square root singularity, it is necessary to use an indirect procedure such as extrapolation of a field parameter to the crack tip or an energy method to determine the stress intensity factors. An alternative to these indirect procedures involve direct embedding of the elastic singularity in the displacement function for the near tip elements.

The method used to calculate J-integrals encoded in the finite element package ABAQUS used in this research is based on the virtual crack extension method [35]. Its implementation does not require a second solution of a slightly different crack size. The program calculates the decrease in total potential energy of the loaded structure caused by an increase in the crack opening area. The virtual crack extension is interpolated from its value at crack front nodal position (see Fig. 4.5) using the same order of interpolation as used in the elements abutting the crack front. A set of equations are then formulated which relate the set of total potential energy changes caused by crack advance at each crack front nodal position to the J-integral values of the same crack front nodal positions, which can be solved for these nodal position values of J.

The path independence of the J-Integral may be used to estimate several values by moving the crack tip nodes or by moving all the nodes within some closed contour around the crack tip.

4.3. Assumptions Made in the Finite Element Analysis of Fillet Welded Cruciform Joint

The finite element models of the cruciform fillet welded joints were based on the following assumption:

1. Applied tensile stresses distribute themselves uniformly along the length of the four fillet welds.

2. The four welds connecting the two attachments are assumed identical in size.
3. A consequence of 1 and 2 above only quarter of the joint needs to be modelled, taking advantage of symmetry.
4. The unpenetrated depth between fillet welds could be modelled as a crack of size equal to the thickness of the attachments for the zero weld penetration assumed.

4.4. Modelling the Cruciform Fillet Welded Joint

The unpenetrated depth between the fillet welds forms a sudden discontinuity which disturbs the uniform flow of stress in the loaded attachment forcing the stress stream to change direction suddenly, and pass through the fillet weld.

Consequently the root of the fillet weld is of prime interest. The stress field at the root of the fillet weld is assumed singular.

To organise the modelling of the cruciform joint and because the models had to be prepared manually it was convenient to define two zones in the joint. The area zone one consisted of the elements surrounding the crack tip (root of the fillet weld) and parts of the attachment and central plate. Zone two consisted of the rest of the mesh. Special crack tip elements which are a modification of the conventional eight noded quadrilateral elements were used in the core area. One edge of the 8-noded quadrilaterals is collapsed and the mid side nodes of the two edges either side of the collapsed one are

shifted to the one-quarter position. Sixteen of these collapsed, degenerate elements were positioned around the crack tip. Figure (4.6) shows how these elements are positioned around the root of the fillet weld. The crack itself was modelled by two lines of nodal points immediately adjacent to each other but not connected. The spacing of the lines was arbitrary taken as .01mm and sloping linearly to zero at the fillet weld root position. Welds were modelled as equal leg length throughout.

An average of 250, 8-noded biquadratic, reduced integration plain strain elements were used in each mesh analysed. The element and the integration points are shown in Fig (4.7). The elements each have four integration points and sixteen degrees of freedom. As can be seen from Figs. (4.8 and 4.9) representing two typical meshes, the mesh in core region is generally fine. Also elements within the weld are quite small to accommodate the complex state of stress which exists. The meshes get coarser away from the root as the stress gradient diminishes.

The nodes at the top of the figures at the mid-thickness of the main plate were fixed in the vertical y-direction. The nodes at the mid-thickness of the attached plate were restrained in the horizontal direction, x-direction. The load was applied on the elements at the end of the attachment as a pressure load of severity 1 N/mm^2 uniformly distributed.

In a single run the program calculates the J-integral for three contours of elements surrounding the crack tip of the root of the fillet weld. The geometries analysed are shown in Table (4.1).

The meshes are capable of accommodating five contours around the crack tip, consequently five J-integral values were evaluated for selected meshes to demonstrate further the efficiency of the meshes and the technique which maintains to a high degree the contour independence feature.

4.5. Results of the Finite Element Analyses

The J-integrals calculated for the geometrical conditions described in Table (4.1) are averaged for the three contours and the resulting stress intensity factor for each geometry is calculated for linear elasticity using equation (3.14).

One standard expression for the stress intensity factor if finite boundary conditions are introduced for a strip of width W with a central crack of length $2a$ is the tangent finite width correction given as:

$$K = \sigma_p \sqrt{W \tan \pi a / W}$$

where

$$\sigma_p \text{ is the remote stress} \quad (4.7)$$

The stress intensity factors per unit remote stress in the attachment plates from the finite element analysis are normalised by the above tangent finite width correction.

A plot of the normalised stress intensity factor against the geometrical ratio a/W is shown Fig. (4.10). The parameter a is half the crack size. W is the width of the cruciform joint given as:

$$W = t_p + 1.4142L \quad (4.8)$$

where L is the fillet weld leg length
 t_p is the attachment thickness.

The variation of the normalised stress intensity factors is linear and can be expressed as:

$$K_{f.e}/K_{tan} = 2.8817(a/W) - 0.074 \quad (4.9)$$

This formula represents a simple means of calculating the stress intensity factors of the fillet weld root of a cruciform joint given the dimensions of the parts joined and the fillet weld leg length.

The stress intensity factors calculated from the J-Integrals obtained from the finite element study of the cruciform joint represented in a normalised form Fig. (4.10) are compared again normalised using the tangent finite width correction with the stress intensity factor estimated using CTOD equation Fig. (4.11.) The K_{CTOD} is:

$$K_{CTOD} = \delta E / \sqrt{4\pi r} \quad (4.10)$$

where δ is relative displacement of the crack faces with r chosen as .222 which is 25% of the crack tip element size. The values of stress intensity factors from K_{CTOD} are in good agreement with those calculated from J-Integrals.

For the purpose of studying the stress distribution in the cruciform joint specially in the root area much more closely a set of elements Fig (4.12) were defined in the post-processor FEMVIEW available at the SERC PRIME AT UMIST for model CR22 Fig (4.8).

Fig (4.13) shows the displaced shape of the model in the chosen area of interest. The dashed lines represent the original conditions before the application of a unit remote pressure. On closer examination the stress contours in the 16 crack tip elements show the state of stress more clearly Fig (4.14). The displaced shape representation, stress contours in y direction for model Fig (4.8) are also shown in Figs. (4.15, 4.16) respectively. Also for model Fig. (4.8) the displacement variation on the crack face against position inside the crack is shown Fig. (4.17). Zero being the crack tip position.

4.6. Fatigue Life Estimation

The method used in this research to estimate the fatigue life

of the cruciform joints analysed theoretically using the finite element method is based on the fracture mechanics analysis of cracks under fatigue loading.

This approach assumes that:

- a) The real cracks may be idealised as a sharp tipped cracks.
- b) The cracks propagate at a rate da/dN which is a function of the range of stress intensity factor ΔK .
- c) While the overall relationship between da/dN and ΔK is normally observed to be a sigmoidal curve in a $\log da/dN$ vs $\log \Delta K$ plot, for practical purposes, it is usually conservative and sufficiently accurate to assume that the central linear portion applies [PD6493] for all values of ΔK from ΔK_0 , (below which no significant crack growth will occur) up to failure.

The relevant equation is:

$$da/dN = C (\Delta K)^m \dots \quad (4.11)$$

where da/dN is the rate of crack propagation

c , m are constants which depend on the material and the applied conditions, including environment.

ΔK is the range of stress intensity factor corresponding to the applied stress, cycle and instantaneous crack size. For $\Delta K < \Delta K_0$, da/dN is assumed to be zero.

The data required for the fatigue life assessment is a relationship which describes the variation of stress intensity factor range with the structural geometrical parameters and the crack size.

For the cruciform joints analysed in this chapter, equation (4.9) provides the needed relationship of the stress intensity factor range required for fatigue life estimation at the joints which on substitution in equation (4.11) gives:

$$da/dN = C (\Delta\sigma_p \sqrt{(W \tan\pi a/W)} (2.8817(a/W) - 0.074))^m \quad (4.12)$$

The overall life is predicted by integrating this equation from an initial crack size a_i , to a final tolerance crack size a_f . The initial crack size $2a_i$ is assumed to be equal to the unpenetrated depth between the fillet welds, which is equal to half the attachment thickness for zero penetration. To calculate the tolerance crack size it is assumed that the crack will grow from an initial crack size to the tolerance crack size leaving a ligament of weld carrying a stress level equal to 400 N/mm^2 taken as the yield stress of the weld metal. hence the tolerance crack size is calculated as follows:

$$2a_f = W - 2 \Delta w \quad (4.13)$$

where w is the remaining ligament size defined as

$$2\Delta w = F/\sigma_{wl} \quad (4.14)$$

σ_{wl} is the limiting stress in the weld = 400 N/mm²

F is the applied load = $p \times$ thickness of attachment
substituting back in equation (4.3) gives:

$$2a_f = W - \sigma_p (2a_i/\sigma_{wl}) \quad [4.15]$$

This equation defines the tolerance crack size in terms of the limiting stress in the weld, nominal stress in the attachment and the width of the joint W . Equation (4.15), above defines an absolute tolerance and initial crack sizes, it is better expressed generally as:

$$a_f/W = 0.5 - \frac{\text{nominal stress applied}}{\text{tolerance weld stress}} (a_i/W) \quad (4.16)$$

The normal stress in the attachment plate can be converted to stress on the fillet weld throat for design purposes, thus:

$$\sigma_p = \sqrt{2} \sigma_w \cdot L/t_p \quad (4.17)$$

where σ_w is the stress on the weld throat.

The fatigue life of fillet welded cruciform joints analysed can be evaluated by integrating the crack propagation law, thus substituting for ΔK obtained theoretically from the

finite element analysis in equation (4.1) gives equation (4.17) which is re-arranged here to give:

$$W d(a/W) / ((\tan \pi a/W)^{m/2} (2.8817a/W - 0.074)^m (W)^{m/2}) = C (\Delta \sigma_p)^m dN \quad (4.18)$$

Further rearranging the equation above to give:

$$d(a/W) / ((\tan \pi a/W)^{3/2} (2.8817(a/W) - 0.074)^3) = C (\Delta \sigma_p)^3 \sqrt{W} dN \quad (4.19)$$

Integrating this equation between the limits calculated earlier, i.e. a_i/W , a_f/W to give:

$$\int_{a_i/W}^{a_f/W} d(a/W) / ((\tan \pi a/W)^{3/2} (2.8817(a/W) - 0.074)^3) = I = C (\Delta \sigma_p)^3 \sqrt{W} dN \quad (4.20)$$

where I is the fatigue life integral, thus the fatigue life N is given as:

$$N = I / C (\Delta \sigma_p)^3 \sqrt{W} \quad (4.21)$$

This equation is similar to the S-N equation, but the method of presentation is superior because of the greater number of relevant parameters involved.

For the purpose of this work the following constants are assumed

$$C = 2.0 \times 10^{-13}, m = 3.0 \quad (4.22)$$

The above equation will give the fatigue life N_i for the joint for a given applied stress range i . To find the fatigue strength N_j for some other stress range j we can use the relationship:

$$(\Delta\sigma_{ip})^m N_i = (\Delta\sigma_{jp})^m N_j \quad (4.23)$$

$\Delta\sigma_{(i,j)p}$ is the applied stress range on the attachment plate which can be converted to stress range on the fillet weld throat.

4.7. Evaluation of the Integral I and the Construction of the S-N Family of Curves for Fatigue Design

The approach used to evaluate the integral equation (4.19) is to divide the range from the initial crack ratio (a_i/W) to the final crack ratio (a_f/W) into very small increments and summing the contributions from each increment. The procedure is performed by the computer, and Simpson's rule was used to evaluate the integral for a large number of increments (= 2000).

The area is evaluated for ratios of L/t_p from 0.1 to 1.2 and stress ranges on fillet weld throats, 20 N/mm^2 to 160 N/mm^2 . The fatigue life integral is plotted in Fig (4.18), the

effect of stress range on a_f is small and the integral is given by the equation:

$$I = 0.43481 (L/t_p)^{2.6158} \quad (4.24)$$

The fatigue life for each joint was then calculated using equation 4.20 and the design family of S-N curves were constructed for the geometrical ratios L/t_p from .1 to 1.2, Figures (4.19 to 4.21) represent the families of curves for attachment sizes 12 mm, 25mm, and 50mm respectively.

4.8 Comparison of Theoretical Findings with Frank & Fisher

Life Predictions and Code of Practice BS5400

In this section the fatigue life estimates for the cruciform fillet welded joints of Frank are compared with the authors. For the selected attachment size thicknesses 12, 25, 50mm the Frank's integrals are calculated and the fatigue lives predicted are plotted figures (4.22 to 4.24).

Both the authors and Franks predictions are compared with Class W, BS5400 which is the recommended design curve for transversely loaded fillet welded joints. Overlaid transparencies for the three attachment sizes, 12mm, 25mm and 50mm. The three code of practice curves are the mean, mean-1 and mean-2 standard deviations. The theoretical results reasonably agree with Class W, BS5400 and with Fishers & Franks predictions. Further discussion of the findings is given in Chapter 8.

4.9 . Finite Element Investigation of the Influence of Misalignment On the Stress Intensity Factors

The effect of misalignment on the stress intensity factors at the fillet weld root of the cruciform joint analysed earlier is investigated here using the finite element method.

Misalignment would alter the stress distribution within the joint and hence the stress intensity factors of the growing cracks. In an axially loaded joint misalignment introduces secondary bending stresses with the result that the total stress range near the joint is increased.

Two techniques are available:

- a) The bending stress due to misalignment is used directly in conjunction with the appropriate design S-N curve for the aligned joint. The effective stress range applied is then the sum of the applied axial stress and the secondary bending stress due to misalignment.
- b) The secondary stresses introduced by misalignment can be used in a fracture mechanics assessment of a misaligned joint having a crack.

In the case of the fillet welded cruciform joints analysed in this research the effect of misalignment is assessed with respect to throat failure based on the stress intensity factor at the fillet weld root. The finite element method is used again to evaluate the needed stress intensity factors

which in turn will be used in a fracture mechanics assessment to quantify the effects of misalignment.

4.10. Finite Element Modelling of Misalignment

Half the cruciform fillet welded joint was modelled using high order 8-noded isoparametric quadrilateral elements. Again as in section (4.4), a cluster of sixteen crack tip elements focused on the crack tip were used at each fillet weld root position.

Twenty-two meshes were analysed to investigate the influence of geometrical parameters on the stress intensity factor at the fillet weld roots under conditions which simulate the presence of misalignment in the joint. The geometrical conditions analysed are given in Table (4.2).

The boundary conditions were such that the nodes on the middle section of the main plate were restrained in x and y directions. The nodes at the end of the attachment were translated horizontally by an arbitrary chosen lateral displacement of 0.005mm to induce bending moments in the attachment. The translated nodes were also restrained from movement in the y-direction thus simulating the testing machine jaws clamping action. Typical mesh is shown Fig (4.25).

4.11. Results of the Finite Element Study

J-contour integrals were evaluated for three contours surrounding the crack tips. The stress intensity factors were then calculated from the J-integrals using equation (3.14). The values calculated for stress intensity factors were per unit outerfibre remote stress.

The resulting stress intensity factors per unit remote stress (compression and tension side) were again normalised using finite width correction equation and were plotted against the geometrical ratio a/W in Fig (4.26). The relationship is represented by the equation:

$$K_{f.e}/K_{tan} = 0.368(a/W) + 0.0461 \quad (4.24)$$

The results of the evaluated stress intensity factors obtained from J-integrals are compared with estimates of K using the basic equation for CTOD given as:

$$K_{ctod} = \delta E \pi / \sqrt{2\pi r} \quad (4.25)$$

where

δ is the relative displacement of the crack faces at the node position r away from the tip to the inside of the crack.

E is the modulus of elasticity taken as $2.1 \times 10^5 \text{ N/mm}^2$

The resulting stress intensity factors for the meshes analysed are plotted against ratio a/W and compared with J-Integrals values in Fig. (4.27) which confirm the accuracy of the finite element stress intensity factor evaluation.

Models AL16 to AL22 were analysed to investigate the effect of the gap between the fillet welds. The gap size geometry was as described in section 4.10 and the maximum crack faces spacing was varied from, .03 to .3mm, Table (4.2).

The stress intensity factors per unit remote stress for the models AL16 to AL22 are plotted against gap sizes Fig. (4.28). The gap size has little effect on the stress intensity factors at the fillet weld root.

To calculate the influence of alignment on the fatigue life the misalignment stress intensity factors must be added to those of the aligned joint. The effective stress intensity factor should then be used in Paris law.

4.12. The Use of Interface Elements to Check Surface Contact

In this section special elements were used in the gap area of the cruciform fillet welded joint. These elements were placed between the two surfaces of the gap to investigate, especially in the compression region, the possibility of contact.

These interface elements are made up of corresponding nodes on each of the gap surfaces. The boundary conditions (contact or not) are monitored by measuring the relative positions of the two surfaces in the normal direction in terms of a strain means.

$$\epsilon = (X_A - X_B) \cdot n \quad (4.25)$$

When the surfaces are sensed to be in contact, Lagrange multipliers are used to constrain the strain to be zero. The signs of the Lagrange multiplier which gives the pressure between the surfaces are monitored by the program to check for subsequent surface separation.

The interface elements were incorporated in one of the models analysed earlier AL9. The results obtained from the analyses indicate that there is contact between the surfaces of the gap very close to the root position on the compression side.

The contact on the compression side had no effect on the stress intensity factor evaluated from the J-integrals on the tension side, but on the compression side the effect is very evident. The J-integral values estimated for the three contours surrounding the crack tip at the compression side were found to be contour dependent. The reason for losing the contour independence status is that the numerical technique employed for the estimation of the J-integrals is

fundamentally based on crack surfaces being traction free (the technique encoded in ABAQUS). It is possible, however, to account for tractions on the crack surfaces if they exist by adding an extra term to the J-integral equation. This term is not included in ABAQUS code.

A consequence of closure on the compression side would be that the stress intensity factors are not damaging, but many factors control the degree of damage which must be considered like the residual stresses present in welded joints.

TABLE 4.1: GEOMETRICAL CONDITIONS STUDIED (CRUCIFORM JOINT)

CASE	Att tp/2 plate	BASE T/2 plate	WELD LEG LENGTH
CR1	7.5	25	5
CR2	7.5	30	5
CR3	7.5	30	7.5
CR4	7.5	30	10
CR5	10	10	7.5
CR6	10	15	5
CR7	10	15	7.5
CR8	12.5	10	7.5
CR9	12.5	15	5
CR10	12.5	15	7.5
CR11	15	15	5
CR12	15	15	7.5
CR13	15	15	10
CR14	15	30	5
CR15	15	30	7.5
CR16	15	30	10
CR17	15	25	7.5
CR18	22.5	30	10
CR19	22.5	30	15
CR20	22.5	30	20
CR21	30	30	10
CR22	30	30	15
CR23	30	30	20
CR24	45	30	7.5
CR25	45	30	10
CR26	45	30	15
CR27	45	45	7.5
CR28	45	45	10

Table4.2: Geometrical Conditions Analysed (Misalignments)

Case	Att plate size	Base plate size	Weld Leg Length	Gap
AL1	12	50	5	.01
AL2	20	50	5	.01
AL3	25	50	5	.01
AL4	40	50	5	.01
AL5	50	50	5	.01
AL6	25	50	8	.01
AL7	25	50	10	.01
AL8	25	50	12	.01
AL9	50	50	8	.01
AL10	50	50	10	.01
AL11	50	50	12	.01
AL12	50	50	15	.01
AL13	25	25	5	.01
AL14	25	30	5	.01
AL15	25	40	5	.01
AL16	25	50	5	0.03
AL17	25	50	5	0.05
AL18	25	50	5	0.1
AL19	25	50	5	0.15
AL20	25	50	5	0.2
AL21	25	50	5	0.25
AL22	25	50	5	0.30

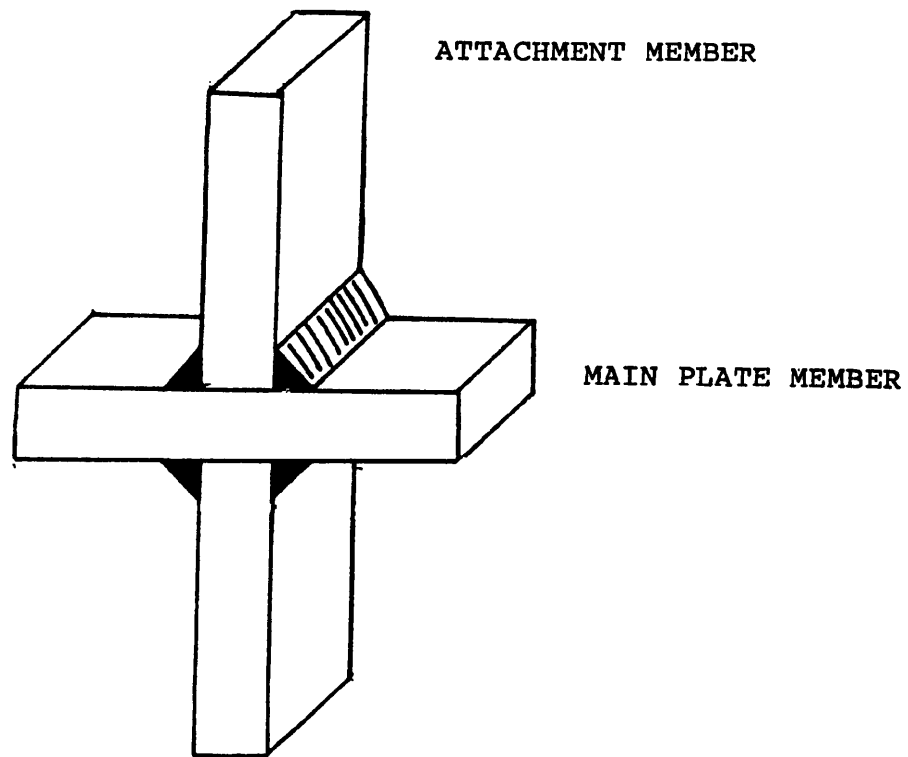


Fig. (4.1). Cruciform Fillet Welded Joint.

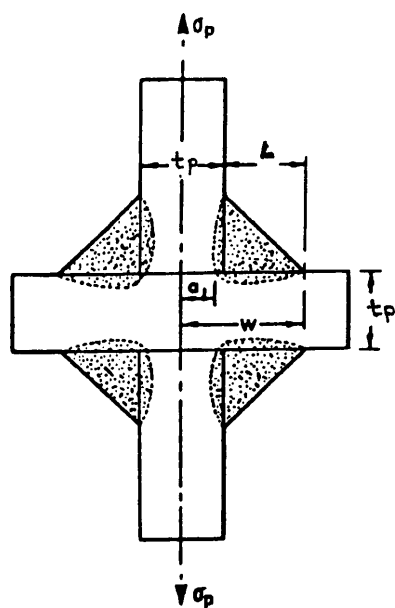


Fig. (4.2). Cruciform Joint Geometrical Parameters^{ref 33 definitions}

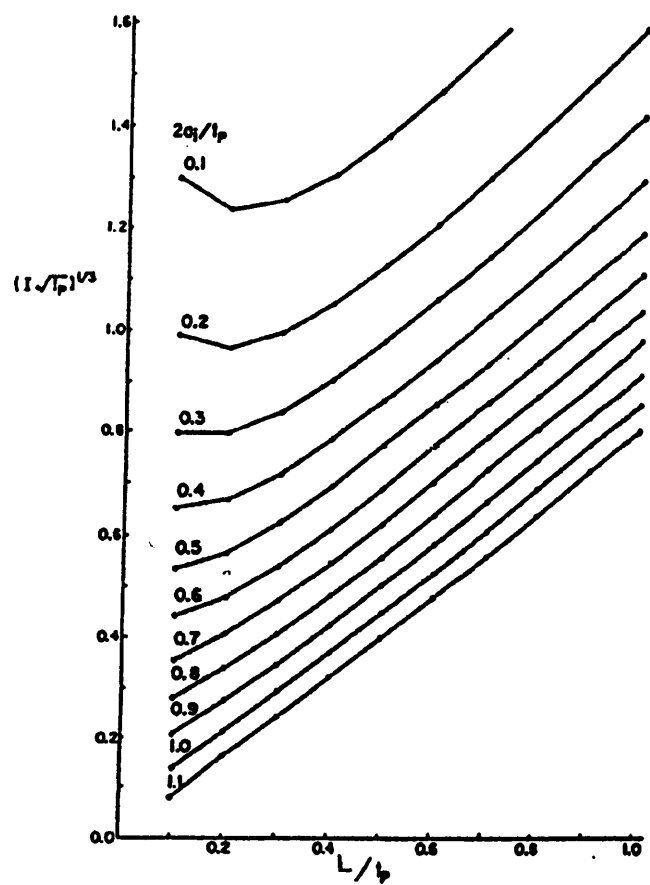


Fig. (4.3). The Fatigue Life Integral [33].

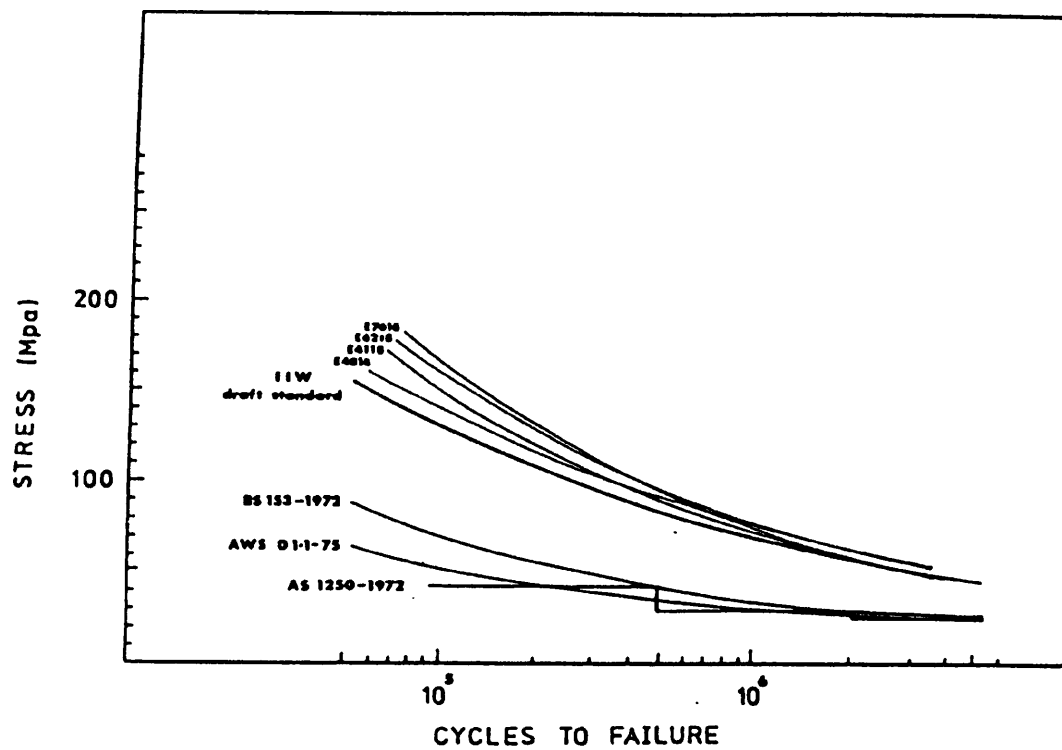


Fig. (4.4). Comparison of S/N Curves for Different Strength Weld Metals with Stresses Permitted Under Different Standards. [49]

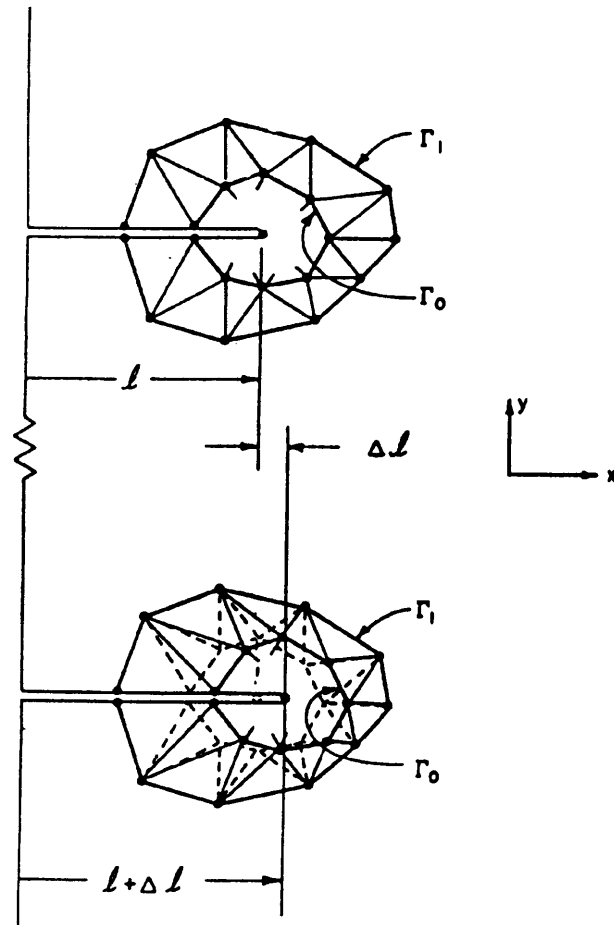


Fig. (4.5). Accommodation of Crack Extension by Advancing Nodes. [35]

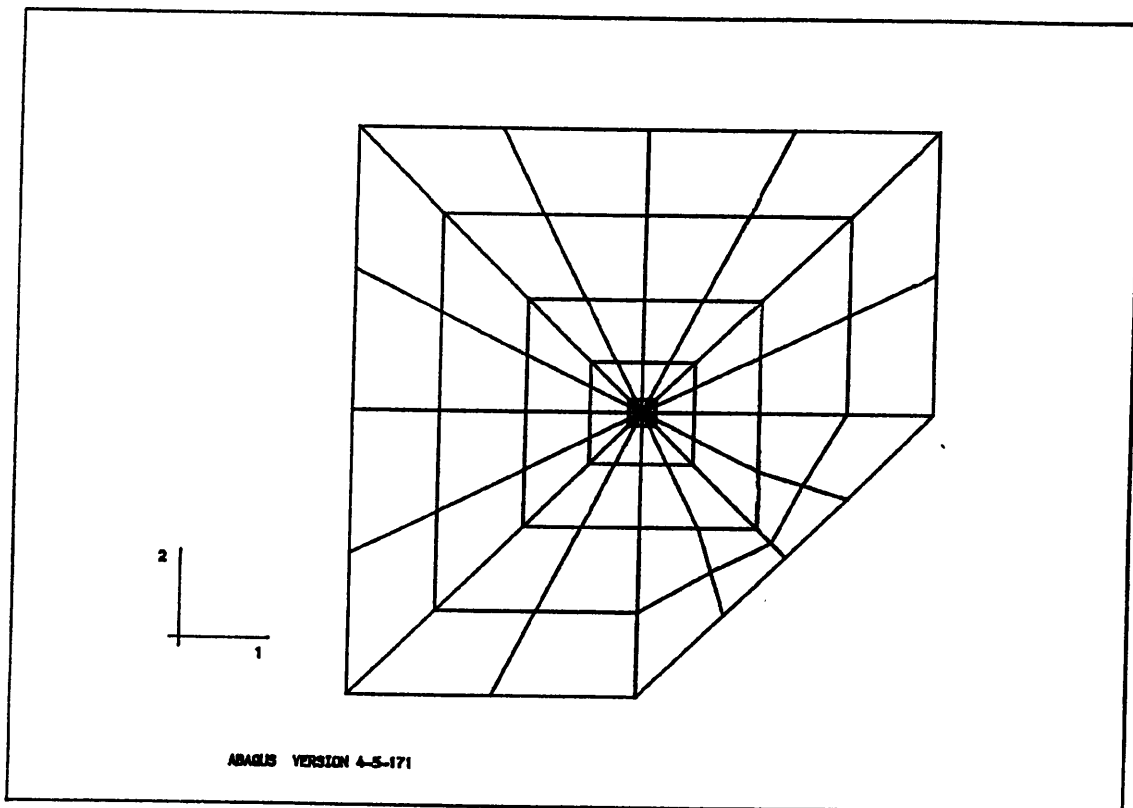


Fig. (4.6). Finite Element Mesh Around the Root Showing the Cluster of 16 Crack Tip Elements.

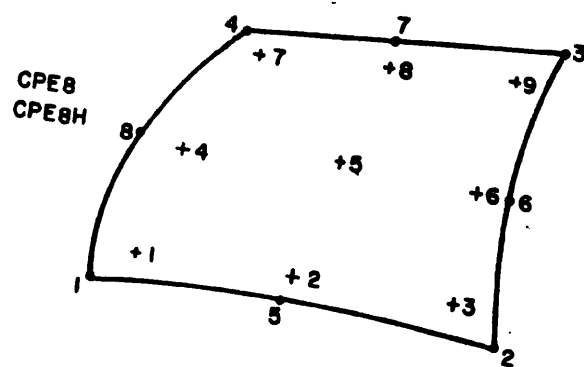
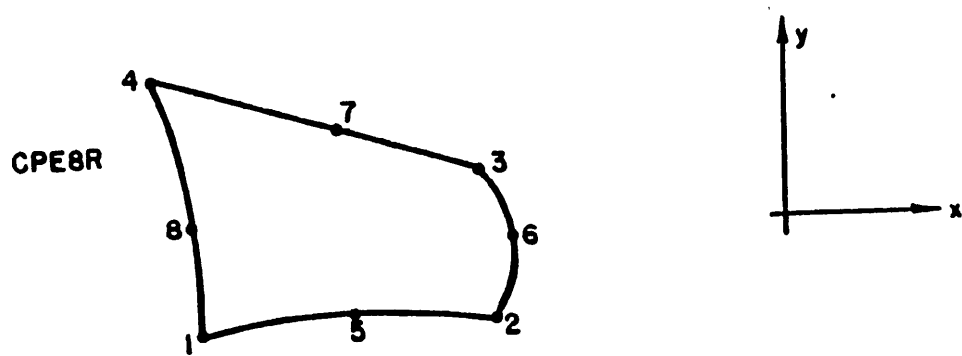


Fig. (4.7). Element CPE8R and Integration Points [45]

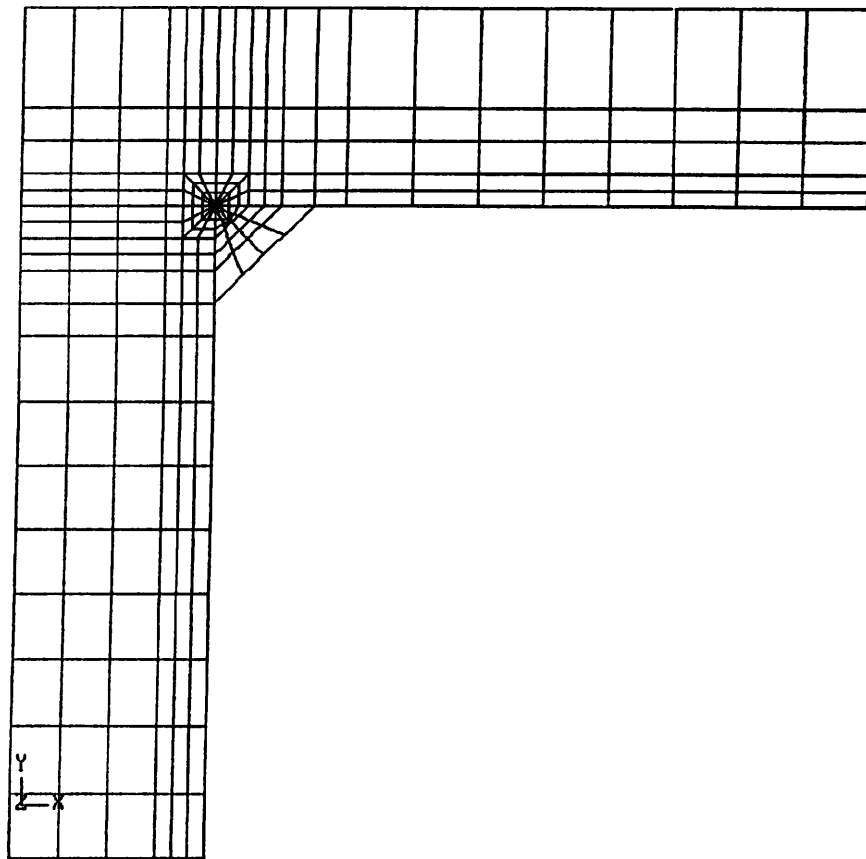


Fig. (4.8). Typical Finite Element Mesh for Cruciform Fillet Welded Joint.

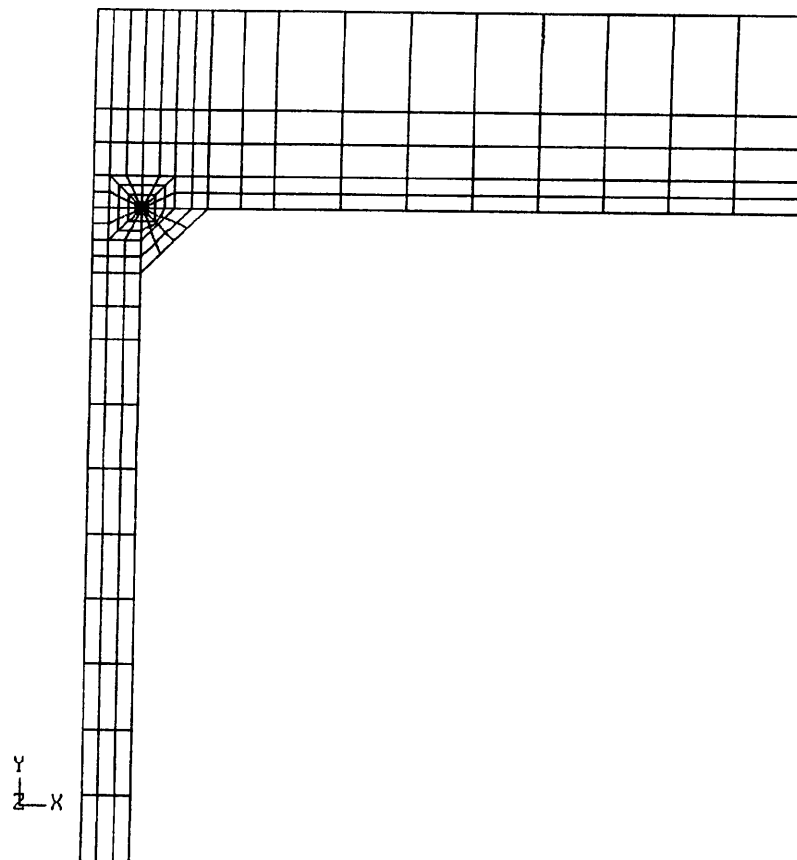


Fig. (4.9). Finite Element Mesh of Cruciform Welded Joint.

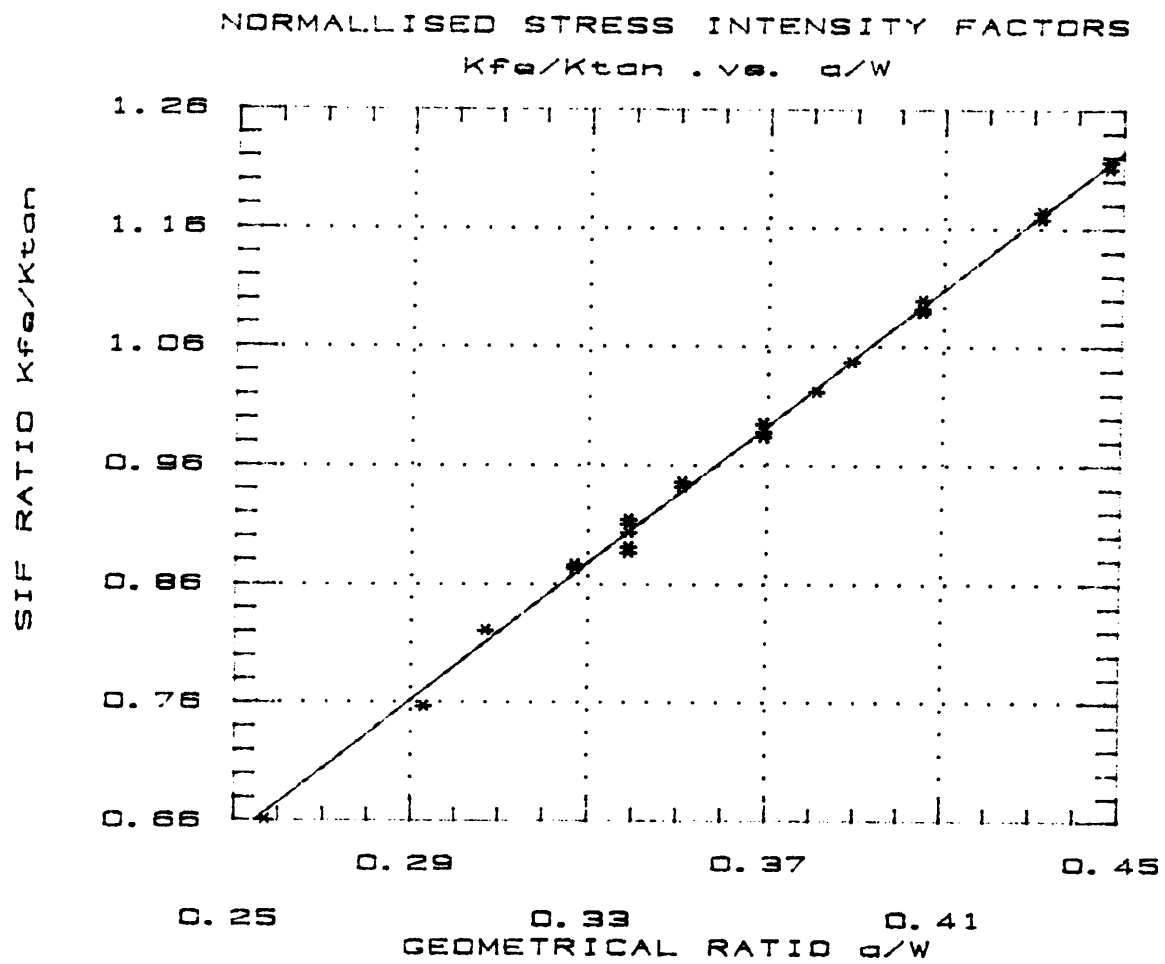


Fig. (4.10). Normalised Stress Intensity Factor vs. Geometrical Ratio a/W .

NORMALISED $KFe(J-INTGRAL)$ VS. NORMALISED $Kctod$ AGAINST RATIO α/W

$\times 10^{-2}$

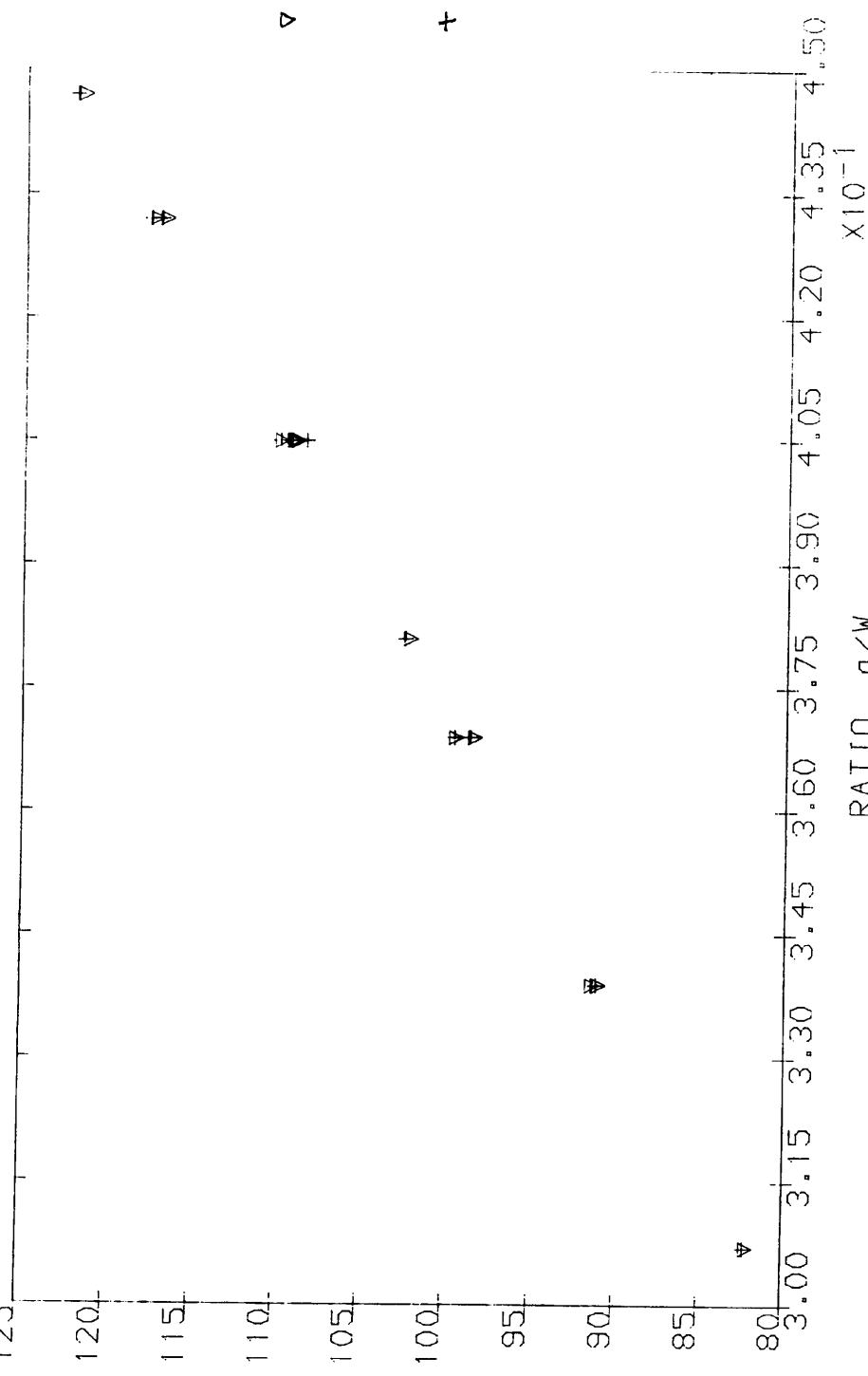


Fig (4.11)

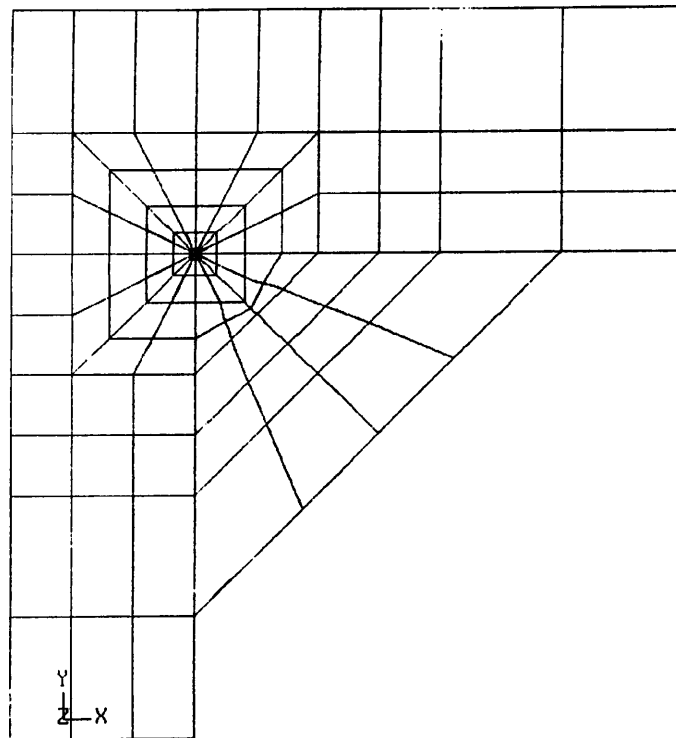


Fig. (4.12). The Finite Elemenet Set Defined for Displaying Stress and Displaced Shapes.

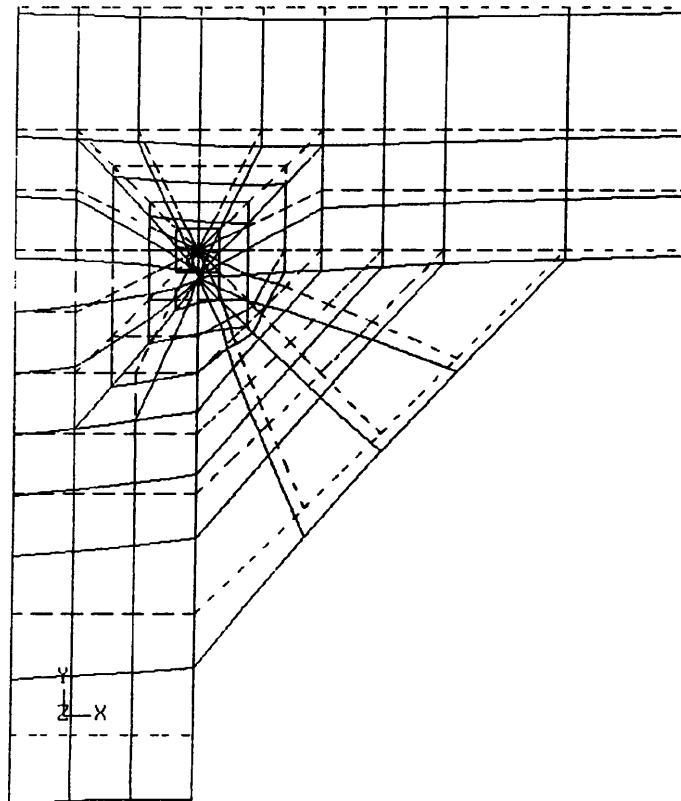


Fig. (4.13). Displaced Shape of Finite Element Model.

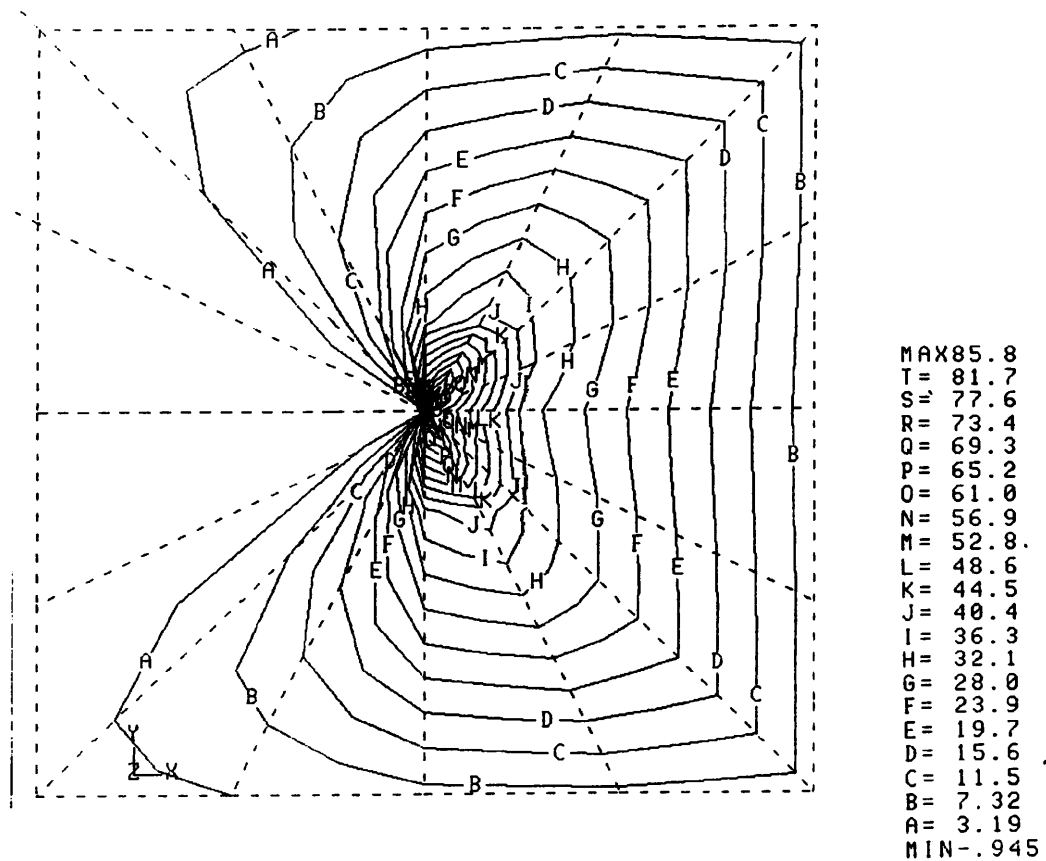


Fig. (4.14). Stress Contours in Y-draft in the Cluster of Crack Tip Elements Model CR22.

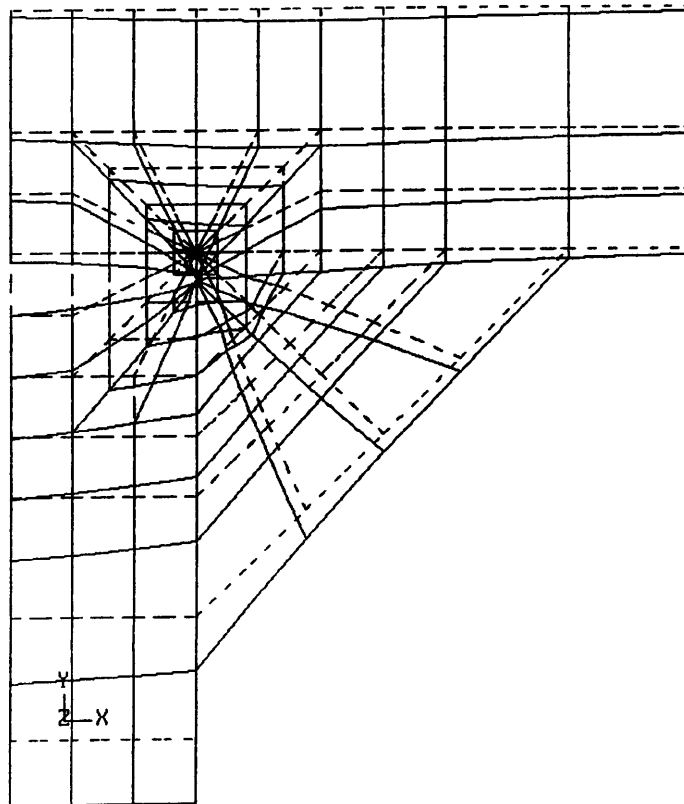


Fig. (4.15). Displaced Shape of Finite Element Model.

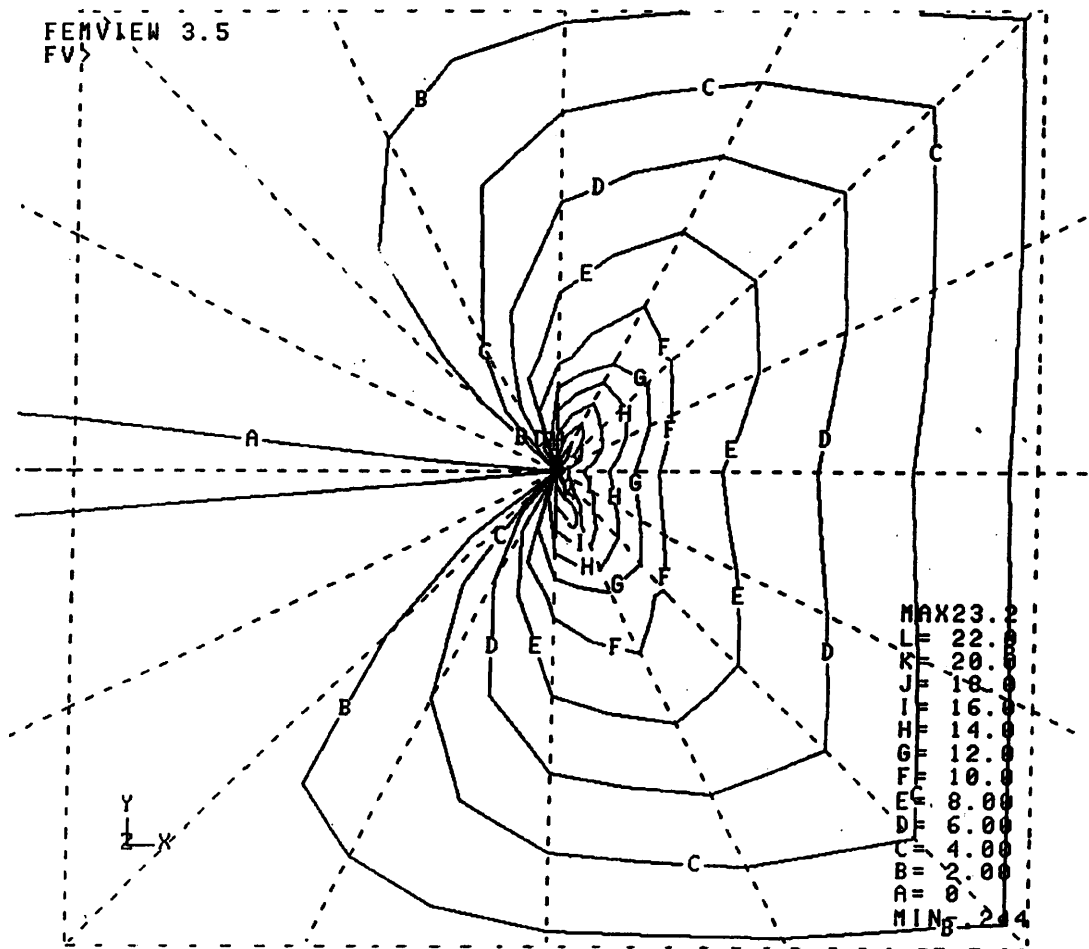


Fig. (4.16). Stress Contours in the Y Direction In the Cluster of Crack Tip Elements.

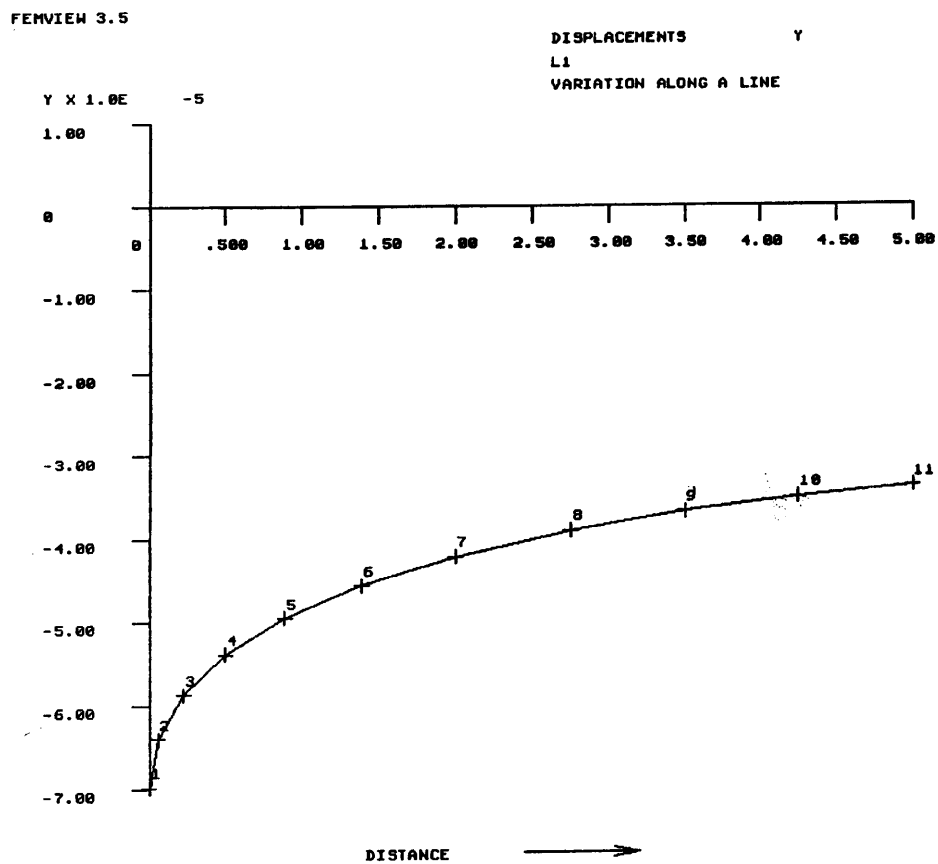


Fig. (4.17). Displacement Variation on the Crack Face Against Position Inside the Crack.

FATIGUE LIFE INTEGRAL VS. RATIO L/t_p

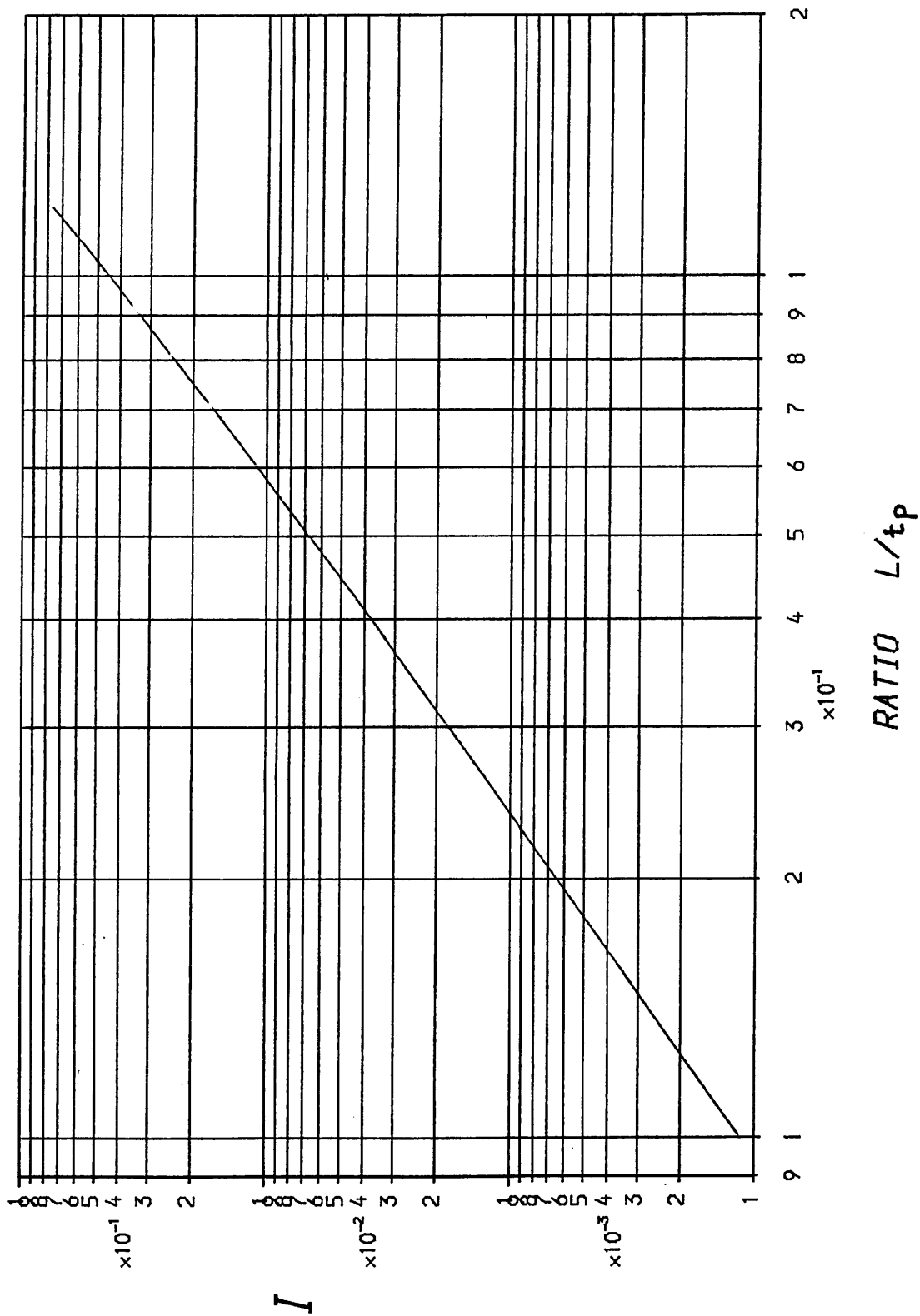
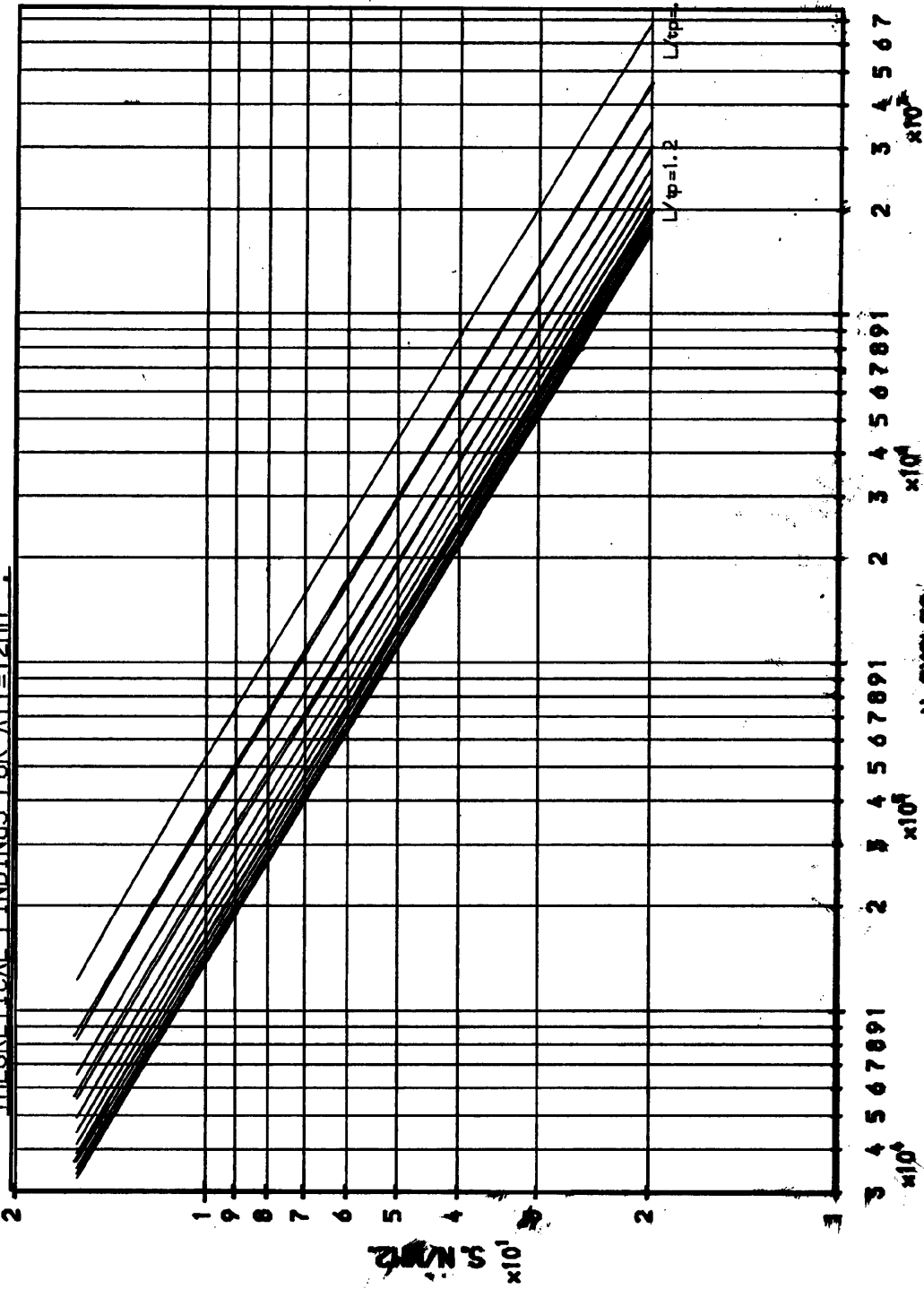


Fig (4.18)

JOINT CLASSIFICATION BS5400 PT. 10 CLASS W LOAD CARRYING WELD METAL

WELD STRESS RANGE, VS. ENDURANCE, N.,

THEORETICAL FINDINGS FOR AIT=12MM



CLASS. W.

WELD METAL IN LOAD-CARRYING

JOINTS MADE WITH FILLET OR

PARTIAL PENETRATION WELDS

BASED ON NOMINAL SHEAR

STRESS ON THE MIN. THROAT



RATIO L/tp VARIES FROM .1

TO 1.2 IN INCREMENT OF .1

MEAN

MEAN-1SD

MEAN-2SD

N-CYCLES

Fig-4.19-

JOINT CLASSIFICATION BS5400 PT. 10 CLASS W
LOAD CARRYING WELD METAL
WELD STRESS RANGE, VS. ENDURANCE, N..

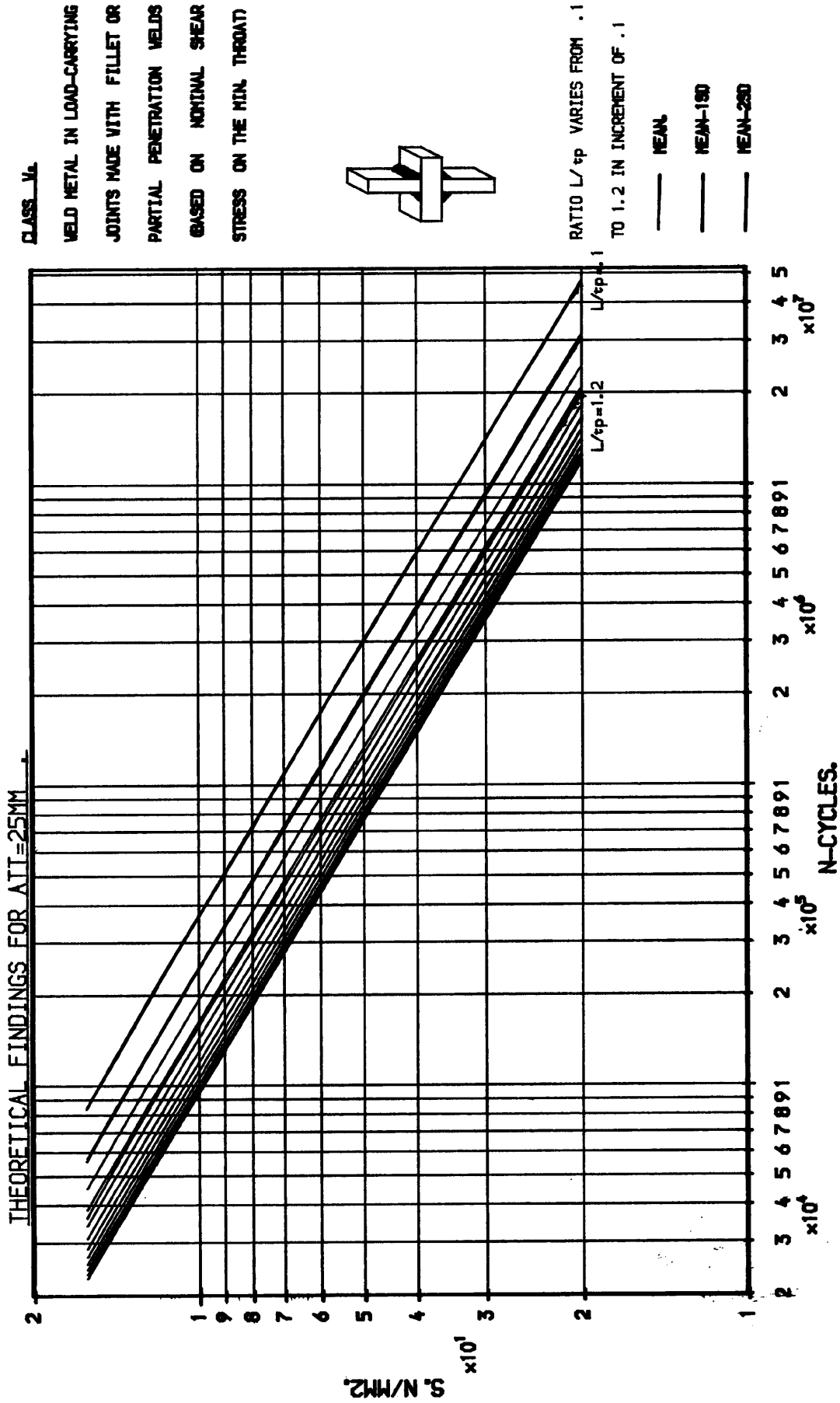
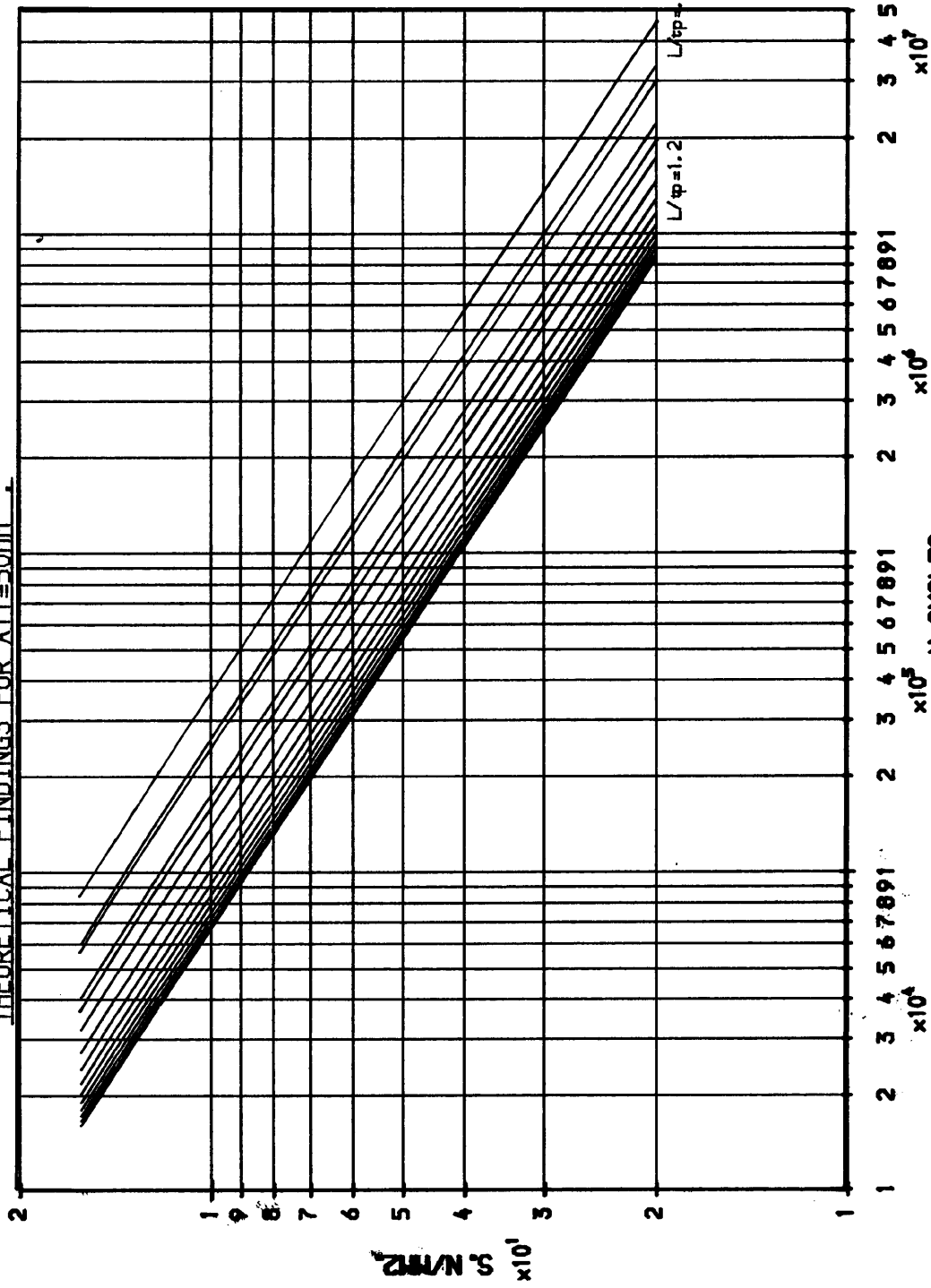


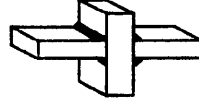
Fig - 4. 20 -

JOINT CLASSIFICATION BS5400 PT. 10 CLASS W
LOAD CARRYING WELD METAL
WELD STRESS RANGE VS. ENDURANCE. N..

THEORETICAL FINDINGS FOR $A_{T1}=50MM$



CLASS W
 WELD METAL IN LOAD-CARRYING
 JOINTS MADE WITH FILLET OR
 PARTIAL PENETRATION WELDS
 BASED ON NOMINAL SHEAR
 STRESS ON THE MIN. THROAT



RATIO L/tp VARIES FROM .1
 TO 1.2 IN INCREMENT OF .1

— MEAN
 — MEAN-1SD
 — MEAN-2SD

N-CYCLES.

Fig. 4. 21 -

JOINT CLASSIFICATION BS5400 PT. 10 CLASS W
LOAD CARRYING WELD METAL
WELD STRESS RANGE, VS. ENDURANCE, N.

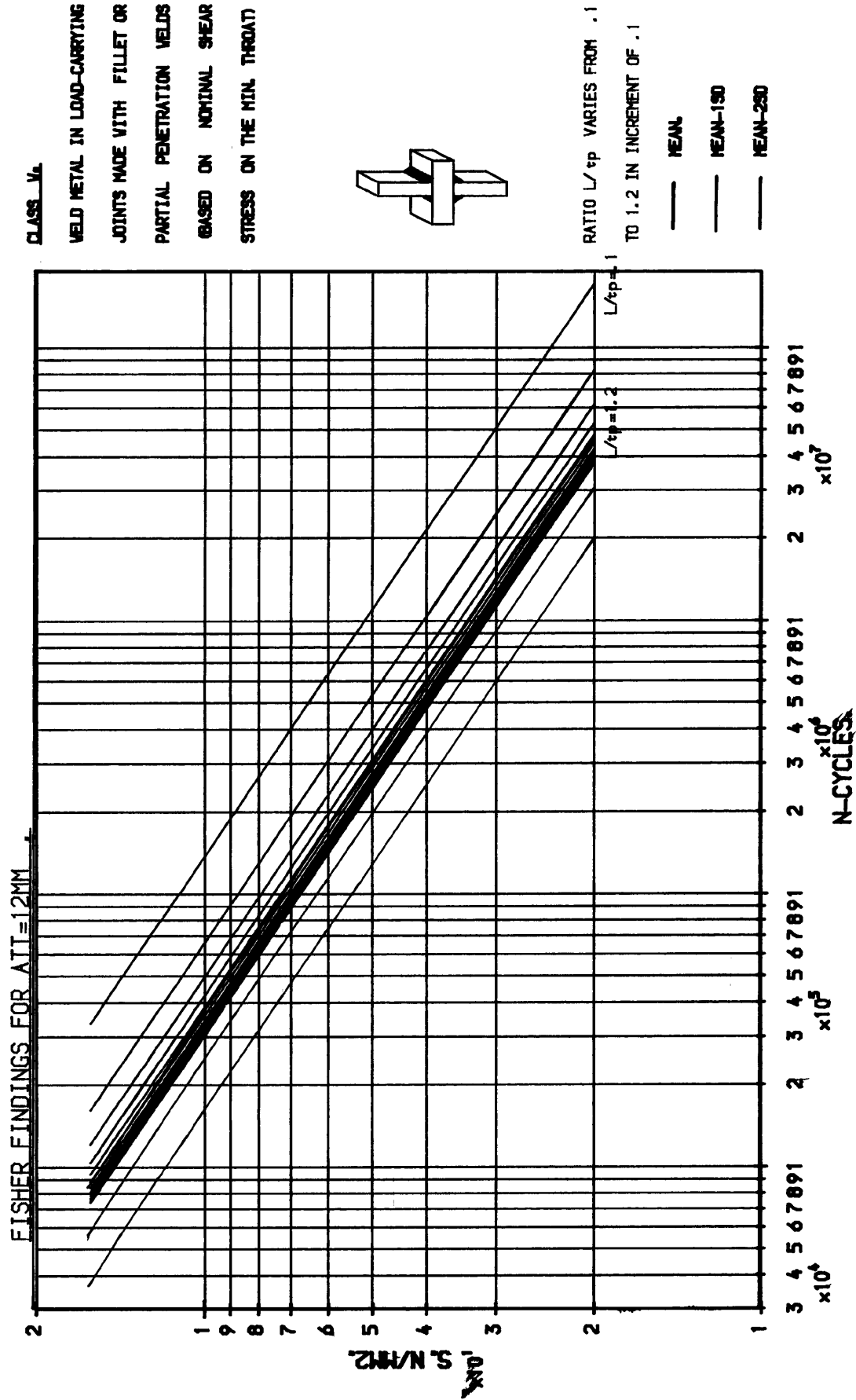


Fig - 4.22 -

JOINT CLASSIFICATION BS5400 PT. 10 CLASS W LOAD CARRYING WELD METAL

WELD STRESS RANGE VS. ENDURANCE, N..

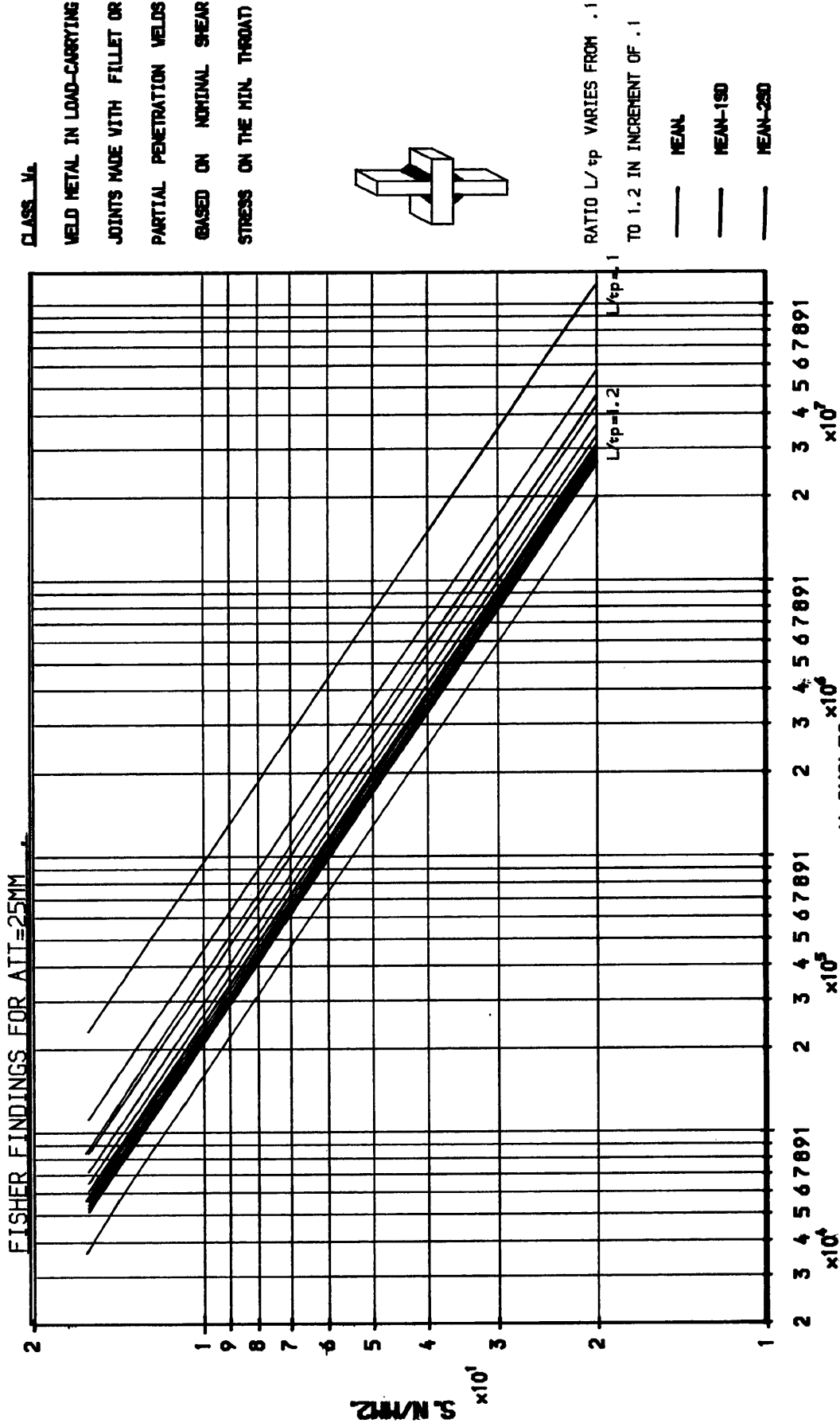
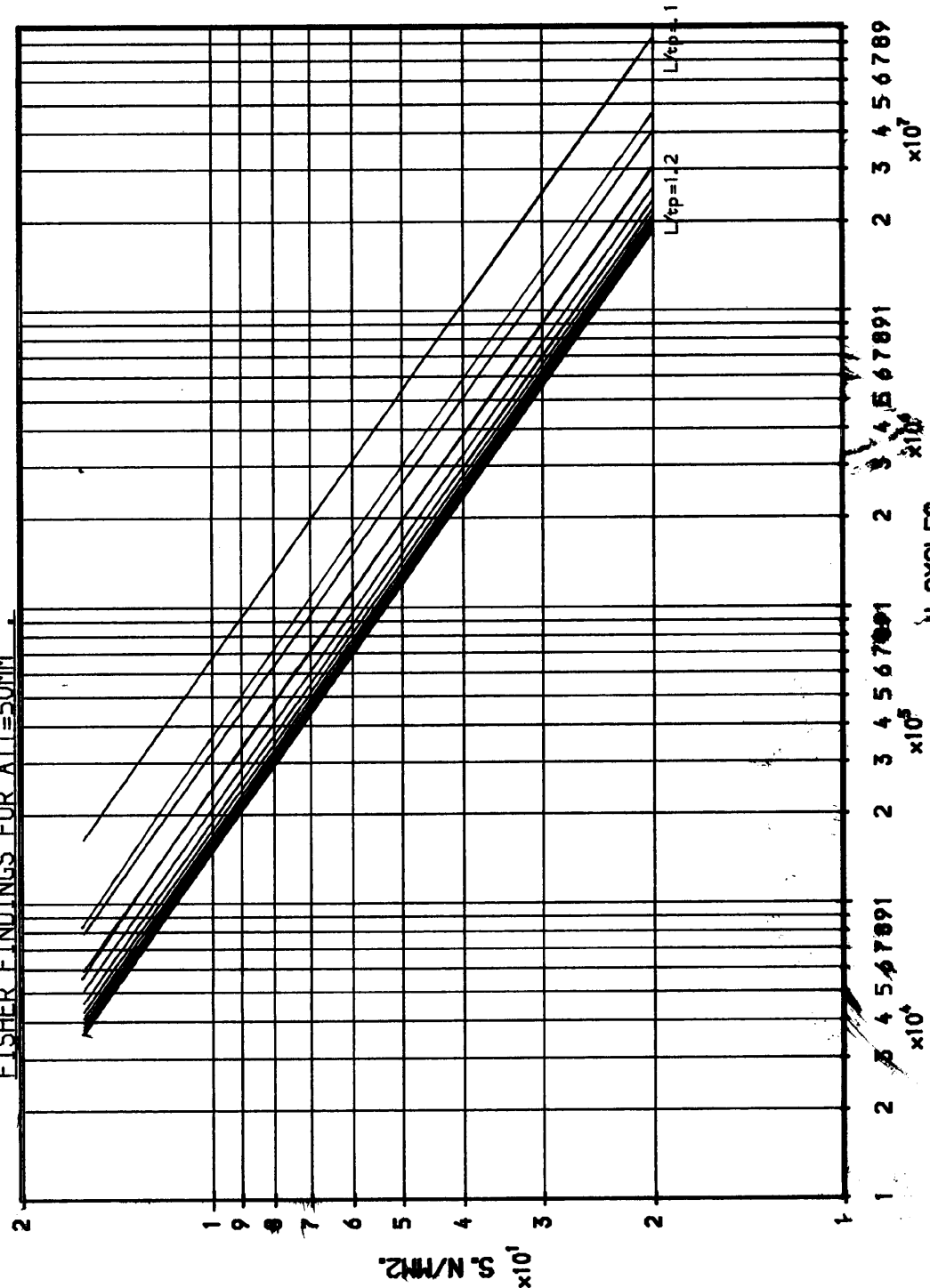


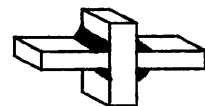
Fig - 4.23 -

JOINT CLASSIFICATION BS5400 PT. 10 CLASS W
LOAD CARRYING WELD METAL
WELD STRESS RANGE, VS. ENDURANCE, N.

FISHER FINDINGS FOR AIT=50MM



CLASS VL
 WELD METAL IN LOAD-CARRYING
 JOINTS MADE WITH FILLET OR
 PARTIAL PENETRATION WELDS
 BASED ON NOMINAL SHEAR
 STRESS ON THE MIN. THROAT



RATIO L/tp VARIES FROM .1
 TO 1.2 IN INCREMENT OF .1
 — MEAN
 — MEAN-1SD
 — MEAN-2SD

Fig. 4.24 -

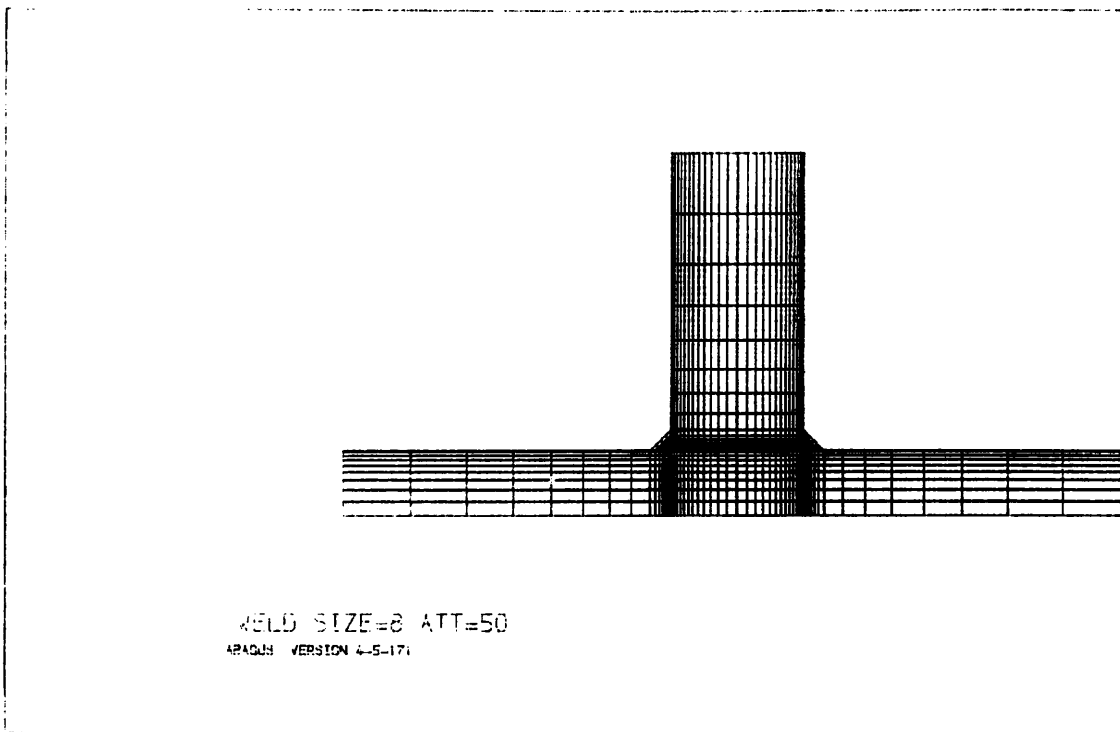


Fig. (4.25). Typical Finite Element Mesh of the Cruciform Welded Joint. (Misalignment Study).

SIF FINITE ELEMENT/SIF TANGENT
VS. RATIO a/w MISALIGNMENT ANALYSIS

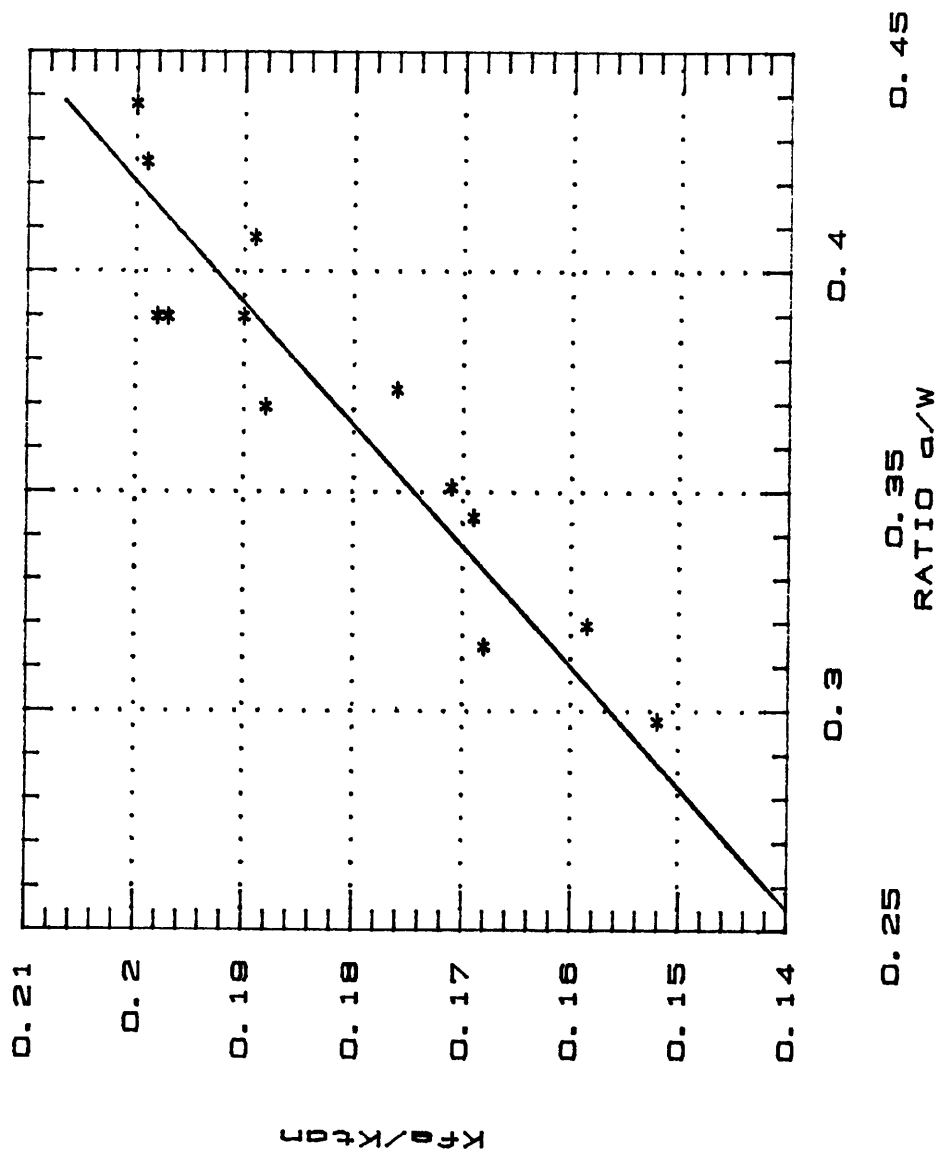


Fig (4.26)

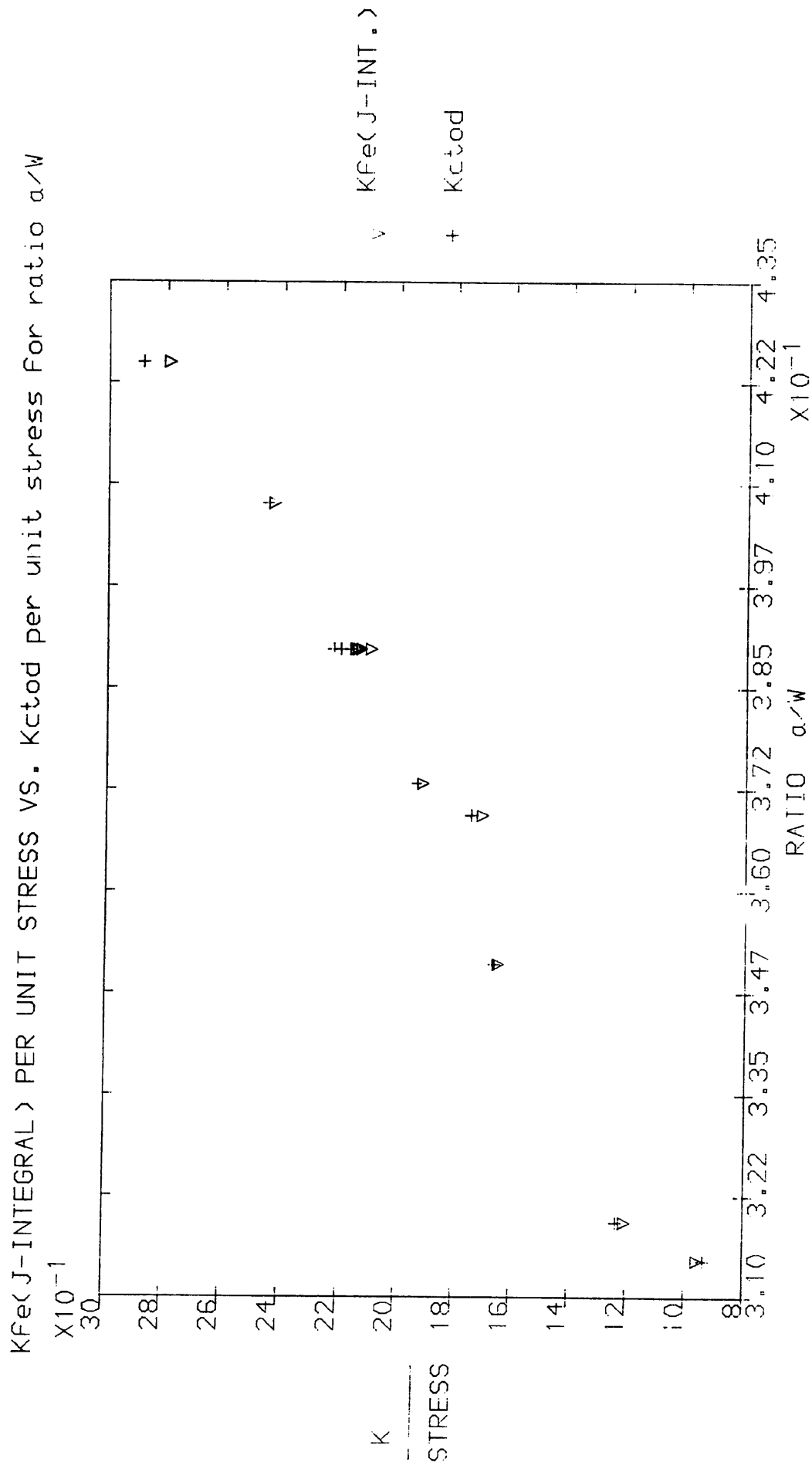


Fig 4.27

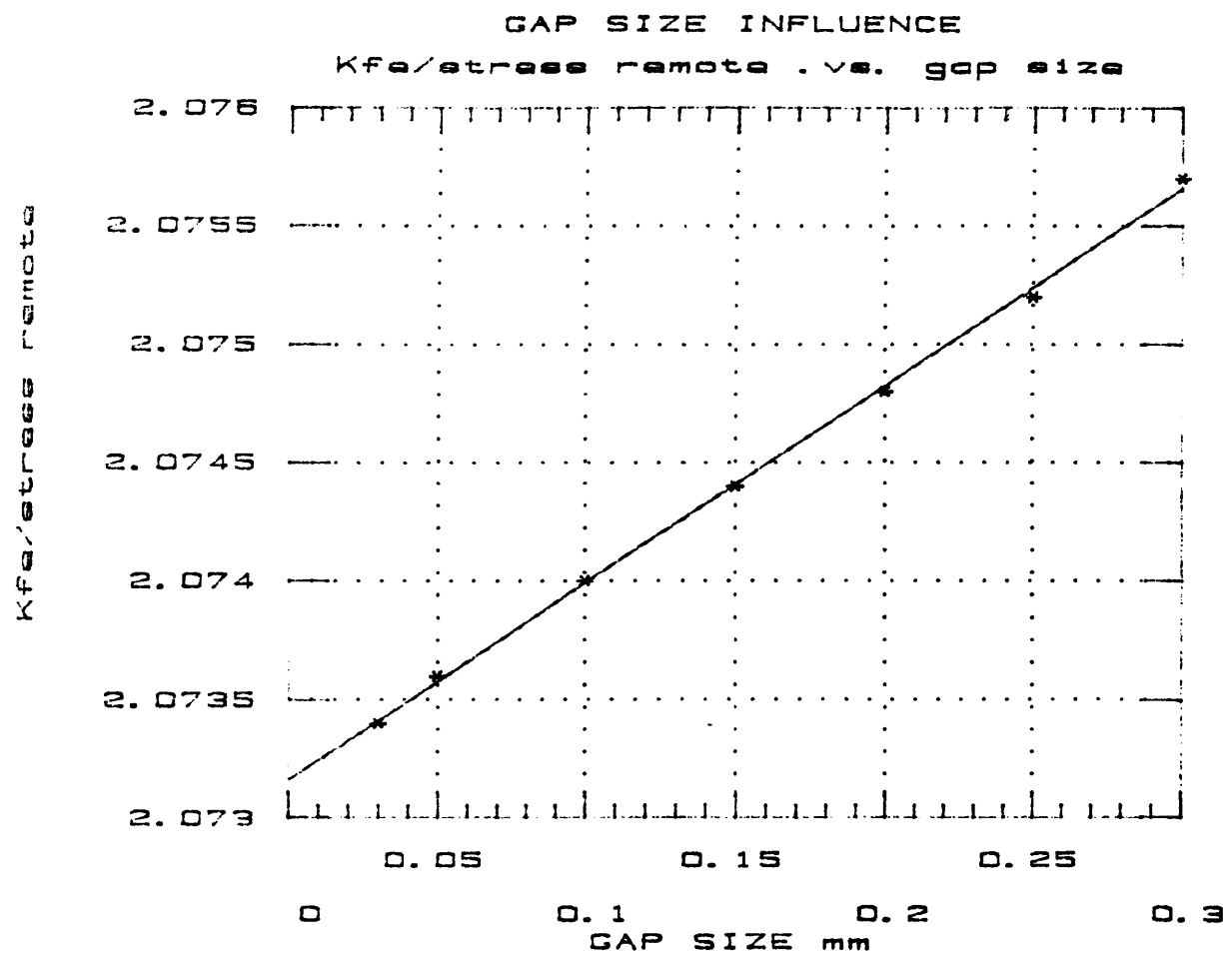


Fig. (4.28). Stress Intensity Factor Per Unit Remote Stress Against Ratio a/W .

CHAPTER 5
THEORETICAL STUDY PHASE 2 (SHS JOINTS)

5.0. Introduction

**5.1. Summary of the Research into the Fatigue Behaviour of
Structural Hollow Section Joints.**

5.2. Finite Element Model

5.3. Results of the Finite Element Analyses

5.4. Fatigue Life Estimation

CHAPTER FIVE

THEORETICAL STUDY PHASE 2 (SHS JOINTS)

5.0. INTRODUCTION

Hollow structural sections are finding increased use in civil engineering structures because of their excellent structural properties. These sections can be either circular (CHS) or rectangular or square. Combinations of these types can also be found in trusses. The design of welded connections made of hollow sections in lattice construction requires more understanding of structural engineering than that required for the general design of steel structures made of plates and open sections.

In this chapter the fatigue behaviour of fillet welded cruciform joints made of Square Hollow Sections is investigated. A numerical analysis using the finite element technique is conducted to study the influence of geometrical parameters on the fatigue behaviour of these joints. The objective is to develop parametric equations that enable the calculation of stress intensity factors and the estimation of fatigue strength of square hollow section joints having different geometries. Further also to establish a relationship which relates the fatigue strength of joints analysed earlier in phase (1) to that of SHS joints using the concept of stress intensity magnification factors.

The detailed analyses conducted to study the fatigue behaviour of SHS fillet welded joints is preceded by a summary of research done in this area namely the fatigue behaviour of Structural Hollow Section joints.

5.1. Summary of Research into the Fatigue Behaviour of Structural Hollow Section Joints

Sufficient information is now available on the fatigue behaviour of circular hollow section (CHS) joints for basic design purposes. This information has been collected from major research projects in the fields of offshore structures and crane construction. A large number of fatigue tests have been carried out on CHS joints and data derived from these tests was used to set up rules for the fatigue design of these joints. The simplest approach for the fatigue design of welded tubular steel joints still permitted in some codes is to keep the direct and punching shear stresses under the maximum storm design wave conditions to low levels. In general, however, the fatigue design of tubular joints for offshore structures is carried out by using parametric formulae to calculate the hot spot stress ranges for the geometric conditions given and the loading applied [3,4&38]. These parametric formulae were derived either from finite element stress analysis or from results of strain gauged model acrylic tube tests [5,6]. The hot spot stress range method employs a single basic S-N design curve which is modified for different thicknesses. Miner's Law is assumed valid for the wave loading spectrum relevant to the platform location. The validity of this approach was examined by major

experimental programmes of which UKOSRP and European Community programmes on tubular joints have formed a major part. In recent years there has been increasing attention drawn to the thickness effects and fracture mechanics analysis and experimental work has shown that there may be serious reductions in fatigue life in thick section joints as compared to thin laboratory tests [39,40 & 41].

A review of the design recommendations for the fatigue design of welded square hollow sections indicates that no specific design rules for the fatigue strength of square hollow section joints are included in the American [42], or British [1] specifications. Up to quite recently very little research work had been carried out on the behaviour of square hollow sections, however, the launch of an extensive experimental programme in 1975, sponsored by the European Coal and Steel Community (ECSC), and the Studiengesellschaft für Anwendungstechnik which was completed in 1980 yielded valuable data. This research recognised the difficulties of understanding the fatigue behaviour of hollow section joints due to the relatively large number of influencing parameters, which for a comprehensive design these must be taken simultaneously into account. The general approach adopted by CIDECT [19] involved the establishment of the individual effects of influencing parameters on the fatigue strength to try to predict the overall effect on the basis of relative priority given to various parameters. The approaches were primarily based on studying the results of tests conducted on

a number of structural hollow section joints having different geometries. A review of various methods of fatigue analysis and influencing parameters is found in [19] and is summarised here.

It is common in analysing fatigue data to determine the relation between the number of cycles (fatigue life) and certain stress or strain ranges. For the square hollow section, at present no operational definition of failure criterion is available which can be used to determine a number of cycles. The methods available for the determination of the stress or strain to describe the fatigue behaviour could be in principle distinguished by methods based on the hot spot stress or strain range, and methods based on nominal stress.

Using methods based on nominal stress, the stress concentration is taken indirectly into account by analysing test results of similar joints separately, and the results plotted against the nominal stress range in the bracings.

If the differences are small a classification can be given based on the type of joint, joint geometrical parameters and loading conditions. This method is used for analyses of square hollow section joints where insufficient information regarding strain or stress concentration factors exist. [21].

In methods based on hot spot stress or strain range, in the case of square hollow sections only very limited information on the stress concentration factors exist. In Japan [43] the fatigue strength of circular hollow sections joints (Load range P_r) is given in relation to the static strength of the joint (ultimate load P_u) for a certain steel grade. This approach assumes that both fatigue and static strength depend on the same geometrical parameters. No similar connection is established for square hollow section joints.

The conclusion of this summary must be that method available for the design of square hollow section joints described are primarily based on studying the results of tests. Assessed test results are only valid over the tested parameter range. More tests would be necessary to extend the application of the test results beyond that range.

An approach based on numerical analysis which involve three dimensional finite element modelling of square hollow section joint to develop parametric equations and the use of fracture mechanics principles to predict crack growths and estimate fatigue strengths of these joints is favoured here and details of the piece of work aimed at achieving the above objectives are described here in this chapter.

5.2. Finite Element Model

For structural hollow section joints due to their relative geometric complexity, it is necessary to resort to numerical

technique such as the finite element method to study their behaviour under different loading conditions. Discretisation of the three dimensional geometry of hollow sections poses a difficult task which if attempted manually will inevitably give solutions prone to error and will be time consuming.

The availability of FEMGEN (finite element mesh generator) on SERC PRIME 9955 at UMIST [44] allowed the process of mesh generation to be speeded up considerably. The proper selection of an adequate finite element mesh is essential to an accurate analysis. To study the behaviour of SHS fillet welded cruciform joints, particularly at the root area of the fillet welds, required the design of a fine mesh in the vicinity of the root where the gradients of the stresses are large and a coarser mesh in the regions where the stresses are more evenly distributed.

The analyses were conducted using the finite element package ABAQUS. The type of elements used in modelling the cruciform fillet welded SHS joint were three dimensional 20-node brick element (C3D20R) [45] with three degrees of freedom per node. In order to generate the mesh efficiently, the joint was divided into a number of basic regions on the flat surfaces to be swept to generate the total volume of the structure. Those regions corresponded to the different levels of mesh refinement. The core region corresponded to the high stress gradient area at the fillet weld roots. The wall thickness of the chord member was modelled by a minimum of three layers of

brick elements to enable the bending of the wall to be modelled accurately. In the brace member also three layers of brick elements across the thickness were used in a relatively coarser mesh than in the chord and around the intersection area because the stresses are more evenly distributed. Advantage of symmetry was taken and only one quarter of the cruciform joint was modelled. Each mesh consisted of 860 brick elements with 14844 degrees of freedom. The mesh design maintained aspect ratios and element inside angles within acceptable limits as far as possible. The mesh generation was conducted with great care to ensure that the geometry was correctly modelled and element numbering difference was kept to a minimum to enable the avoidance of spilling out of main memory during the frontal solution technique employed by ABAQUS. Having to spill out of main memory core increased the routine substantially and is to be avoided.

Twenty-eight different geometrical conditions were analysed to study the influence of geometrical parameters b/B , t/T , and L/t and sensitivity to weld angle. These geometrical conditions are given in Table (5.1). Correct boundary conditions were needed and applied to simulate the full square hollow section joint on the planes of symmetry and were checked in the preprocessor (FEMGEN) and in the analysis run. The ends of the chord were unrestrained and checked for effects on the J-Integral evaluated at the root. The length of the chord away from the intersection was taken to be 1.25 times the largest chord width analysed which, if increased

further, no influence is reflected in J-integrals calculated. In the core area a cluster of eight crack tip elements with the mid-side nodes moved to the quarter position on those element edges that focus onto the crack tip nodes at the roots of welds. This provides a strain singularity and so improves the modelling of the strain field adjacent to the crack tip.

Loads were applied at the brace free ends to simulate the axial loads. Uniformly distributed pressure loads were prescribed on the surfaces of elements at the end of the brace member. The magnitude of the distributed pressure was unity.

5.3. Results of the Finite Element Analyses

The unpenetrated depth at the intersection of brace and chord member modelled in this phase as a crack necessitated the evaluation of the stress intensity factor along the crack front. In all the meshes analysed the J-integrals were computed by the program at 25 positions along the crack front from the middle of the side wall to the middle of the cross wall. At each crack tip position J-integrals were evaluated for three contours surrounding the crack tips. The J-integral values for the three contours at each crack front position were close to each other preserving the contour independence feature. The values of J were averaged for the three contours and the variation of the stress intensity factors per unit nominal stress in the brace calculated from

J values for linear elasticity using equation (3.14) were plotted against crack front position in groups of geometrical conditions analysed Fig. (5.1 - 5.7).

The values of stress intensity factors at the root of the fillet weld per unit stress in brace show a rather smooth variation along the crack front with maximum stress intensity factors in the middle of the cross wall and slightly lower values at the middle of the side wall. The brace wall thickness effect is observed on comparing the group of plots presented, Figs. (5.1, 5.3, 5.5.) Increasing the brace wall thickness increases the stress intensity factor at the fillet weld root positions, thus demonstrating again the thickness effect. The bending degree governed by the geometrical ratio b/B also has a great effect on the stress intensity factors evaluated. This ratio, as will be demonstrated in the next section, forms the basis of derived relationships for fatigue life estimation using fracture mechanics principles.

Maximum stress intensity factors per unit stress in brace for the geometrical conditions analysed are normalised with the results obtained for the cruciform plate fillet welded joints in phase 1 of the theoretical work with the attachment thicknesses in the plate joints correspond to combined thickness of the two cross walls representing the full cruciform square hollow section joint. The variation of the normalised stress intensity factors from the three dimensional analyses were plotted against the important b/B

ratios analysed Fig (5.8, 5.9). The variation producing the most critical conditions can be represented by the fitted equation:

$$\frac{K_{f.e.3-D} \text{ (SHS members)}}{K_{f.e.2-D} \text{ (plates)}} = -7.003b/B + 5.429 \quad (5.1)$$

An upper bound curve can also be fitted to the data.

Typical meshes used in the analysis are shown in Figs. (5.10 to 5.13). The intersection region is shown in Figs. (5.14 to 5.16), showing also the crack tip cluster of elements. The displaced shape of a typical mesh is also shown in Fig. (5.17).

5.4. Fatigue Life Estimation

The fatigue strength of cruciform fillet welded joints of SHS members is estimated in the same way as the plate joints examined in phase 1, using the fracture mechanics principles.

The fatigue life N is essentially calculated by integrating the classical Paris Law to give:

$$N = \int_{a_i}^{a_f} da / C(\Delta K)^m \quad (5.2)$$

So that when a_i , the initial crack size, a_f the limiting crack size, and the relationship between the stress intensity

factor range ΔK and the crack size a is known; N can be calculated.

The stress intensity factors calculated from the finite element analysis are normalised by the stress intensity factors from the plate joints equation which gives, for the initial condition of the fillet weld before fatigue crack growth:

$$K_{3-D}/K_{2-D} = Mg = -7.003(b/B)+5.429 \quad (5.3)$$

where

Mg is a stress intensity magnification factor

b , B are the brace and the chord member widths respectively.

The 3-D stress intensity factor range at the start of fatigue crack growth can be expressed as

$$\Delta K_{3-D} = \Delta \sigma_b Mg \Delta K_{2-D}$$

where

(5.4)

$\Delta \sigma_b$ is the nominal stress range in the brace

W is defined as:

$$W = 2t + 1.4142L \quad (5.5)$$

where

t is the brace wall thickness

L is the fillet leg length.

Substituting for ΔK in equation 5.2 from equation 5.4 and separating the variables to integrate, the integration is:

$$\int_{a_i/W}^{a_f/W} d(a/W) / (K_{2-D})^3 (Mg)^3 = (\Delta \sigma_b)^3 C N^* \quad (5.6)$$

As a first estimate, it is reasonable to assume that Mg remains approximately constant for a given joint geometry, as the crack grows, the effect of crack growth being included in the 2D solution for K as a function of a/W . Thus Mg is a function of brace to chord widths ratio and can be taken out of the integration to give:

$$\int_{a_i/W}^{a_f/W} d(a/W) / (K_{2-D})^3 = (\Delta \sigma_b)^3 C (Mg)^3 N^* \quad (5.7)$$

The integral on the left-hand side of the equation had been evaluated numerically in phase 1 and is defined as:

$$\int_{a_i/W}^{a_f/W} d(a/W) / (K_{2-D})^3 = I \sqrt{W} \quad (5.8)$$

substituting back to give the fatigue life equation for the cruciform fillet welded joint from square hollow sections:

$$N^* = I / (\Delta \sigma_b)^3 (Mg)^3 C \sqrt{W} \quad (5.9)$$

where N^* is the fatigue life for crack growth from a_i/W to maximal admitted ratio a_f/W for a cruciform fillet welded joint with a magnification factor Mg and brace nominal stress range $\Delta \sigma_b$.

Recalling equation (4.21) which gives the fatigue strength N

for the plate joints analysed in phase 1 which is:

$$N = I / (\Delta \sigma_b)^3 C \sqrt{W} \quad (5.10)$$

Further, for design purposes the fatigue life of cruciform fillet welded SHS joint N^* can be related to the fatigue life of cruciform plate joint analysed in phase 1 by substituting back for N in equation (5.9) to give:

$$N^* = N / (Mg)^3 \quad (5.11)$$

This relationship is plotted Fig. (5.18) for ratios of b/B between .1 and .7 analysed theoretically.

Table (5.1) Geometrical Conditions Analysed (SHS Joints)

Case	Brace Size	Chord Size	b/B	t/T	L/t
SHS 1	60x60x10	120x120x10	0.5	1.0	0.5
2	60x60x10	150x150x10	0.4	1.0	0.5
3	60x60x10	180x180x10	0.33	1.0	0.5
4	60x60x10	240x240x10	0.25	1.0	0.5
5	60x60x10	90x 90x10	0.67	1.0	0.7
6	60x60x10	120x120x10	0.5	1.0	0.7
7	60x60x10	150x150x10	0.4	1.0	0.7
8	60x60x10	180x180x10	0.33	1.0	0.7
9	60x60x10	240x240x10	0.25	1.0	0.7
10	60x60x7.5	120x120x10	0.5	0.75	0.67
11	60x60x7.5	150x150x10	0.4	0.75	0.67
12	60x60x7.5	180x180x10	0.33	0.75	0.67
13	60x60x7.5	240x240x10	0.25	0.75	0.67
14	60x60x7.5	90x 90x10	0.67	0.75	0.93
15	60x60x7.5	120x120x10	0.5	0.75	0.93
16	60x60x7.5	150x150x10	0.4	0.75	0.93
17	60x60x7.5	180x180x10	0.33	0.75	0.93
18	60x60x7.5	240x240x10	0.25	0.75	0.93
19	60x60x5.0	120x120x10	0.5	0.5	1.0
20	60x60x5.0	150x150x10	0.4	0.5	1.0
21	60x60x5.0	180x180x10	0.33	0.5	1.0
22	70x70x10	140x140x10	0.5	1.0	0.7
23	70x70x10	175x175x10	0.4	1.0	0.7
24	70x70x10	210x210x10	0.33	1.0	0.7
25	70x70x10	280x280x10	0.25	1.0	0.7
26	60x60x7.5	180x180x10	0.33	0.75	0.67
27	60x60x7.5	240x240x10	0.25	0.75	0.67
28	60x60x7.5	180x180x8	0.33	0.94	0.93

BRACE WALL	CHORD WALL	WELD	b/B	t/T	L/t	BRACE SIZE
10	10	5	0.25-0.50	1	0.5	60X60X10

NORMALISED STRESS INTENSITY FACTOR IN FILLET WELD PER UNIT NOMINAL
 $\times 10^{-1}$ STRESS IN BRACE VS. POSITION ALONG CRACK FRONT

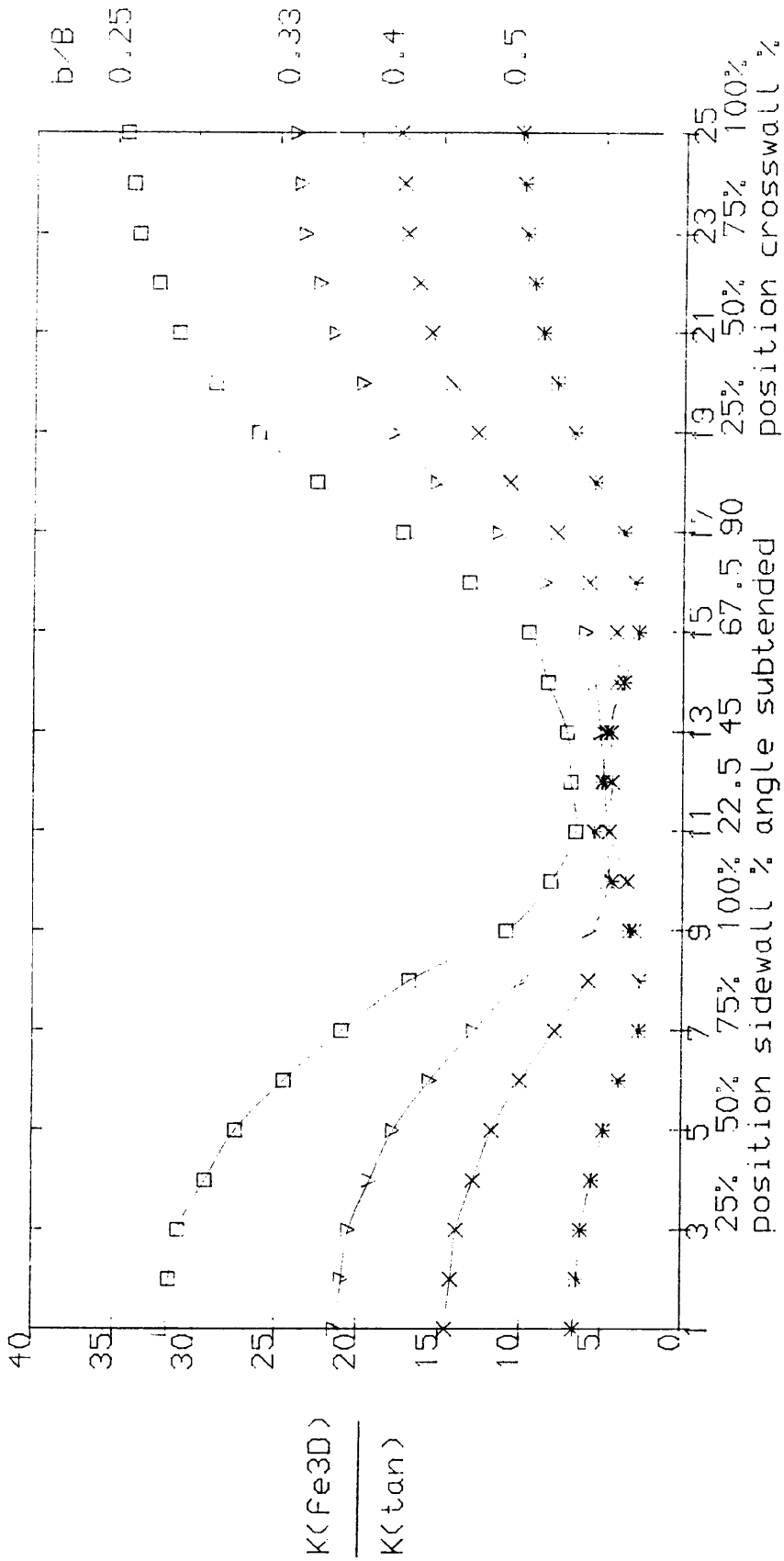


Fig (5.1)

BRACE WALL CHORD WALL WELD b/B t/T L/t BRACE SIZE

10 10 7 0.25-0.67 1.0 0.70 60X60X10

NORMALISED STRESS INTENSITY FACTOR IN FILLET WELD PER UNIT NOMINAL
 X10⁻¹ STRESS IN BRACE VS. POSITION ALONG CRACK FRONT

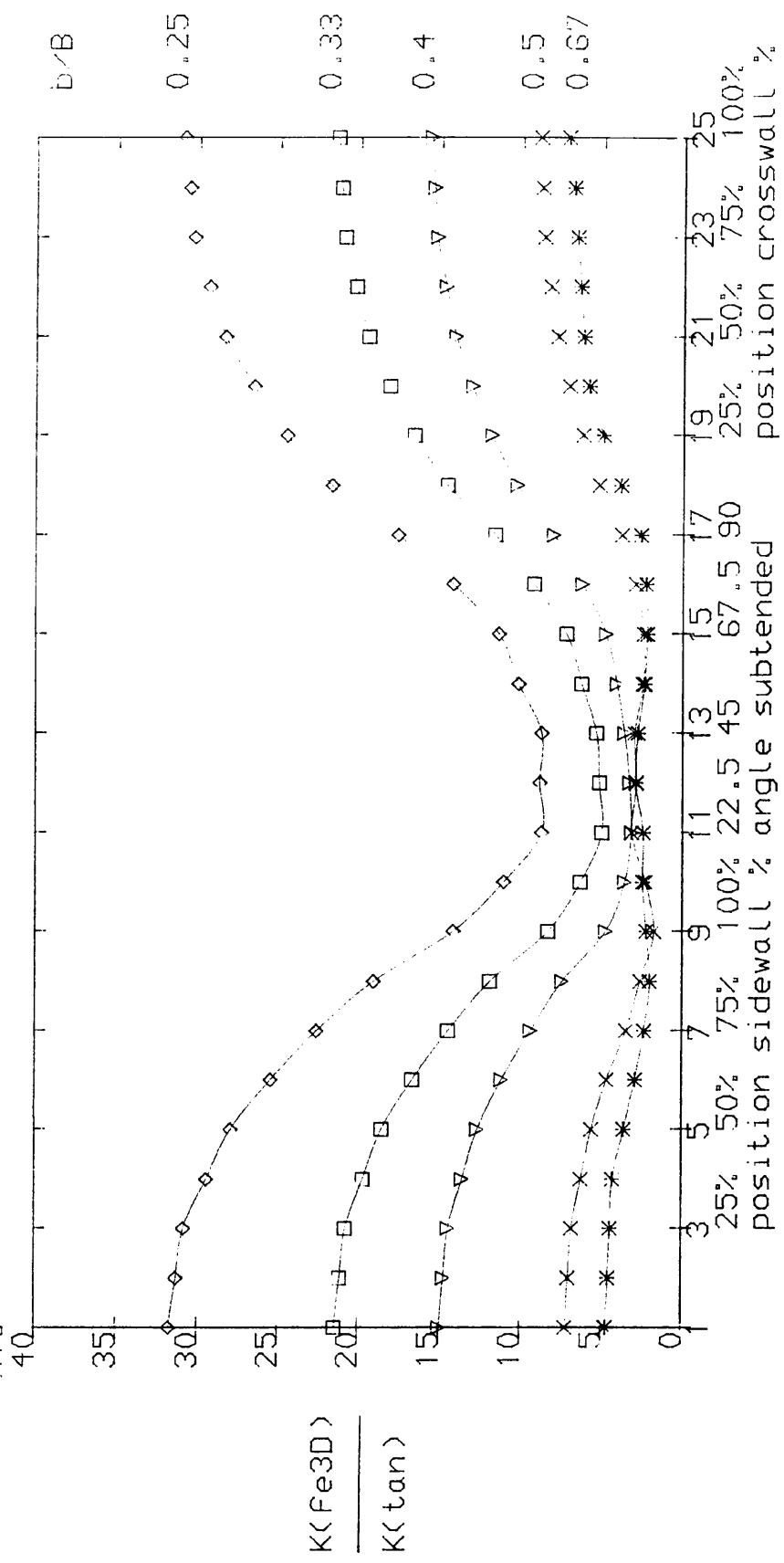
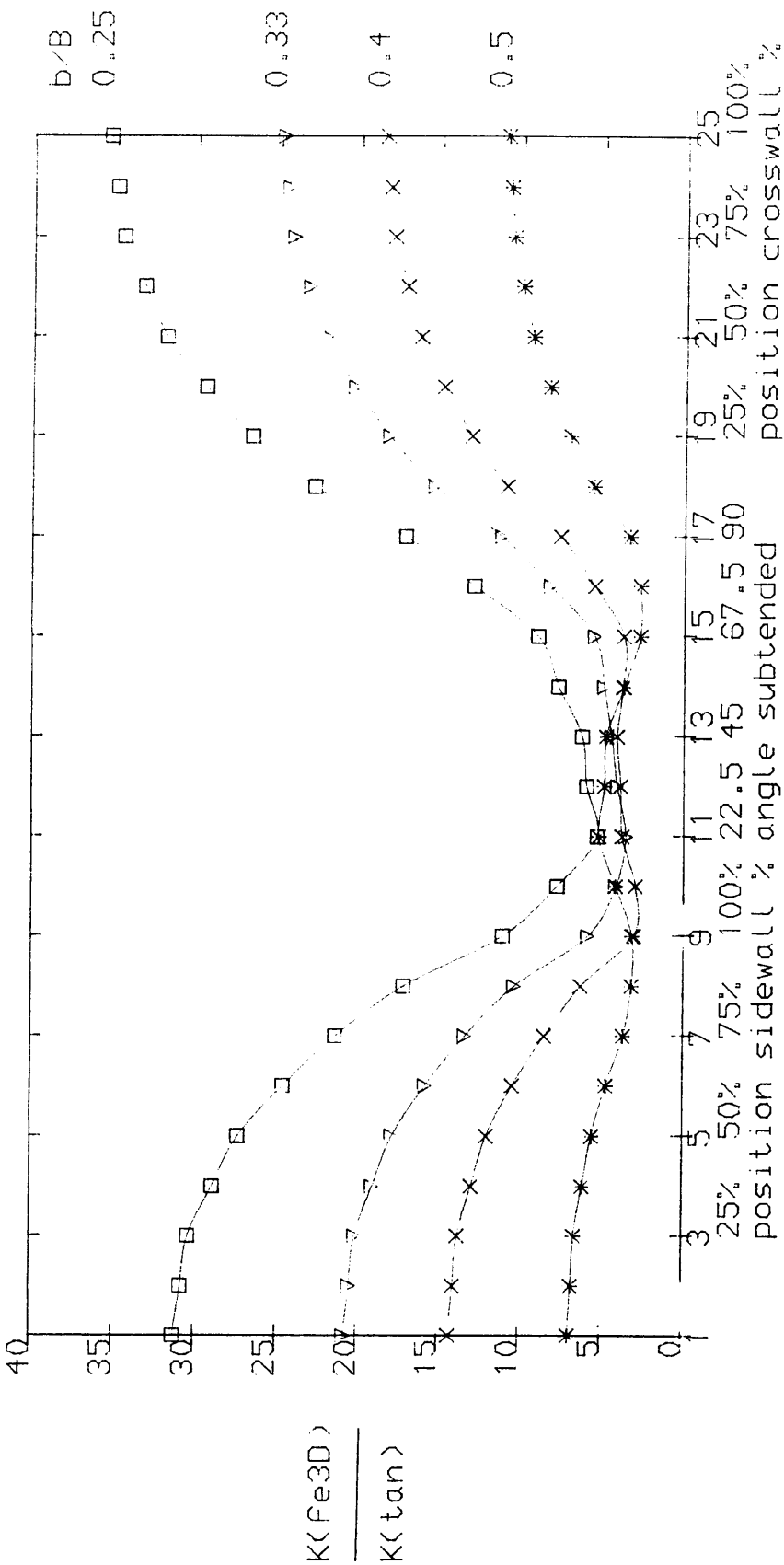


Fig (5.2)

BRACE WALL CHORD WALL WELD b/B t/T L/t BRACE SIZE
 7.5 10 5 0.25 0.50 0.75 0.67 C0X60X7.5

NOPMAL ISED STRESS INTENSITY FACTOR IN FILLET WELD PER UNIT NOMINAL
 STRESS IN BRACE VS.POSITION ALONG CRACK FRONT



FIG(5.3)

BRACE WALL CHORD WALL WELD b/B t/T L/t BRACE SIZE
 7.5 10 7 0.25-0.67 0.75 0.93 60X60X7.5

NORMALISED STRESS INTENSITY FACTOR IN FILLET WELD PER UNIT NOMINAL
 X10⁻¹ STRESS IN BRACE VS. POSITION ALONG CRACK FRONT

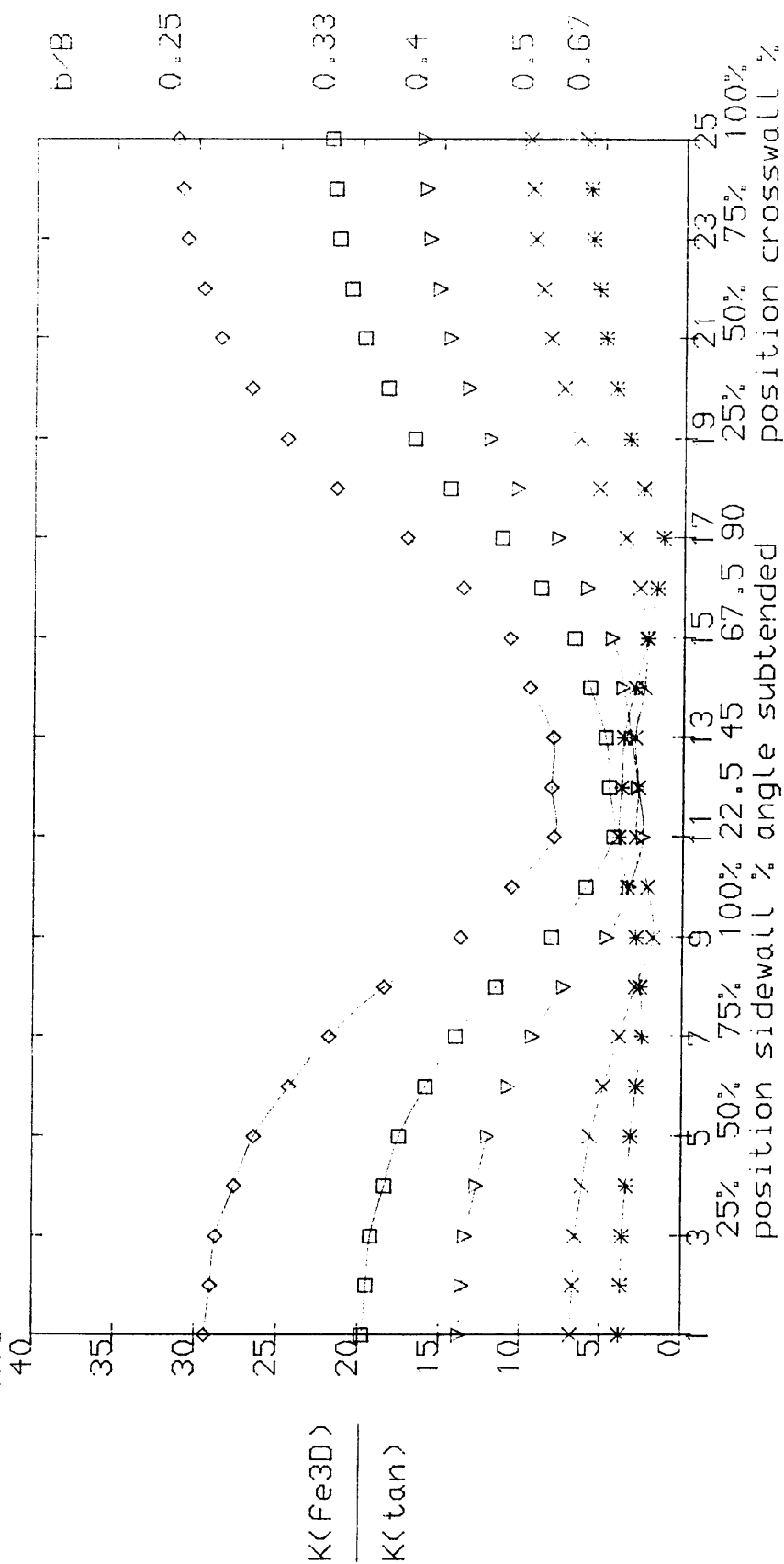
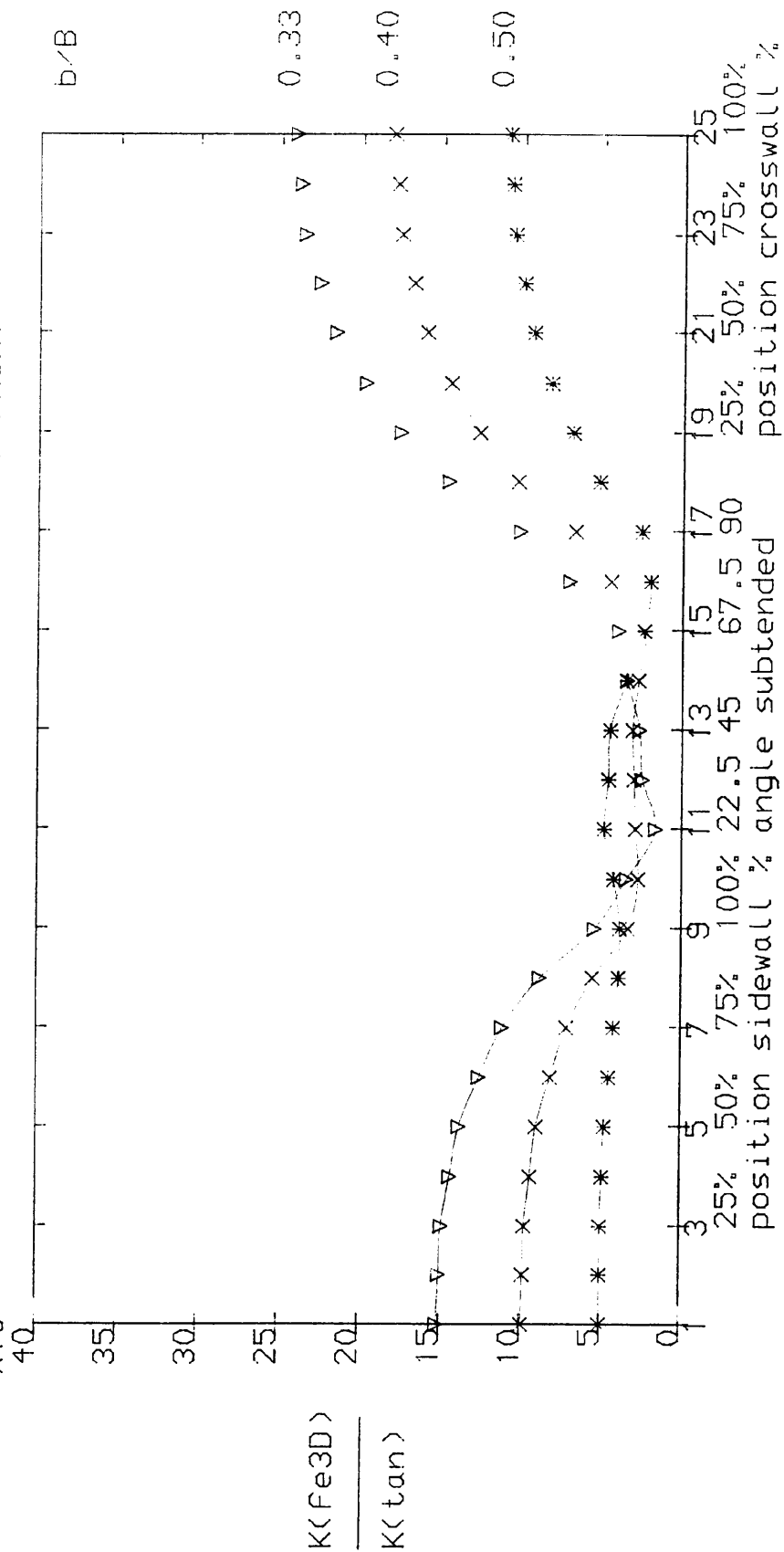


Fig (5.4)

BRACE WALL CHORD WALL WELD b/B t/T L/t BRACE SIZE
 5 10 5 0.33-0.50 0.5 1.0 60x60x5

NORMALISED STRESS INTENSITY FACTOR IN FILLET WELD PER UNIT NOMINAL
 X10⁻¹ STRESS IN BRACE VS. POSITION ALONG CRACK FRONT



Fig(5.5)

BRACE WALL CHORD WALL WELD b/B t/t L/t BRACE SIZE
10 10 7 0.25-0.50 1 0.7 70x70x10

NORMALISED STRESS INTENSITY FACTOR IN FILLET WELD PER UNIT NOMINAL
x10⁻¹ STRESS IN BRACE VS. POSITION ALONG CRACK FRONT

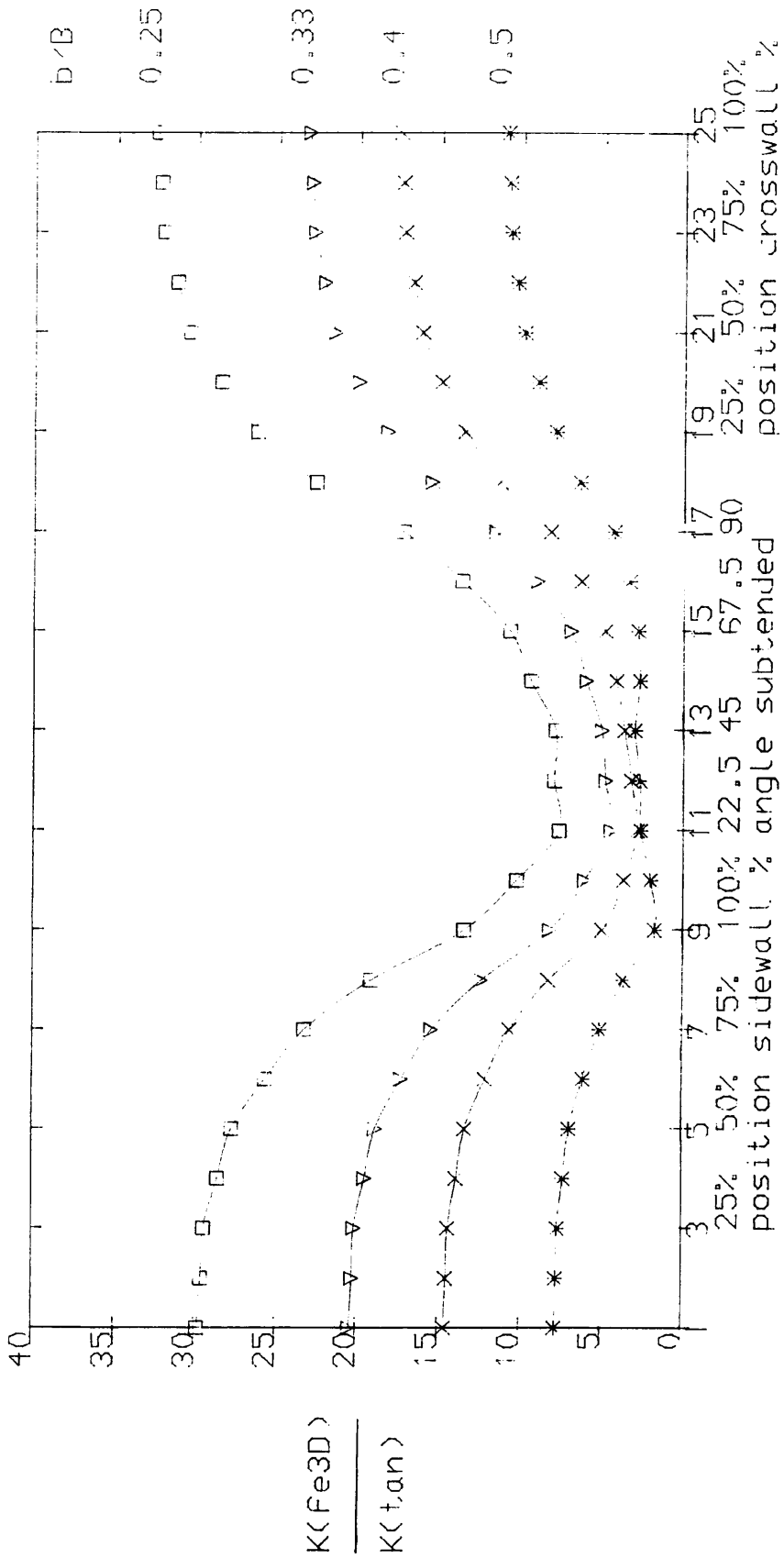
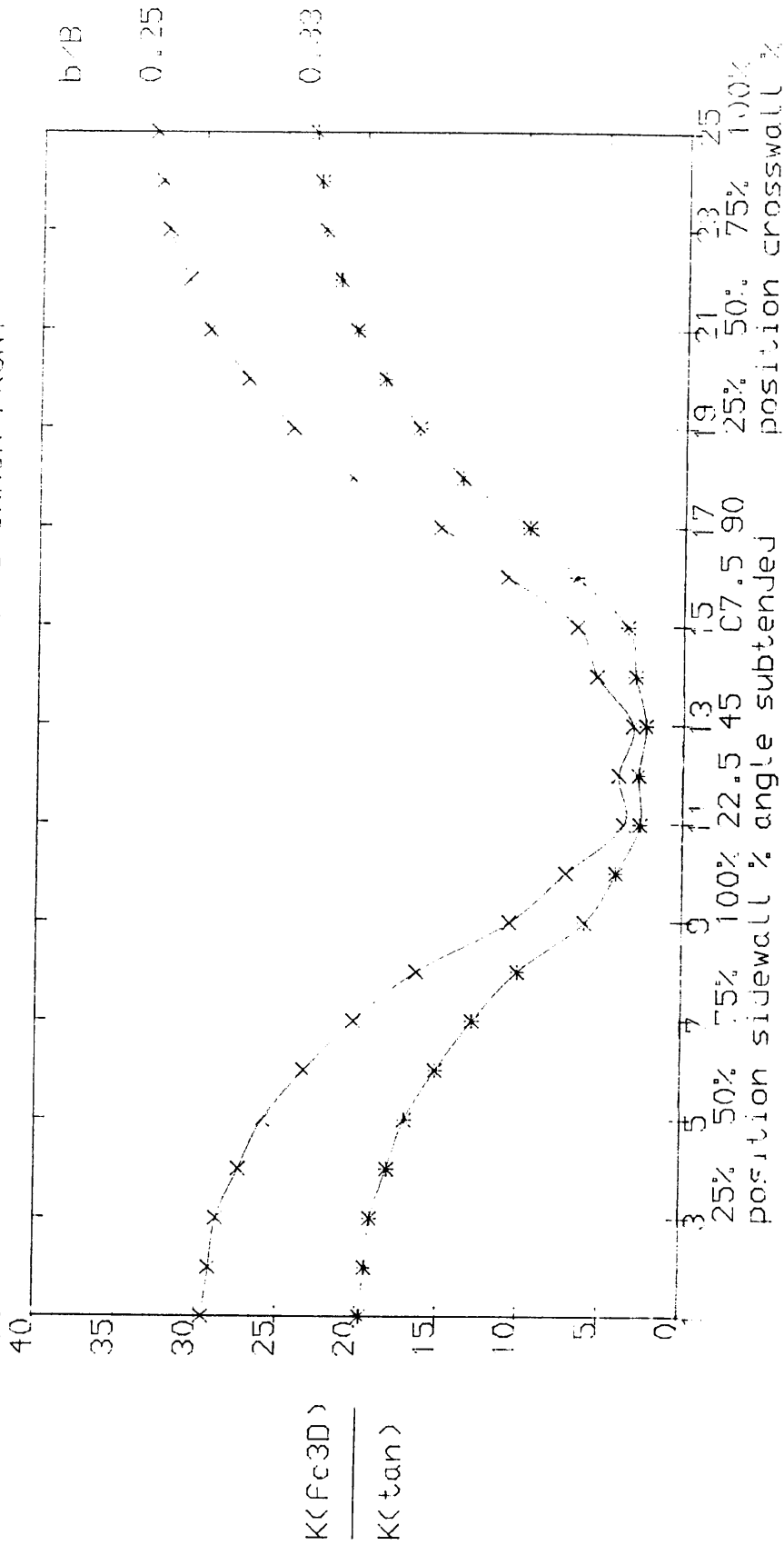


Fig (5.6)

BRACE WALL CHORD WALL WELD b/B t/T L/t BRACE SIZE
 7.5 10 0.25-0.33 0.75 0.93 60x60x7.5

NORMALISED STRESS INTENSITY FACTOR IN FILLET WELD PER UNIT NOMINAL
 $\times 10^{-1}$ STRESS IN BRACE VS. POSITION ALONG CRACK FRONT



Fig(5.7)

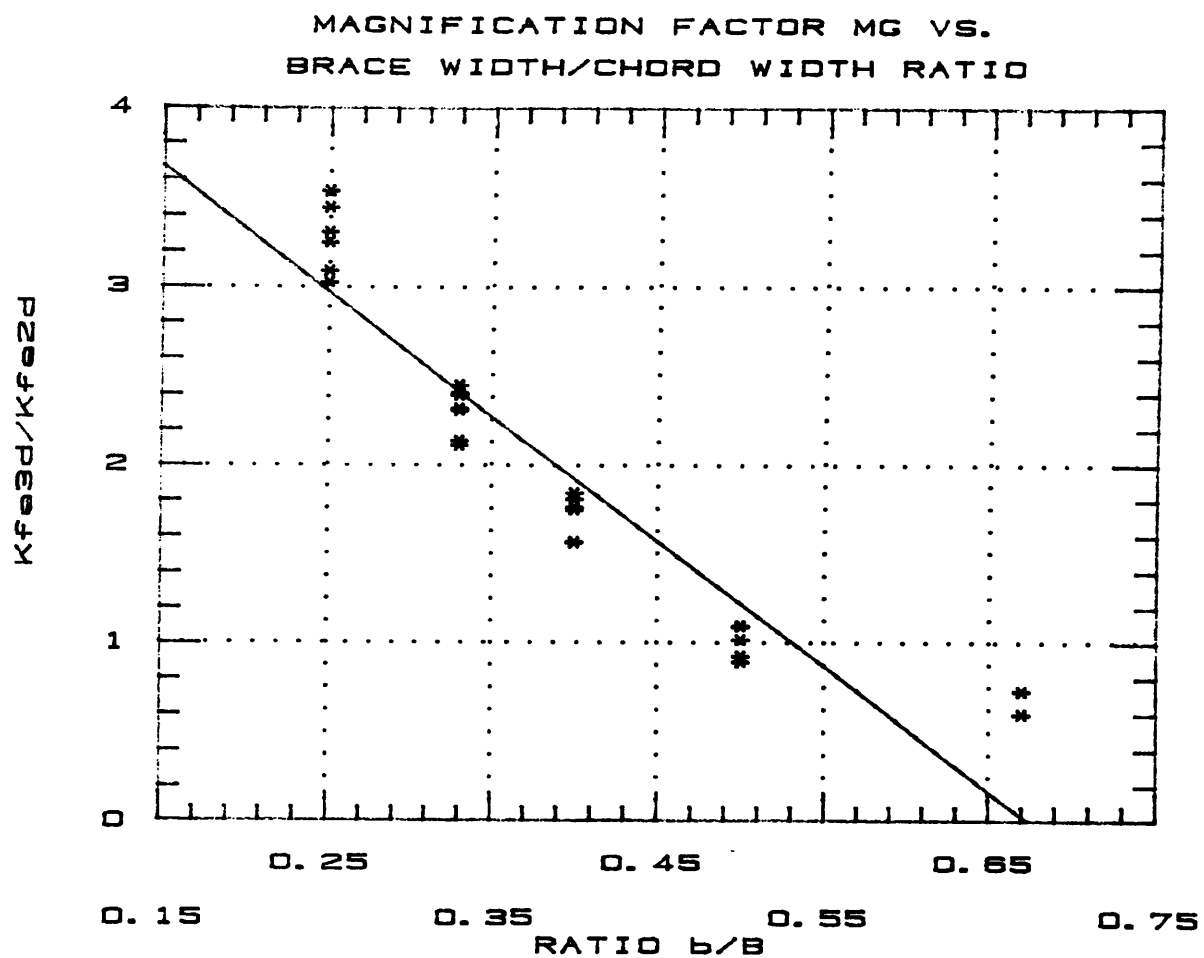


Fig. (5.8). Stress Intensity Magnification Factor for SHS joints vs. the Geometrical Ratio b/B (Straight Line Fit).

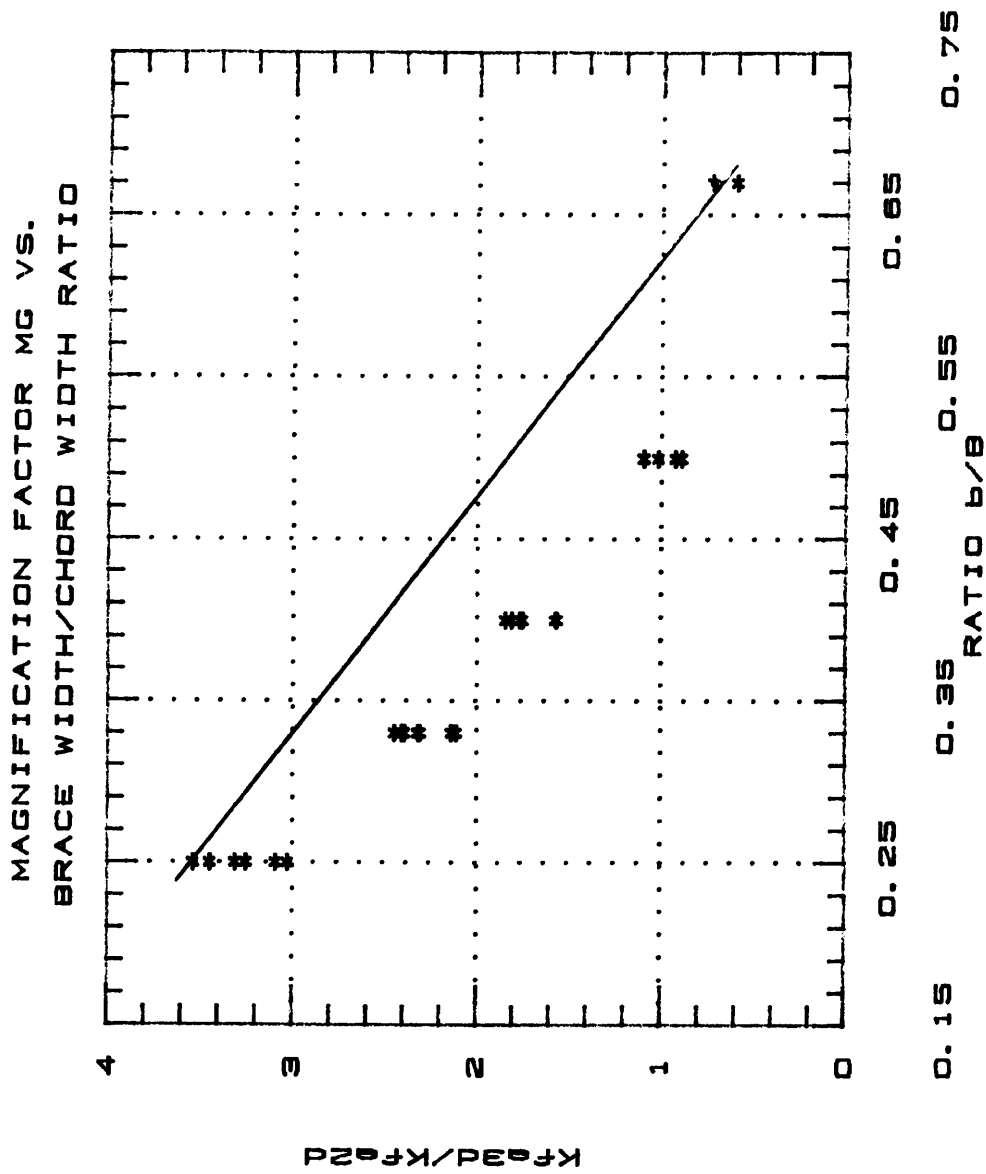


Fig (5.9)

FEMVIEW 3.5
FV>

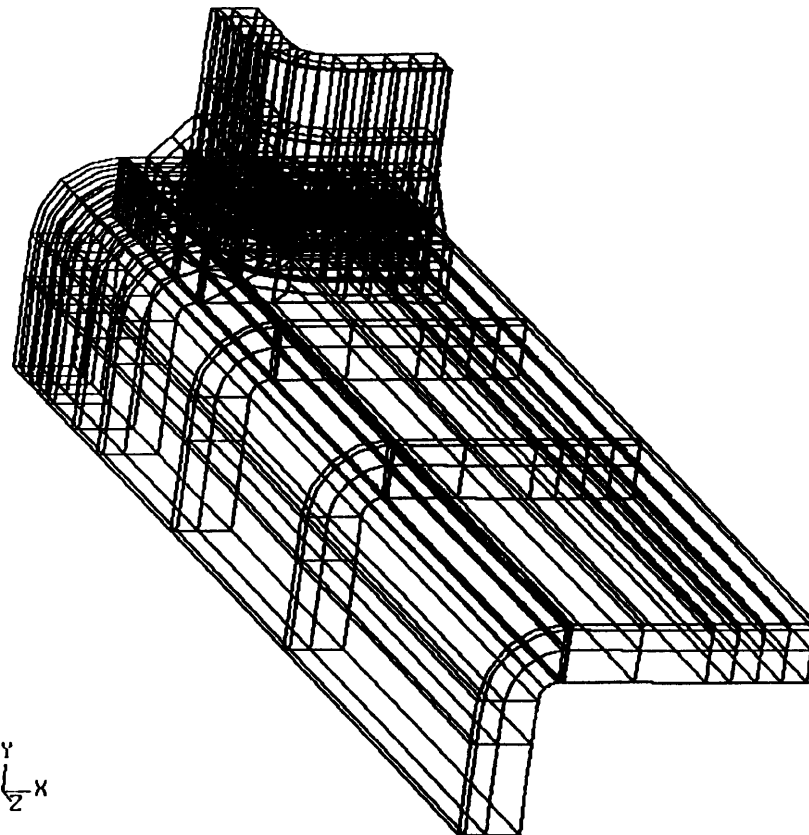


Fig. (5.10). Square Hollow Section Joint Finite Element Mesh.

FEMVIEW 3.5
FV>

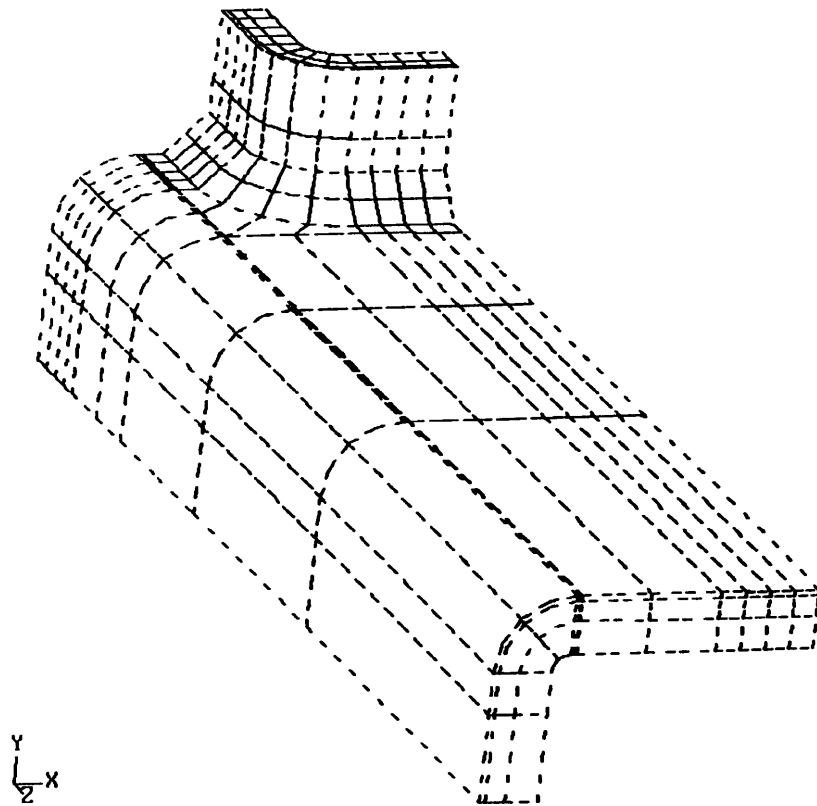


Fig. (5.11). Finite Elements Model.

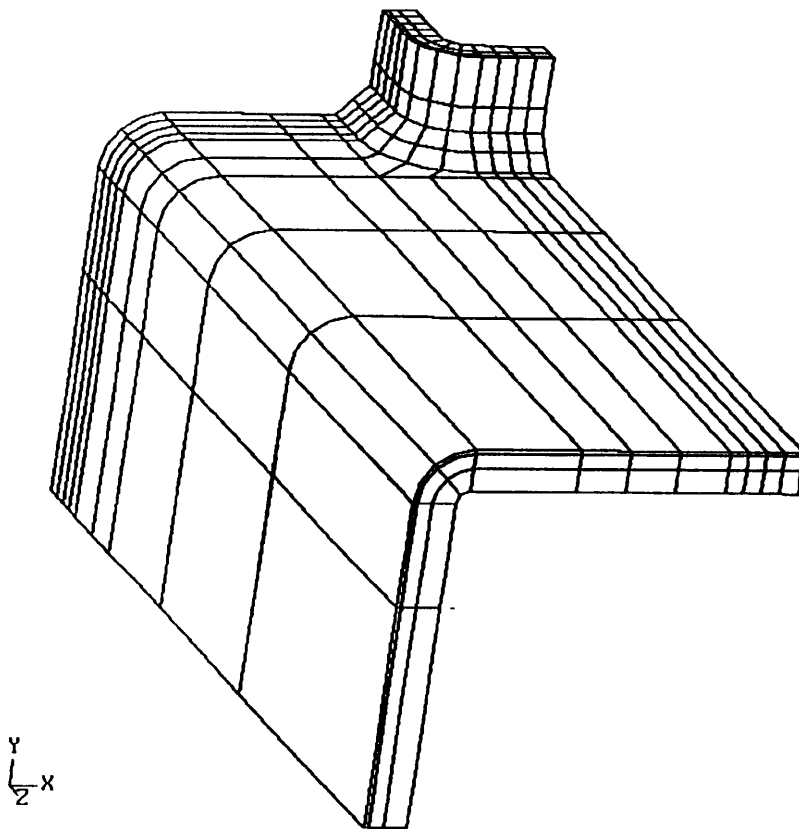


Fig. (5.12). Typical Finite Element Model of SHS Joint.

FENVIEW 3.5
FV>

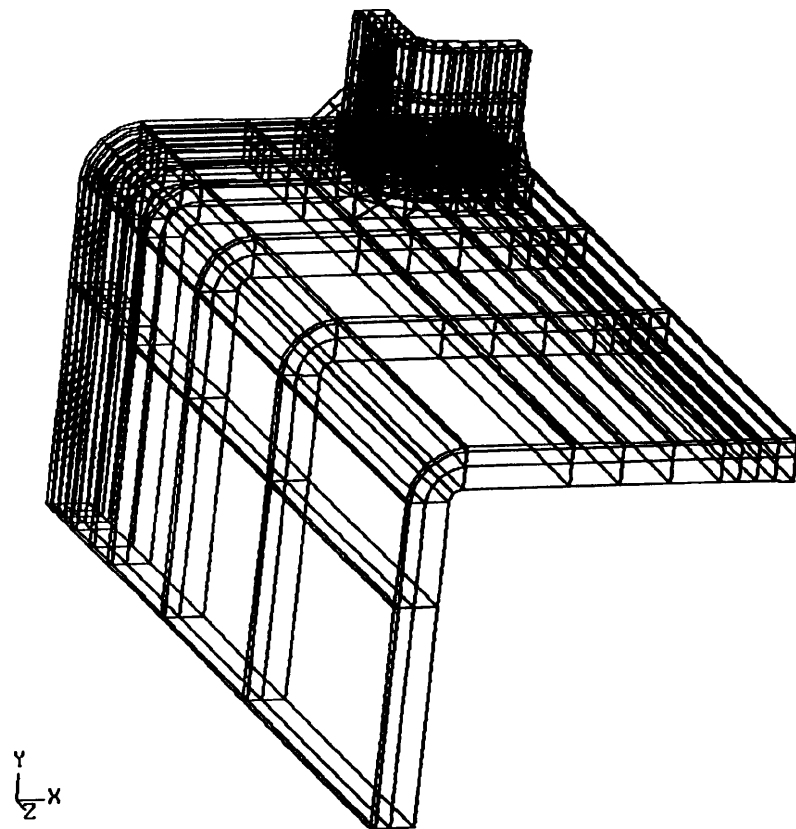


Fig. (5.13). Typical Finite Element Model of SHS Joint.

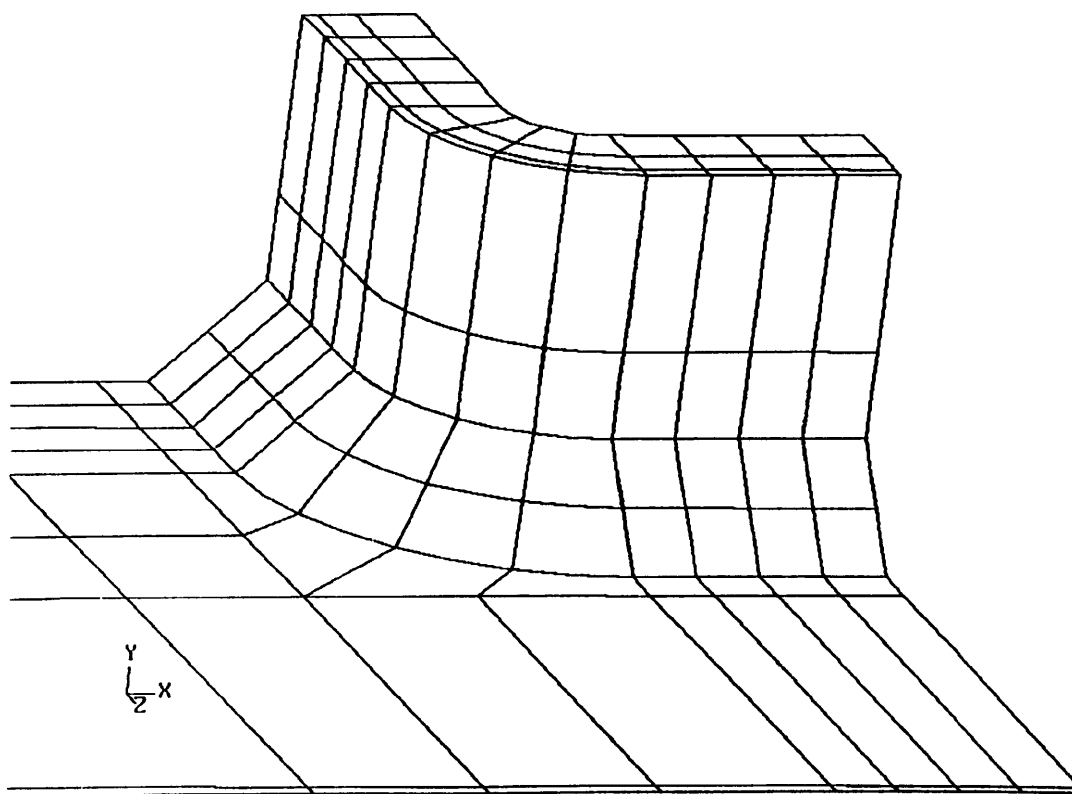


Fig. (5.14). The Intersection Region of the SHS Fillet Welded Joint.

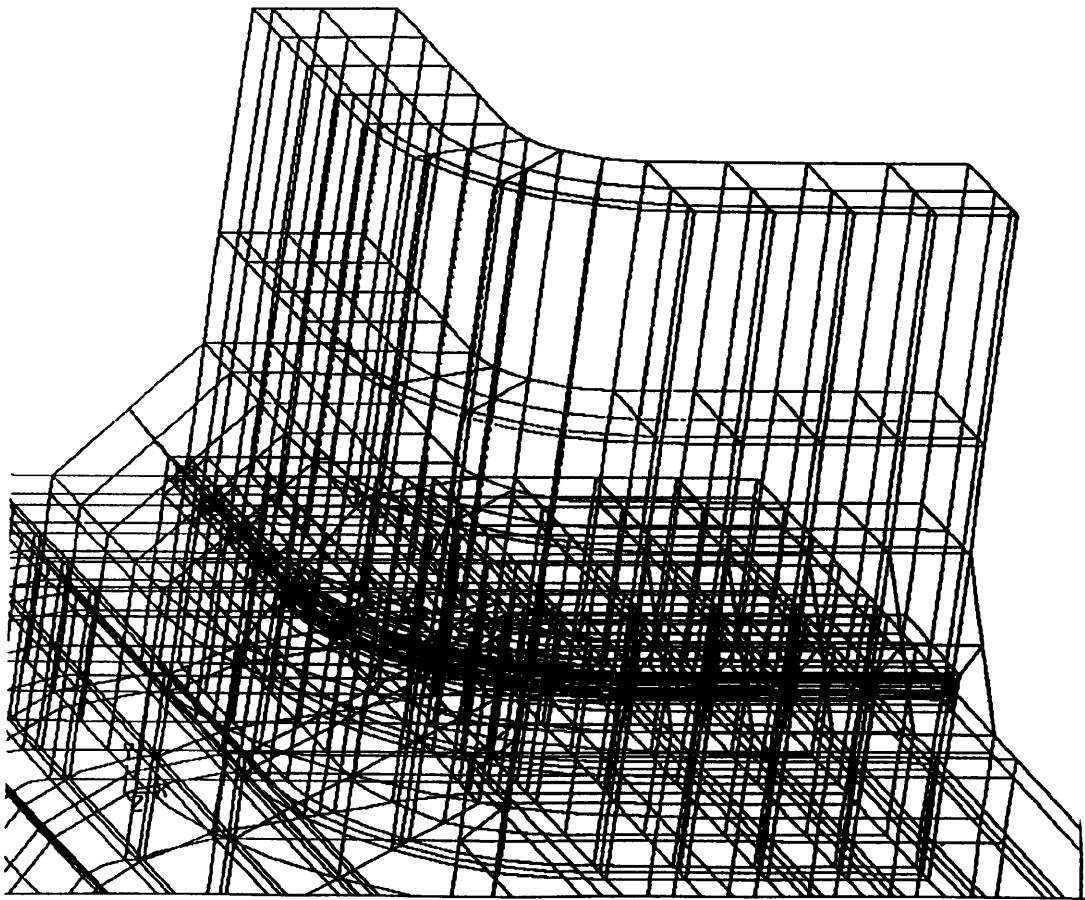


Fig. (5.15). Detailed Representation of Finite Element Model SHS Joint in the Intersection Area.

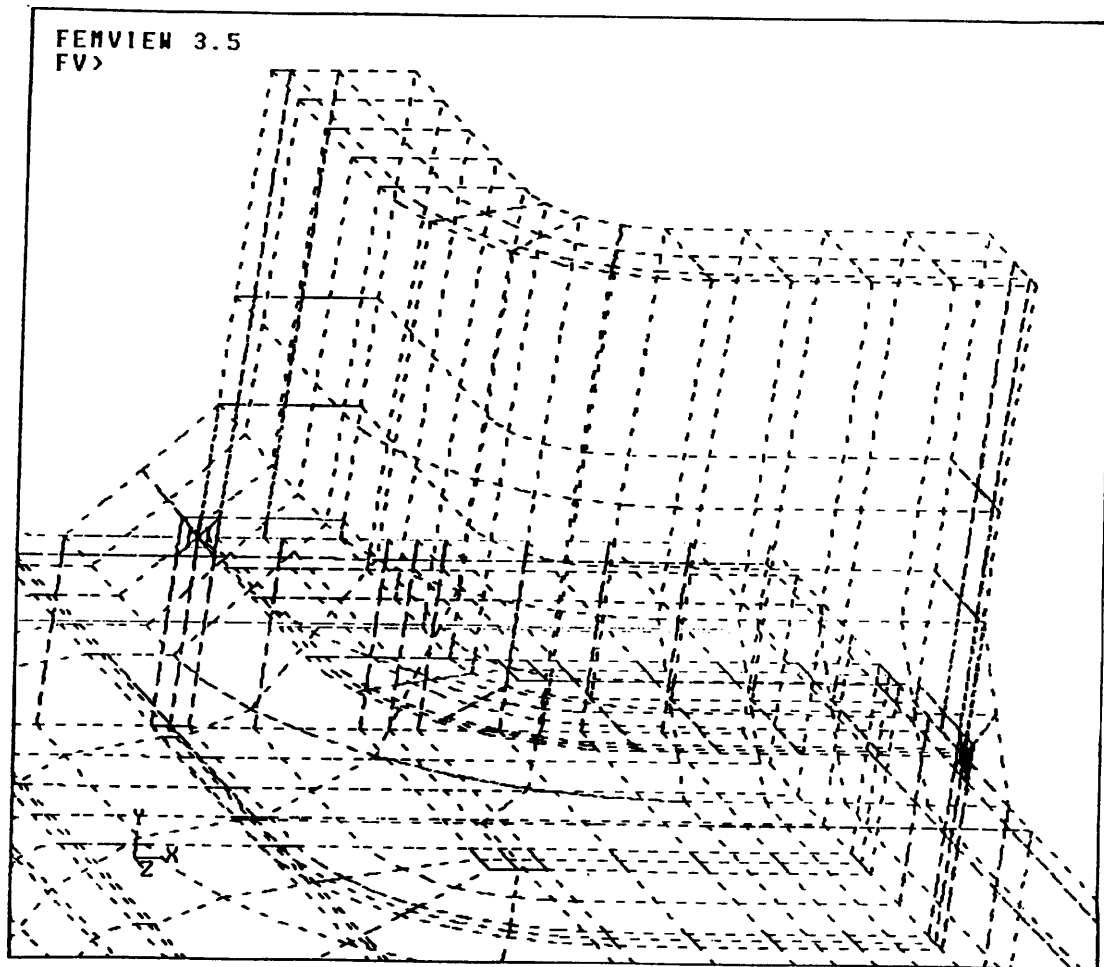


Fig. (5.16). Detailed Representation of Finite Element Model SHS Joint in the Intersection Area.

FEMVIEW 3.5
FV>

DISPLACEMENTS Y

FACTOR = .542E4

MAX = .203E-2

MIN = -.160E-3

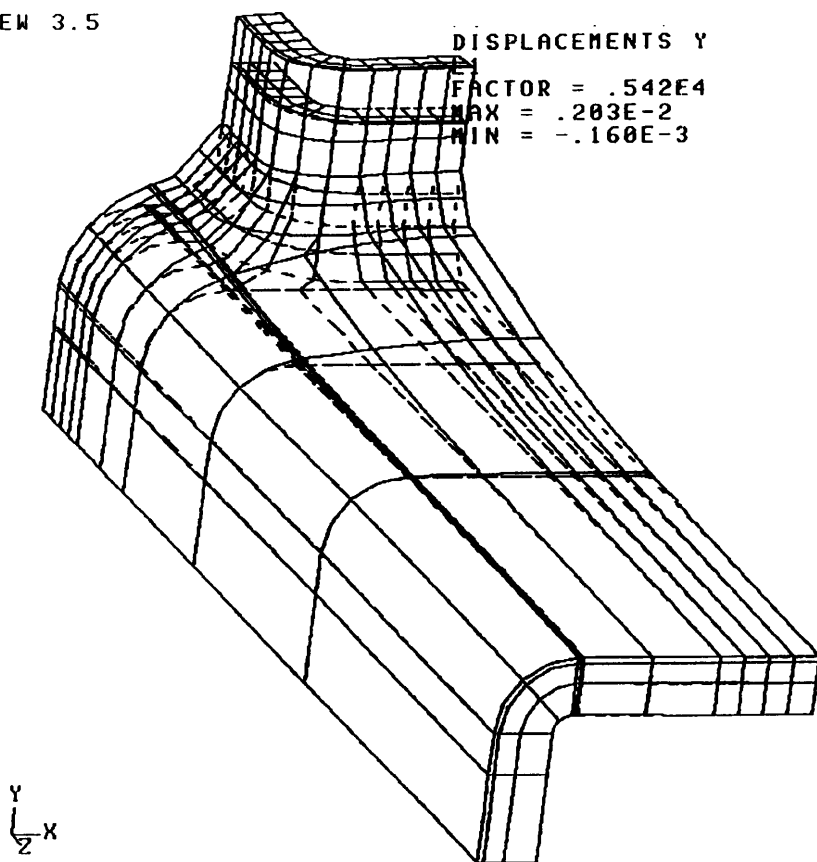


Fig. (5.17). Displaced Shape of a Typical Mesh of SHS Joint.

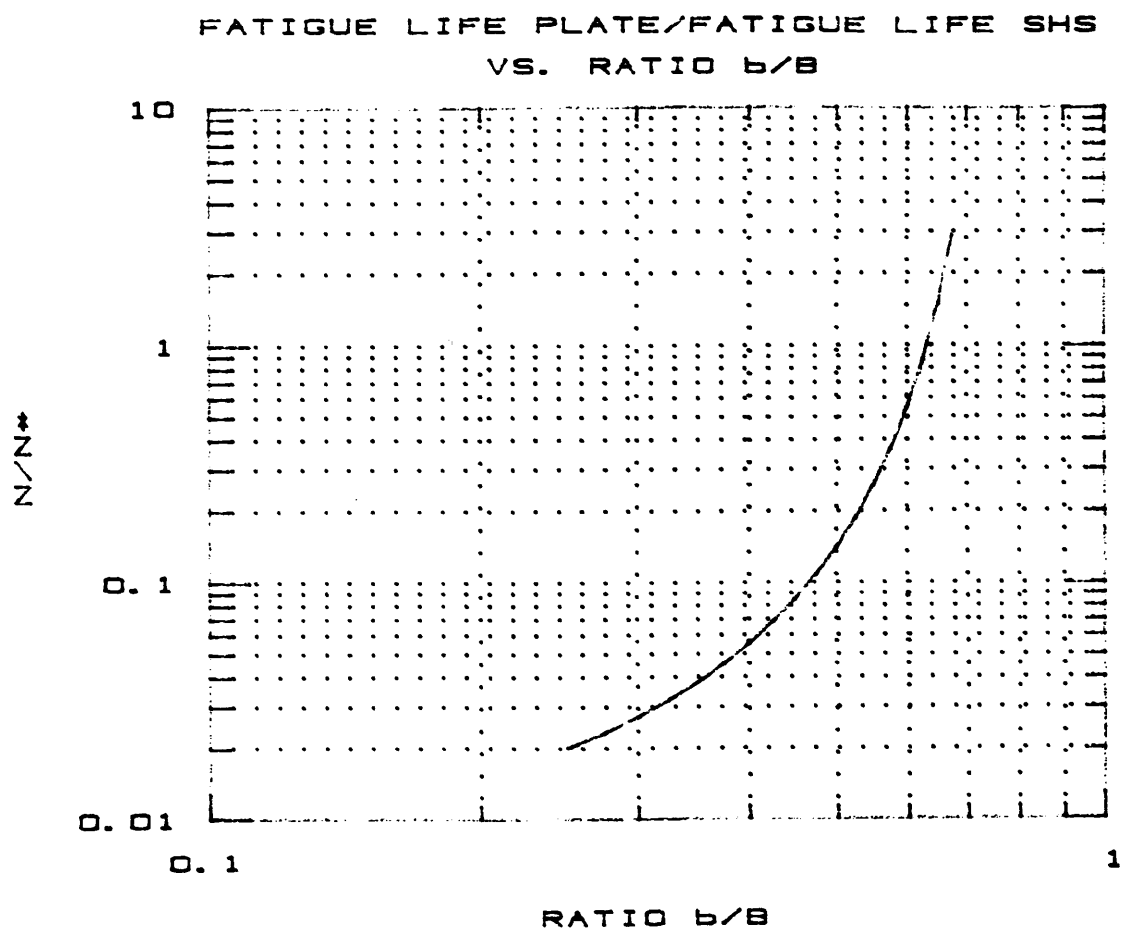


Fig. (5.18). Ratio Fatigue Life of Plate Joint to that of SHS Joint vs. Geometrical Ratio b/B .

CHAPTER SIX

THEORETICAL STUDY PHASE 3

6.0. Crack at the Weld Toe in SHS Connection

6.1. Finite Element Model and Results

CHAPTER SIX

THEORETICAL STUDY PHASE 3

6.0. CRACK AT THE WELD TOE IN SHS CONNECTION

In this chapter an exploratory attempt is made to examine the severity of conditions at the weld toe rather than on the fillet weld throat. A semi-elliptical crack was incorporated in a three-dimensional finite element model of the square hollow section fillet welded joint at the fillet weld toe position in an attempt to investigate the stress intensity factors at the crack tip. The finite element model used for this study is described together with the results for the particular joint and crack geometry modelled here.

6.1. FINITE ELEMENT MODEL AND RESULTS

Modelling a semi-elliptical crack at the toe of a fillet weld in SHS joints necessitates the use of a large number of elements. The finite element model used here was generated using FEMGEN which was used earlier for the generation of the three dimensional models in Chapter 5. The type of element used was the three dimensional 20-node brick element (C3D20R) with three degrees of freedom per node. The technique used for the efficient generation of the mesh was to generate the fine mesh needed around the crack and then build the body of the surrounding parts around that mesh. The mesh generated

around the semi-elliptical crack with the crack is shown Fig. (6.1) five layers of brick elements were used in the chord wall in the area surrounding the crack body. One quarter of the joint was modelled by taking advantage of symmetry. The mesh away from the crack body was similar in design to the type of mesh used earlier in Chapter 5. The semi-elliptical crack was placed at the toe area of the fillet weld with maximum depth of 0.4mm at the middle of the cross wall and of length equal to 19mm. The chord size was 120x120x5mm and the brace member was 60x60x5mm. The fillet weld leg length was 5mm. A cluster of eight crack tip elements were used around the crack tip. The number of elements C3D20R used was 1,337 and the total number of degrees of freedom = 24,000. The mesh allowed the estimation of the stress intensity factor at 17 positions along the crack front. J-contour integrals were evaluated at each crack front position and the results of the three contours around the crack tip were close except in the area where the crack meets the free surface and the crack depth becomes very small ≤ 0.1 mm. Further refinement could improve the results in this area. The J-integral values were averaged for the three contours, and the variation of the stress intensity factor calculated per unit brace stress along the crack front as a function of θ is shown in Fig. (6.2). The mesh is also shown in Fig (6.3).

The results confirm the viability of the approach, and if extended, would enable a comparison of susceptibility to failure at the weld toe and weld throat positions. Such an investigation is beyond the scope of the present programme.

The stress intensity factor per unit stress in the brace member at the fillet weld throat for the joint geometry analysed here with a semi-elliptical crack is higher ($= 7.03$) than that for the toe conditions Fig. (6.2), however, the finite element model attempted is for a notional crack depth of 0.4mm and positioned slightly away from the toe position, dictated by the complexity of the mesh needed to precise positioning of the semi-elliptical crack.

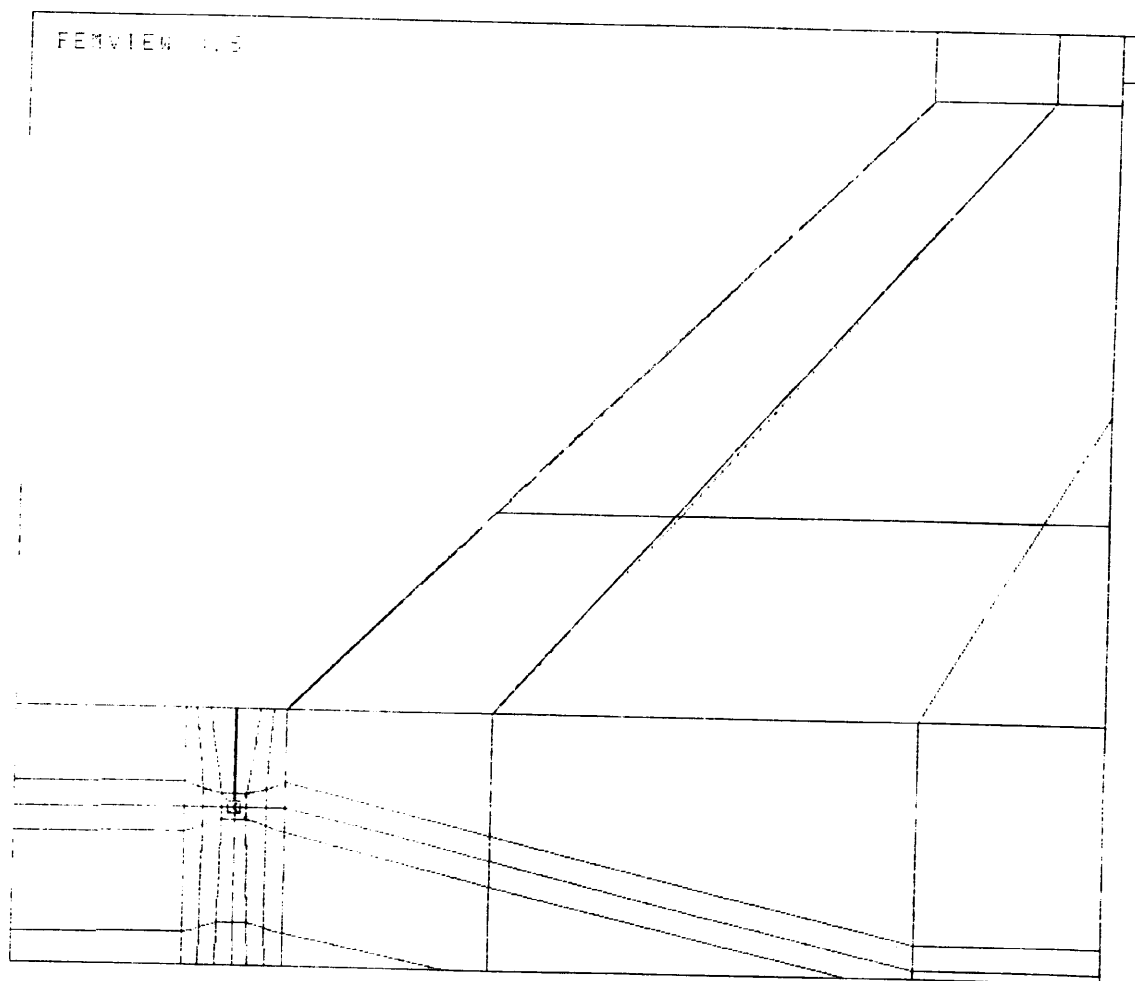


Fig. (6.1). Semi-Elliptical Crack in the Finite Element Mesh Analysed.

STRESS INTENSITY FACTOR PER UNIT STRESS IN THE BRACE
VS. POSITION ALONG THE CRACK FRONT

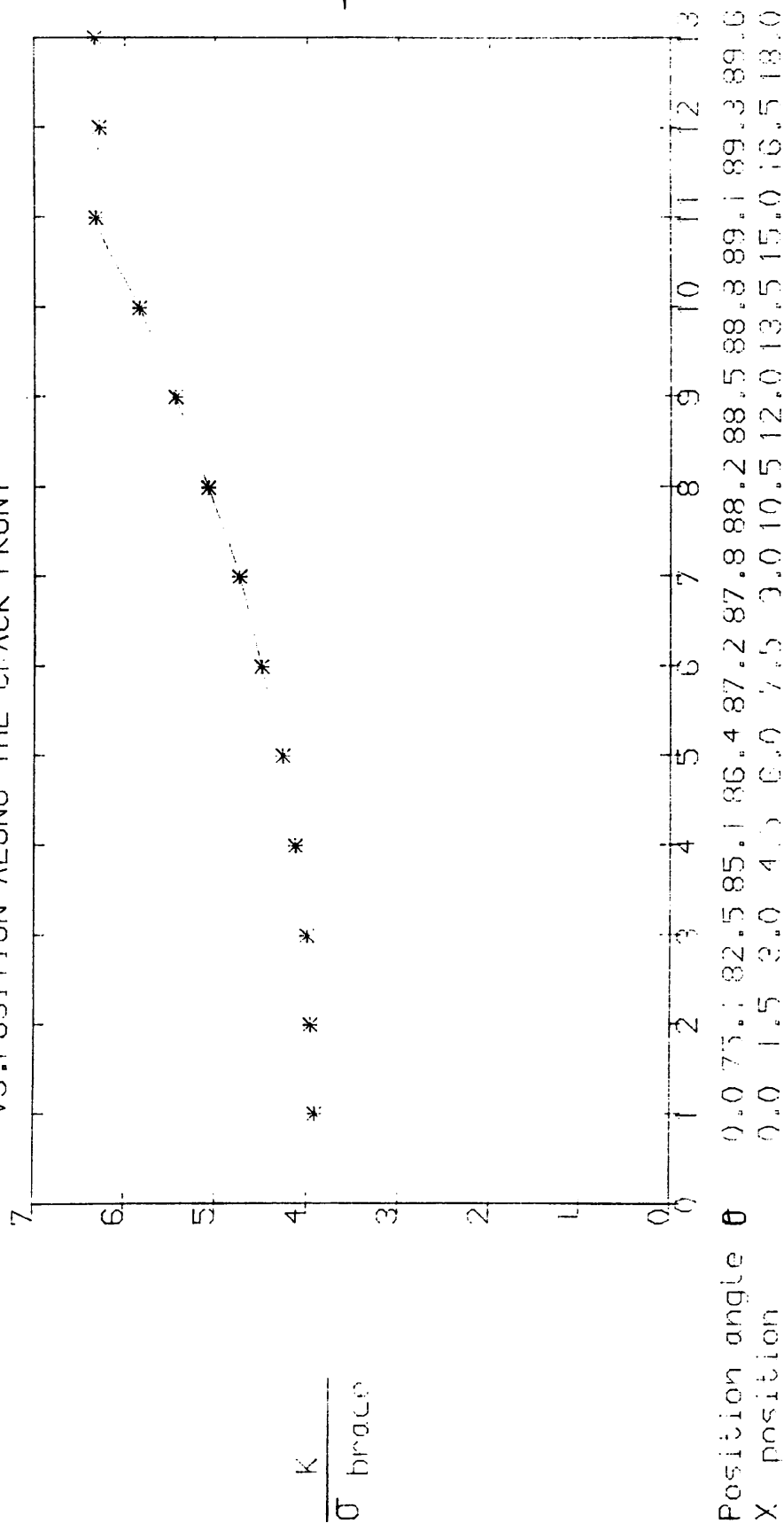


Fig. (6.2)

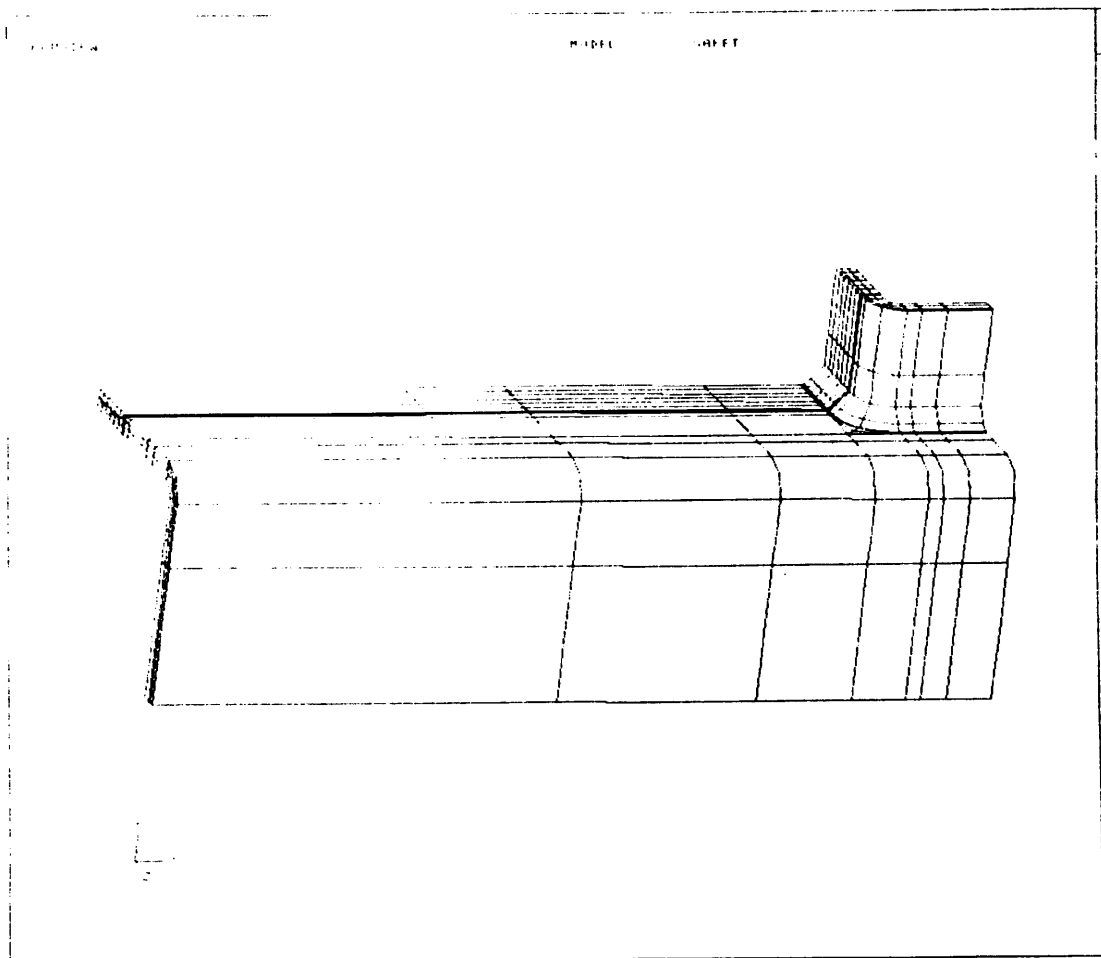


Fig. (6.3). Representation of the Finite Element Mesh.

CHAPTER SEVEN
EXPERIMENTAL PROGRAMME

7.0. General

7.1. Experimental Programme Part A

7.1.1. Cruciform Fillet Welded Joints (Plates)

7.1.2. Welding

7.1.3. Instrumentation and Test Procedure

7.1.4. Failure Mode and Test Results

**7.1.5. Comparison of Test Results with Behaviour
Predicted by Fracture Mechanics Analysis**

7.2. Experimental Programme Part B

7.2.1. Fillet Welded Joints (SHS Members)

7.2.2. Welding and Instrumentation

7.2.3. Test Procedure and Results

7.2.4. Mode of Failure for Tests HKS1, HKS2 and HKS3

7.2.5. Mode of Failure for Tests HKS4 to HKS7

**7.2.6. Comparison of Test Results With Behaviour
Predicted By Fracture Mechanics Analysis**

CHAPTER SEVEN
EXPERIMENTAL PROGRAMME

7.0 GENERAL

In previous chapters, fracture mechanics has been employed to analyse the fatigue behaviour of fillet welded joints of plates in Chapter Four, and SHS members in Chapter Five. These studies yielded quantitative information about the predicted influence of joint geometry upon the fatigue strength. The finite element method has been used to provide accurate estimates of stress intensity factors required for fatigue life estimations.

In this chapter the results of two pieces of experimental work conducted to study the fatigue behaviour of two types of fillet welded joints are described . The joints are stressed perpendicularly to the weld line and are referred to as load-carrying fillet welded joints.

The primary objectives of these tests were:

- 1) To study the behaviour of cruciform joints made of plates and SHS members.
- 2) To determine the stress range - life behaviour and the mode of failure of the joints.
- 3) To correlate the test results with the theoretically estimated fatigue strengths. This is accomplished by

using the stress intensity factors derived from the finite element analysis and fracture mechanics analysis to predict the crack growth behaviour of the joints analysed.

The two part programme was:

Part A:

Cruciform load-carrying fillet welded joints made of a main plate and two load carrying attachments welded transverse to the direction of the applied load.

Part B:

The basic form of the joints tested consisted again of a main member which in this case was a square hollow section member with two SHS attachment members fillet welded directly at right angles to the chord member.

These specimens were selected due to their suitability for testing in a tensile testing machine and they are representative of typical joints found in welded construction. Details of the joints tested, fabrication, test procedure, and results are given in the following two parts.

EXPERIMENTAL PROGRAMME PART A

7.1.1. CRUCIFORM FILLET WELDED JOINTS (PLATES)

The specimens tested were fabricated from 12mm, 25mm, and 50mm thick BS4360 [16] grade 50B plate material. Tables (7.1a, 7.1b, 7.1c) summarise the physical and chemical properties of the steel used. The main plate steel material was 50mm thick steel plate to BS 4360 grade 50D. The through thickness tensile test results provided by the metallurgists are given in Table (7.2). The complete specimens were fabricated from 200mm x 75mm x (12mm, 25mm, 50mm) attachment plates and 300mm x 75mm x 50mm main plates. The plates surfaces were cleaned lightly to remove the mill scale and dirt. The plate edges were also left square. The cruciform joint geometry is shown Fig. (7.1a).

The steel material was chosen in this programme to assure good weldability and avoidance of problems like lamellar tearing which may arise due to member thickness, joint design and welding stress. Lamellar tearing in steel plates can occur in the area of restrained welded joints as the result of shrinkage stresses across the thickness of the plate in the Z or through thickness direction. When stresses are applied in the through thickness direction as a result of weld joint detail as in the case of the cruciform joints in which stresses are transferred through the fillet welds into the main plate, separations may occur along the inclusion

boundaries. Hence the main plate material used for the joints tested in this programme had through thickness properties that improved its resistance to lamellar tearing.

7.1.2. WELDING

It is important when choosing a welding procedure to ensure compatibility of the material and the welding process. The important factors to be considered include composition of the base material and the welding consumables, and thermal input due to pre-heat and the welding process input. The carbon equivalent is an empirical expression which may be used to predict the hardenability and weldability of structural steels:

$$CE = C + Mn/6 + (Ni + Cu)/15 + (Cr + Mo + V)/5 \quad (7.1)$$

Equation (7.1) above was used to calculate the carbon equivalents for the steel material used and the values are given in Tables (7.1a, 7.1b, 7.1c). High strength low alloy steels with carbon equivalent up to 0.45% generally require the use of low hydrogen welding processes to avoid problems with cracking in the heat affected zone. Suitable pre-heat based on guidance given in BS 5135 [46] is 100°C based on the combined thicknesses used in the cruciform joints tested. It was important from the point of view of limiting the variation in weld sizes and ensuring reasonable weld profiles, to choose a welding process to achieve the required

aims. Specimens XI¹, XJ¹, Table (7.3), were fillet welded at UMIST using TIG process and specimens XI², XJ², Table (7.3), were welded, using MIG welding at the fabricators Robert Watsons.

7.1.3. INSTRUMENTATION AND TEST PROCEDURE

Alignment and axially of loading were important factors to be considered in these tests and care had been taken with the manufacture of the specimens. Strain gauges with a gauge length of 3mm were fitted to both sides of each attachment in test series XI¹, XI², to measure the stresses in the attachment plates and ensure axially of the load or otherwise record the stress conditions. Photograph (Fig. A1) shows an instrumented prepared test joint.

All specimens were tested in an Instron Servo-hydraulic testing machine under a constant amplitude cyclic stress. The wave form applied was generated using a Generator Programme mounted on HP9133 computer which controls the testing machine. All tests were conducted under computer control which enables the amplitude, frequency and mean level positions to be adjusted with great flexibility and precision with feed back from the machine. The average frequency used was 20Hz. Tests were also carried out with the machine in load control mode. The advantage of this is that it gives greater control of the loading applied and maintains the loading conditions required better than displacement mode.

The stress range in the fillet weld throat was selected as the controlled experimental variable. The stress range applied in each test was based on the average throat thickness measured for each specimen. The stress ranges on the fillet weld throat were adjusted after the tests based on actual throat thicknesses measured. The tests were run continuously until the specimens fractured. The controlling computer is equipped with a holding feature which enables the programming to hold the test when a limit either on load or displacement is violated. This feature safeguards against overloading the specimens and stops the test when specimens fracture. Details of the geometries of cruciform fillet welded joints tested are given in Table (7.3).

7.1.4. FAILURE MODE AND TEST RESULTS:

The results of the fatigue tests are summarised in Table (7.4). The fatigue strengths observed experimentally are tabulated against the stress ranges on the fillet weld throats. All specimens have failed from cracks which propagated from the initial flaw at the weld root. This discontinuity is due to the unpenetrated depth between the fillet welds. The ratio of the fillet weld leg length to the size of the unpenetrated depth is also given in Table (7.4), which provides the important parameter used in the analytical study described earlier in Chapter 4 to estimate the fatigue life integral and consequently the fatigue strength at cruciform fillet welded joints. The path of the fatigue crack

was observed to be close to the main plate until failure occurred by a final tear fracture.

The test results are plotted in Fig (7.2) where fatigue life of the specimens tested is plotted as a function of stress range on the fillet weld throats.

7.1.5. COMPARISON OF TEST RESULTS WITH BEHAVIOUR PREDICTED BY FRACTURE MECHANICS ANALYSIS

The fatigue behaviour of the cruciform joints tested in this experimental study is evaluated using the principles of fracture mechanics and the results of the theoretical study conducted using the finite element method. The dimensions of the tested joints measured, after the tests were completed, have been used to predict the fatigue strengths. The procedure followed is based on the use of equation (4.21) derived earlier in Chapter 4 by integrating the classical Paris Law from the initial geometrical ratio (a_i/w), where a_i is the initial crack size which is equal to half the unpenetrated depth size observed experimentally to (a_f/w), the limiting ratio. Equation (4.21) which is used to estimate the fatigue life of a cruciform joint is also given here:

$$N = I / (S_p)^3 \sqrt{W} \quad C \quad (7.2)$$

Where S_p is the stress range in the attachment plate which could be converted to stress range on fillet weld throat for design purposes,

W is the width of the joint,

C is the Paris Law constant taken in steel as
 2.0×10^{-13} N, mm units,

I is the fatigue life integral and is given as:

$$I = 0.43481 (L/t_p)^{2.6158} \quad (7.3)$$

where L is the fillet weld leg length,

t_p is the attachment plate thickness for zero fillet weld penetration, or the unpenetrated depth size for partial penetration.

The theoretical estimates of the fatigue strength of the joints tested are given in Table (7.4), and also plotted for the applied stress ranges on the fillet weld throat, Fig. (7.3). The fatigue strengths calculated theoretically are lower than the fatigue strengths observed experimentally. The theoretical results coincide with the lower bound curve of the experimental results. This curve can be used for conservative design. More tests are needed to investigate the geometrical effects fully.

EXPERIMENTAL PROGRAMME PART B

7.2.1. FILLET WELDED JOINTS (SHS MEMBERS)

The experimental study described in this section involves fatigue tests on fillet welded joints made of square hollow section members. Two combinations of β (the brace width/chord width) were studied experimentally to investigate the influence of joint geometry on the fatigue behaviour of these joints. Grade 43 steel was specified for both the chord and the brace members. The chord members used were formed from 255x255x10mm thick square hollow section and 154x154x10mm thick sections. The nominal size of section for the brace was 100x100x10mm thick square hollow section for all the joints tested. Thus the ratios of β were 0.39 and 0.65. .

7.2.2. WELDING AND INSTRUMENTATION

A welding jig frame was designed at UMIST by A. Kirk in an effort to ensure that the brace members were welded in line, thus ensuring axially of loading. Details of the welding frame design are given in Fig. (7.4) Great care was taken with the manufacture of the specimens and the preparation for welding. The joints were fillet welded using the MIG process at the fabricators Robert Watsons.

Each specimen was fitted with eight strain gauges to monitor the stresses in the brace members and check the alignment of the joints tested.

7.2.3. TESTED PROCEDURE AND RESULTS

A total of seven specimens were tested under fatigue loading in an Instron Servo-hydraulic testing machine. The tests were conducted under constant amplitude cyclic stress. The geometrical conditions of the joints tested are given in Table (7.5). The wave form applied was generated using the Generator Programme mounted on an HP 9133 computer which controls the Instron machine. All tests were conducted under computer control in the load control mode, and test frequency averaged 15 Hz. The stress range in the fillet weld throat was calculated based on the average throats measured before the tests.

The results from the strain gauges fitted to the attachments showed axially of loading was reasonably ensured. The stress ranges calculated on the fillet weld throats are given in Table (7.6) against the fatigue strengths of each joint observed experimentally. Photograph (A7) shows the square hollow section joint HKS in the testing machine ready to be tested. And photograph (Fig. A8) shows the full test arrangement and monitoring equipment.

The results of the seven square hollow section joints are plotted in Fig (7.5). The fatigue strengths observed experimentally are plotted for the stress ranges on the fillet weld throats applied.

7.2.4. MODE OF FAILURE FOR TESTS HKS1, HKS2 AND HKS3: $\beta = 0.39$

Joint HKS1 was the first joint tested. This specimen was accidentally overloaded initially on the first load application and was statically loaded and unloaded in the reverse direction to eliminate the curvature (-150KN, + 80KN, - 150 KN). The specimen was then tested under much lower loading conditions. It failed by fatigue cracks observed with a magnifying glass at the toe of the fillet welds on chord side wall, similar cracking appeared on the other chord member on the opposite side.

Specimens HKS2 and HKS3 were then tested at nearly the same stress conditions as HKS1 without the prior overload. Again failure modes were identical to the first test but they had a much lower fatigue life than the specimen HKS1 which had been overloaded. The fatigued specimen HKS2 is shown in photographs (Fig. A5). This photograph shows the toe failure.

7.2.5. MODE OF FAILURE FOR TESTS HKS4 TO HKS7: $\beta = 0.65$

Specimen HKS4 was fatigue tested and failed by cracks observed in the fillet welds and first observed in the weld at the side and then round the joint. Stress intensity factors predicted theoretically were close for the side and

cross wall mid positions, which could explain, together with the variability in weld profile, the start of cracking at that position.

Identical failure modes were observed for tests HKS5, HKS6 and HKS7. The last two tests HKS6 and HKS7 were tested at higher stress ranges on the fillet weld throats to establish an approximate S-N curve for these geometries. Failure for all the specimens tested was specified either due to the complete separation of one or both of the braces or due to the propagation of a crack to such an extent that proper load application was no longer possible. Photograph (A6) shows the weld failure.

7.2.6. COMPARISON OF TEST RESULTS WITH BEHAVIOUR PREDICTED BY FRACTURE MECHANICS ANALYSIS

The fatigue behaviour of the SHS joints tested in this part of the experimental study in which fatigue occurred through the fillet weld throat HKS4 to HKS7 is evaluated using the fracture mechanics principles and based on the theoretical findings in Chapter 5. The procedure is based on evaluating the M_g factors for the joints tested using equation (5.1) which described M_g as a function of β . The fatigue life is then estimated using equation (5.11) given here also.

$$N^* = N / (M_g)^3 \quad (7.3)$$

where N is the fatigue life of the cruciform fillet welded

joint made of plates for which the procedure for evaluation is given in Chapter 4 and in the first part of this chapter. The calculated fatigue strengths are given in Table (7.6). The results obtained are in good agreement with the observed fatigue strengths experimentally. Despite the fact that the number of specimens tested is small, the choice of geometries tested provided vital information on the modes of failure and the influence of geometrical ratios such as β on forcing failure either through the chord wall at the toe of the fillet welds as in tests HKS1 to HKS3 which $\beta = 0.39$ or through the fillet weld throat for tests HKS4 to HKS7 with $\beta = 0.65$.

The results of tests conducted by F. Mang, and O. Bucak [47] on square hollow section joints with geometrical parameter like HKS4 to HKS7 are given as the curve in Fig (7.5). The theoretical results are close to the experimentally observed fatigue strengths for tests HKS4 to HKS7. Further tests would be necessary to investigate the fatigue behaviour of these joints with different β ratios.

7.3. SPATE

General Description of the Technique

When a solid body is subjected to stress fluctuations, small temperature changes are produced which in turn give rise to emissions of infra-red radiation from the surface of the body. If these emissions are measured the stress distribution in the body could be studied. A sensitive detector/display

equipment is available which responds to the infra-red emissions resulting from the temperature changes. The detector operates in a scanning mode and the received signals can be displayed in the form of a colour-contoured plot. The signal received is proportioned to the sum of the principals stress changes.

Research has been carried out at UMIST [48] on the use of SPATE to study the stress patterns in welded samples of transverse fillet welded plates and on model tubular T-joints, and showed the same trends as finite element and other stress analysis methods for the stress concentrations due to the geometric shape.

The SPATE system has a limited resolution and the use of the system to detect accurate values in high stress gradients like the stress gradients at crack tips and estimate the stress intensity factors is not possible.

The SPATE system is used here in this research to show the stress pattern qualitatively in one of the cruciform joints tested. The colour-contoured plot of the signal received from the end face of the cruciform joint showing the pattern of stress in the attachments, welds and the middle plate is given in (Fig. A9). The pattern shows that high stresses exist in the weld root area.

Table 7.1a Chemical and Physical Properties

Description:

200mm x 80mm m 12mm Plate to BS 4360-50B

Physical Properties

Yield stress N/mm ²	Tensile Strength Nmm ²	Elongation %
398	538	27

Chemical Analysis

C%	Mn%	Si%	S%	P%
0.15	1.33	0.40	0.013	0.017

CE = 0.37%

Table 7.1b Chemical and Physical Properties

Description:

200mm x 80mm x 25mm Plate to BS 4360-50B

Physical Properties:

Yield Stress N/mm ²	Tensile Strength N/mm ²	Elongation %
355	534	26

Chemical Analysis

C%	Mn%	Si%	S%	P%
0.16	1.14	0.44	0.023	0.006

CE = 0.35%

Table 7.1c. Chemical and Physical Properties

Description:

200mm x 80mm x 50mm. Plate to BS 4360-50B

Physical Properties:

Yield stress N/mm ²	Tensile Strength Nmm ²	Elongation %
393	515	30

Chemical Analysis

C%	Mn%	Si%	P%	Mo%	Cr%	Ni%	CV%
0.108	1.50	0.391	0.016	0.012	0.024	0.29	013

V%	S%	AL%
0.004	0.003	0.044

CE = 0.37%

Table 7.2 **Physical and Chemical Properties**

Specification - Plate 300mm x 80mm x 50mm thick.

BS 4360 - 50D

Through thickness tensile tests

	Test 1	Test 2
Test piece diameter (mm)	4.5339	4.5339
Section area (mm ²)	16.150	16.150
Yield Stress (N/mm ²)	394	386
Tensile Strength (N/mm ²)	550	547
Elongation on G.L. 4A - %	30	30
Reduction of Area - %	64	63

Chemical Analysis:

C%	Mn%	Si%	P%	So%	Cr%	Nb%	V%
.178	1.39	.403	0.011	0.008	0.024	0.026	0.002

$$CE = 0.41$$

Table 7. 3 Geometries of Cruciform Fillet Welded Joints Tested (Plates).

Joint	tp	T	L
	Attachment Size mm	Baseplate mm	Leg Length mm
XI ¹ ₁	10.75	50.0	7.38
XI ¹ ₂	10.79	50.0	7.99
XI ² ₃	11.00	50.0	8.57
XI ¹ ₄	23.8	50.0	8.58
XI ² ₅	23.75	50.0	8.92
XI ² ₆	24.27	50.0	9.01
XI ² ₇	24.38	50.0	9.28
XI ¹ ₈	49.77	50.0	8.93
XI ¹ ₉	49.34	50.0	7.22
XI ¹ ₁₀	49.48	50.0	9.40
XI ² ₁₁	49.26	50.0	9.32
XI ¹ ₁₂	48.93	50.0	9.9
XI ² ₁₃	49.49	50.0	12.5
XI ² ₁₄	48.9	50.0	12.90
XI ² ₁₅	48.58	50.0	11.77
XI ² ₁₆	49.0	50.0	12.70
XJ ² ₁	12.32	50.0	8.89
XJ ² ₂	12.28	50.0	7.92
XJ ¹ ₃	12.37	50.0	6.15
XJ ¹ ₄	12.33	50.0	7.31
XJ ¹ ₅	12.47	50.0	6.90
XJ ¹ ₆	12.37	50.0	6.21
XJ ¹ ₇	24.81	50.0	8.13
XJ ¹ ₈	24.90	50.0	8.27
XJ ¹ ₉	24.91	50.0	8.62
XJ ¹ ₁₀	24.85	50.0	7.72
XJ ¹ ₁₁	24.82	50.0	9.31
XJ ¹ ₁₂	24.90	50.0	9.22
XJ ¹ ₁₃	24.87	50.0	9.56
XJ ² ₁₄	50.0	50.0	8.10
XJ ¹ ₁₅	49.89	50.0	9.74
XJ ¹ ₁₆	50.0	50.0	10.17

Table 7.4 Fatigue Test Results and Predicted Theoretical Fatigue Strengths On Fillet Welded Plate Joints

Test	R Ratio	L/tp	Stress Range On Weld Throat N/mm ²	Exp Life Cycles	Theo Cycles	Theo/Exp
XI ¹ ₁	0.12	0.61	115.9	193094	133574	0.69
XI ¹ ₂	0.04	0.87	91.9	315177	223473	0.71
XI ² ₃	0.04	0.79	104.3	219758	163469	0.74
XI ¹ ₄	0.13	0.39	93.9	223760	231745	1.04
XI ² ₅	0.05	0.39	106.8	182340	157365	0.86
XI ² ₆	0.04	0.41	100.9	212762	185098	0.87
XI ² ₇	0.04	0.40	103.7	203896	166420	0.82
XI ¹ ₈	0.04	0.21	86.7	349920	285440	0.82
XI ¹ ₉	0.05	0.20	83.9	336432	319918	0.95
XI ¹ ₁₀	0.05	0.26	82.5	350478	309469	0.88
XI ² ₁₁	0.12	0.21	84.6	1048345	296847	0.28
XI ² ₁₂	0.10	0.21	94.3	417422	216462	0.52
XI ² ₁₃	0.05	0.27	92.3	711087	203111	0.29
XI ² ₁₄	0.05	0.28	98.5	250420	163132	0.65
XI ² ₁₅	0.05	0.25	98.1	498558	173138	0.35
XI ¹ ₁₆	0.06	0.28	97.2	1470000	170011	0.12
XJ ² ₁	0.10	0.76	97.0	404972	188809	0.47
XJ ² ₂	0.10	0.72	96.9	551103	190343	0.35
XJ ¹ ₃	0.10	0.52	95.2	286179	251086	0.88
XJ ¹ ₄	0.12	0.82	90.3	320915	247370	0.77
XJ ¹ ₅	0.11	0.71	89.1	332978	262978	0.79
XJ ¹ ₆	0.11	0.61	95.9	352766	238502	0.68
XJ ¹ ₇	0.06	0.39	87.2	548793	280741	0.51
XJ ¹ ₈	0.09	0.35	107.1	233625	152803	0.65
XJ ¹ ₉	0.10	0.43	88.4	313498	260732	0.83
XJ ¹ ₁₀	0.96	0.37	93.6	332655	238502	0.72
XJ ¹ ₁₁	0.95	0.42	88.8	268899	255390	0.95
XJ ¹ ₁₂	0.11	0.44	86.0	338652	280630	0.83
XJ ¹ ₁₃	0.08	0.46	84.5	407589	290030	0.71
XJ ² ₁₄	0.10	0.28	98.7	253410	159213	0.63
XJ ¹ ₁₅	0.11	0.17	97.3	547723	213267	0.39
XJ ¹ ₁₆	0.10	0.21	83.4	474079	303540	0.64

Table 7.5 Geometries of Tests (SHS Joints)

Test	Cord Size	Brace Size	b/B	t/T	L/t
HKS1	255x255x10mm	100x100x10mm	0.39	1.0	0.70
HKS2	255x255x10mm	100x100x10mm	0.39	1.0	0.68
HKS3	255x255x10mm	100x100x10mm	0.39	1.0	0.63
HKS4	154x154x10mm	100x100x10mm	0.65	1.0	0.76
HKS5	154x154x10mm	100x100x10mm	0.65	1.0	0.77
HKS6	154x154x10mm	100x100x10mm	0.65	1.0	0.70
HKS7	154x154x10mm	100x100x10mm	0.65	1.0	0.69

Table 7.6 Fatigue Test Results (SHS Joints)

Test	R Ratio	Stress Range On Weld N/mm ²	Life Cycles
HKS1	0.051	50.19	348131.0
HKS2	0.073	48.98	67511.0
HKS3	0.062	50.45	50590.0
HKS4	0.065	60.40	1.531196x10 ⁶
HKS5	0.056	56.69	1.88761x10 ⁶
HKS6	0.074	98.49	168017.0
HKS7	0.072	96.7	289228.0

**Table 7.7 Comparison Between Fatigue Test Results and
Theoretically Predicted Results (SHS Joints)**

Test	Stress Range On Weld N/mm ²	Experimental Life	Theoretically Predicted Life	Theo/Exp
HKS1	60.40	1.531196x10 ⁶	1.098271x10 ⁶	0.717
HKS2	56.69	1.88761x10 ⁶	1.316854x10 ⁶	0.67
HKS3	98.49	168017.0	265071.0	1.5
HKS4	96.7	289228.0	283679.0	0.98

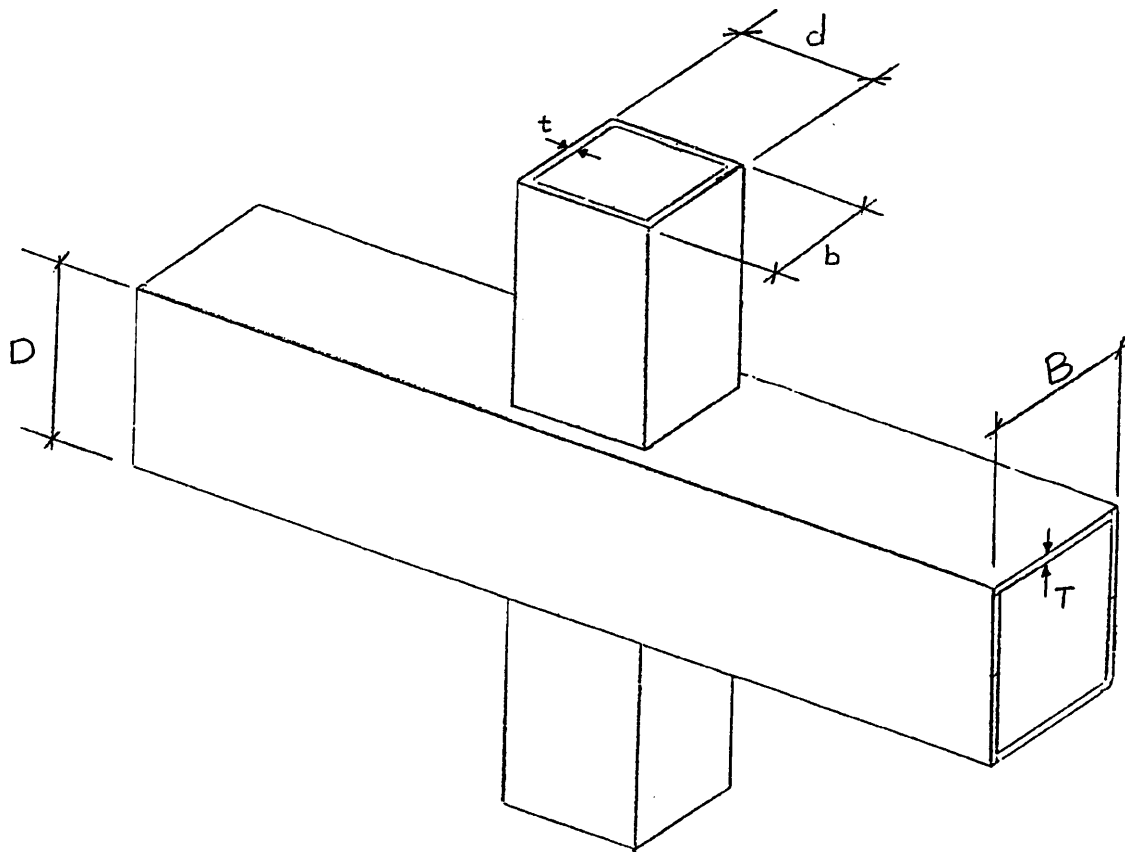


Fig - 7.1-

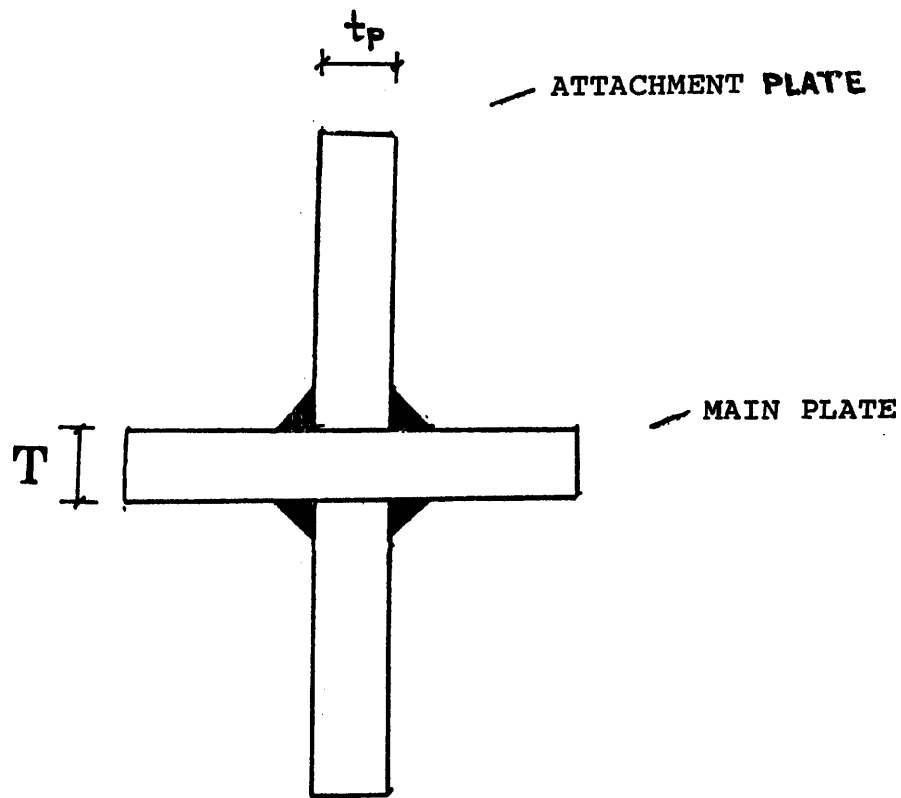
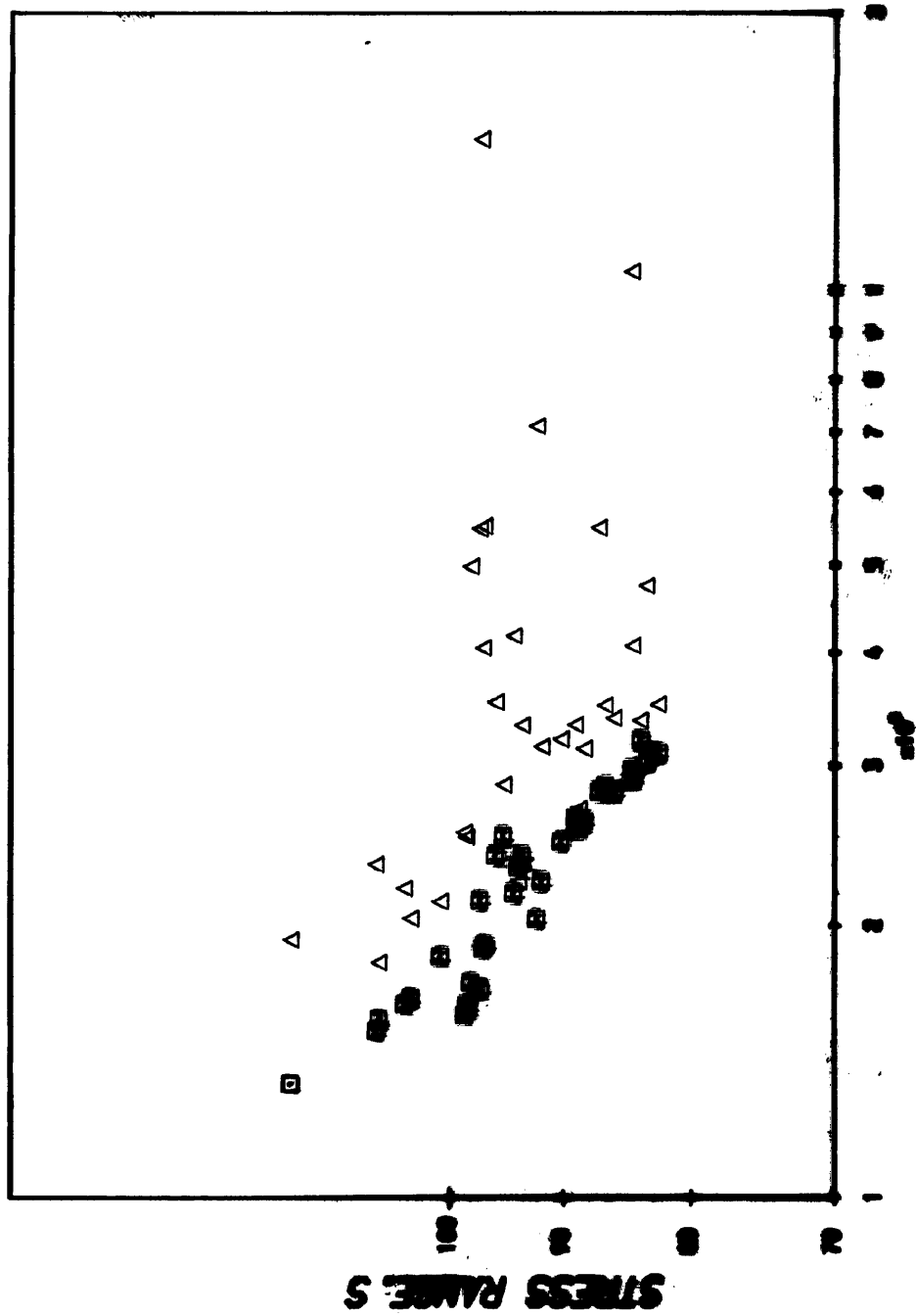


Fig. (7.1a). Cruciform Fillet Welded Joint (Plates)

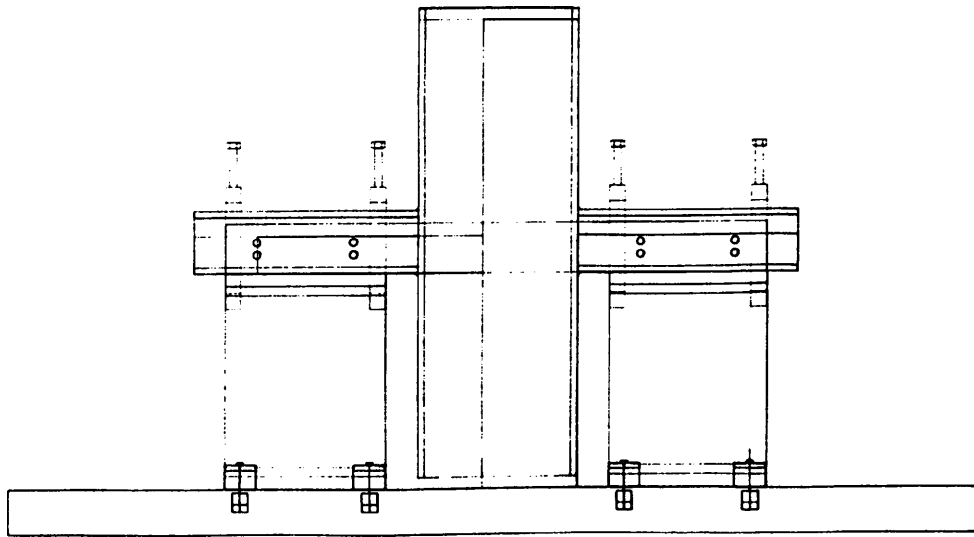
STRESS RANGE ON EILLET YELD THROAT VS. ENDURANCE N (EXPERIMENTAL RESULTS)

STRESS RANGE ON EILLET YELD THROAT VS. ENDURANCE N (THEORETICAL RESULTS)

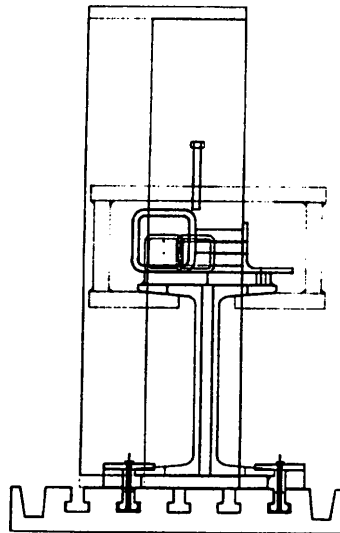


N. CYCLES **P. 9. 10**

Fig - 7.2 -



Front Elevation of the Welding Jig Arrangement



Side Elevation of the Welding Jig Arrangement

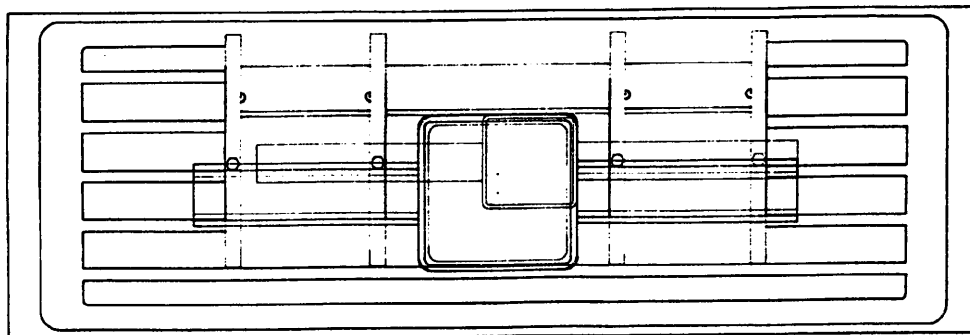


Fig. (7.4). Details of the Welding Jig for SHS Joints.

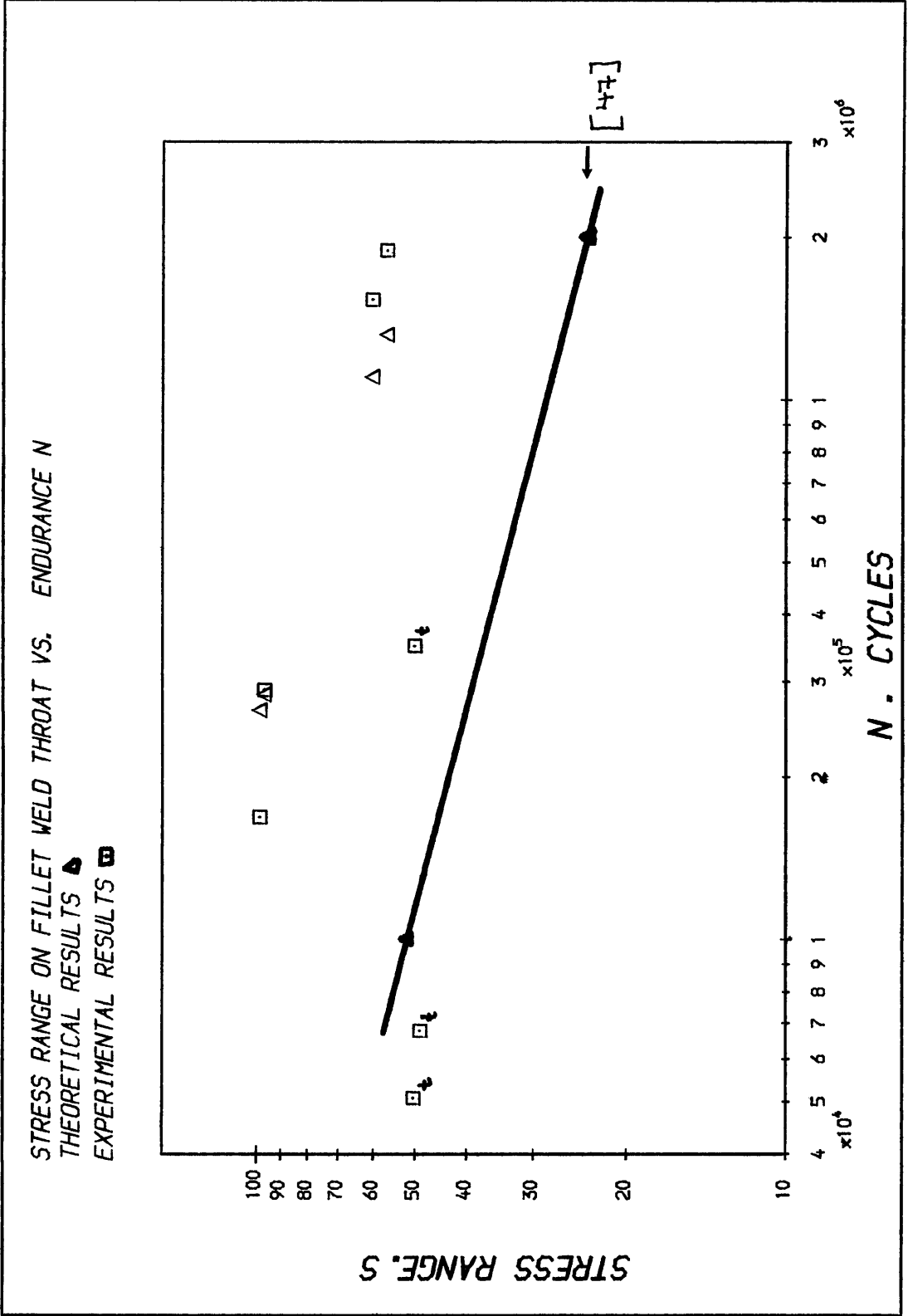


Fig- 7.5 -

CHAPTER EIGHT

8.0. Discussions

8.1. Conclusions

CHAPTER EIGHT

DISCUSSION

The theoretical work used in this research to study the fatigue behaviour of fillet welded connections of plates and square hollow sections was conducted using the finite element method and the fracture mechanics approach. The finite element method was used as a powerful tool to study the behaviour of the described joints. This involved significant 2-D and 3-D analyses to study the geometrical effects on the stress intensity factors at the fillet weld root position. Generally for a given geometry and loading the stress distribution can be expressed as non-dimensional ratios and, scaled with the size of a component. Thus for the cruciform fillet welded joints of plates analysed in Phase 1 of the theoretical study, the general stress distribution will remain the same regardless of the size of the connection provided there are no geometric changes. This distribution, as has been shown earlier, consists of a nominal stress field due to the loading on the attachment members, and a local high stress gradient near the fillet weld root or toe. The stress intensity factor on the other hand is a function not only of the relative crack size/width ratio which scales with components size but also the crack size absolutely. Thus the stress intensity factor will vary with overall component size. This behaviour is visualised when one studies the results of the in depth finite element analysis on both the

cruciform fillet welded plate joints and the SHS members joints. Increasing the attachment size increases the stress intensity factor at the fillet weld root. On the other hand increasing the weld size reduces the stress intensity factors, whilst the main plate thickness has little effect on SIF in the fillet weld.

A general parametric relationship has been developed from the finite element analysis results relating the normalised stress intensity factors using finite width correction formula and the geometrical conditions of the joint. Further a fracture mechanics calculation was developed to predict the fatigue strength of welded joints. The results are presented in a family of design curves comparable with S-N design curves in BS5400, part 10.

The fatigue strengths estimated showed variations in life by factors of the ratio of 4 for ratios of fillet weld leg length to attachment plate thickness varying from 0.1 to 1.2 at the same attachment thickness (weld size effect). When the attachment thickness was varied from 12mm to 50mm a deterioration in life by a factor of 2 is predicted at the same stress range (thickness effect). All of these cases are treated as the same category W in the design codes.

For practical fillet weld sizes in the range 5mm to 12mm leg length, the variation in fatigue life over the plate thicknesses 12mm to 50mm is of the order of two, although

larger variations would be predicted for higher attachment thicknesses.

The theoretical results are compared with the current design recommendations for class W in Figs. (4.19 - 4.21). Clearly there is reasonable agreement. It should be borne in mind that the fracture mechanics results do depend on the constants assumed in the Paris ~~crack~~ propagation law, and could therefore be calibrated by a sufficient data bank of experimental results. The experiments in this programme were insufficient in number to be definitive, but were in broad agreement. The theoretical results were in good agreement with those of Frank and Fisher, but the present analysis gives a simpler presentation of stress intensity factors and fatigue performance by parametric formulae.

The most important aspect of the theoretical results is confirmation that a geometric thickness/size effect exists for fatigue failure in fillet welds just as it does for fatigue cracks growing in plate from the toe of fillet welds. Present design rules do not allow for this effect for class W, fillet weld details on the weld throat.

The experimental tests in this programme showed significant effects due to slight misalignment of the attachments and special precautions had to be taken by machining completed specimens. Without these precautions, found necessary as a

result of strain gauging individual specimens, considerable scatter occurred in results. Routine testing by other laboratories must be expected to give rise to such scatter for cruciform type tests. Further variability occurred due to weld root defects and variations in weld size. Great care is essential in experimental work to obtain consistent results, and the implications for service structures need to be considered carefully.

In phase 2 of the theoretical study again geometrical effects on stress intensity factors were evaluated and the results showed that the bending of the wall thickness of the chord member elevated the stress intensity factors at the fillet weld root,. Increasing the ratio of brace width to chord width increased the stress intensity factor, also increasing the brace wall thickness increased the stress intensity factors. Increasing the weld size as in phase one decreased the stress intensity factors. A parametric relationship was developed which related the stress intensity factors for the 3-D finite element analysis,

normalised by the 2-D finite element analysis results for the plate joints, to the geometrical ratios . This relationship was used in a fracture mechanics based calculation to estimate the fatigue strength of SHS joints, and the results were expressed in relation to the fatigue strength of fillet welded plate joints. The use of these findings for the estimation of fatigue strengths which are completely based on the finite element results and the

use of fracture mechanics principles is a sound alternative to the empirical design methods which are based on assessing tests results and which are often valid only over the tested joint range. Experimental results are required to calibrate the theoretical approach. The analysis conducted using the finite element in which a semi-elliptical crack was incorporated in the SHS joint at the fillet weld toe showed that this approach could be developed with further study, to indicate the design behaviour for weld toe failure.

The experimental work conducted on cruciform fillet welded joints of different attachment sizes and weld leg lengths despite the scatter in the results obtained showed that theoretical estimates of the fatigue strengths corresponded with the lower bound curve to the experimental results. This indicates that the use of the theoretical recommendations for the design of cruciform joints will result in a safe design. The results of the tests conducted on square hollow section joints on the other hand despite the small number of tests conducted revealed very valuable information regarding the fatigue behaviour of such joints and the modes of failure. On comparing the theoretically estimated fatigue strengths with the experimental results good correlation is found for the specimens which failed in the fillet weld with $\beta = 0.65$. In both the cruciform joints and the SHS member joints further tests are recommended.

8.1. CONCLUSIONS

In the light of the work reported in this thesis the following conclusions can be drawn:

1. The suitability and value of the finite element method for the parametric study of the fillet welded joints of plates and square hollow section members has been established in this investigation.
2. The accuracy of the finite element results for both general stress distribution and stress intensive factors due to the unpenetrated thickness between the fillet welds has been confirmed by comparison with results obtained by other investigations, namely Frank for the cruciform fillet welded joints of plates, and by comparing the results from the J-Integrals with those predicted using crack opening displacement formulae.
3. Parametric relationships have been developed from the in depth finite element analysis in phase 1 on plate fillet welded joints and in phase 2 on the square hollow section joints which related the stress intensity factors at the fillet weld root position with geometry.
4. The stress intensity factors at the fillet weld root increased with increasing the attachment thickness in the plate and SHS joints and decreased with increasing the fillet weld leg length. The bending of the wall of the chord member

in SHS joints magnified the stress intensity factors at the toe.

5. The effect of misalignment investigated in phase 1 indicated that its presence in cruciform joints of plates causes secondary stresses which increase the stress intensity factor at the fillet weld root. A relationship was established which relates the stress intensity factors with the joint geometrical parameters. The total effect is to magnify the stress conditions.

6. An exploratory finite element study was conducted in Chapter 6 in which semi-elliptical crack was incorporated in a 3-D model of SHS joint. This confirmed the practicability of the approach to investigate cases when fatigue failure would occur preferentially at the weld toe as opposed to on the weld throat, but further investigation is beyond the scope of the present programme.

7. The use of fracture mechanics principles in this thesis to estimate the fatigue strength of plate fillet welded joints yielded a family of curves relating the stress ranges on the fillet weld throat to the fatigue strength for the geometrical conditions of the joint. These findings were in good agreement with those of Frank. The code of practice recommendation for the design of load carrying fillet welded joints class W does not take account of different geometry effects and results in uneconomical joints in certain plate

thicknesses and in unsafe design for attachment size 25mm with ratios of weld leg length to attachment size greater than 0.5.

8. The fracture mechanics calculation performed for SHS joints resulted in the derivation of a fatigue strength equation which related their strengths to that of plate joints using a stress intensity magnification factor. This provides a basis for much simpler and improved design guidance than that based on empirical findings.

9. The experimental fatigue plate joints resulted in lower bound curve that matched the theoretical predictions. This can be used for safe design.

10. The Experimental study on fatigue tests of SHS joints, though small in number, revealed valuable information on the fatigue behaviour and showed that fatigue failure occurred at the weld toe for $\beta = 0.39$ and on the weld throat for $\beta = 0.65$. A good correlation was obtained between experimental and theoretical findings for the joints which failed through the weld with $\beta = 0.65$.

11. More experimental fatigue tests are necessary to calibrate the geometric and size effects on plate and SHS fillet weld fatigue behaviour.

APPENDIX A

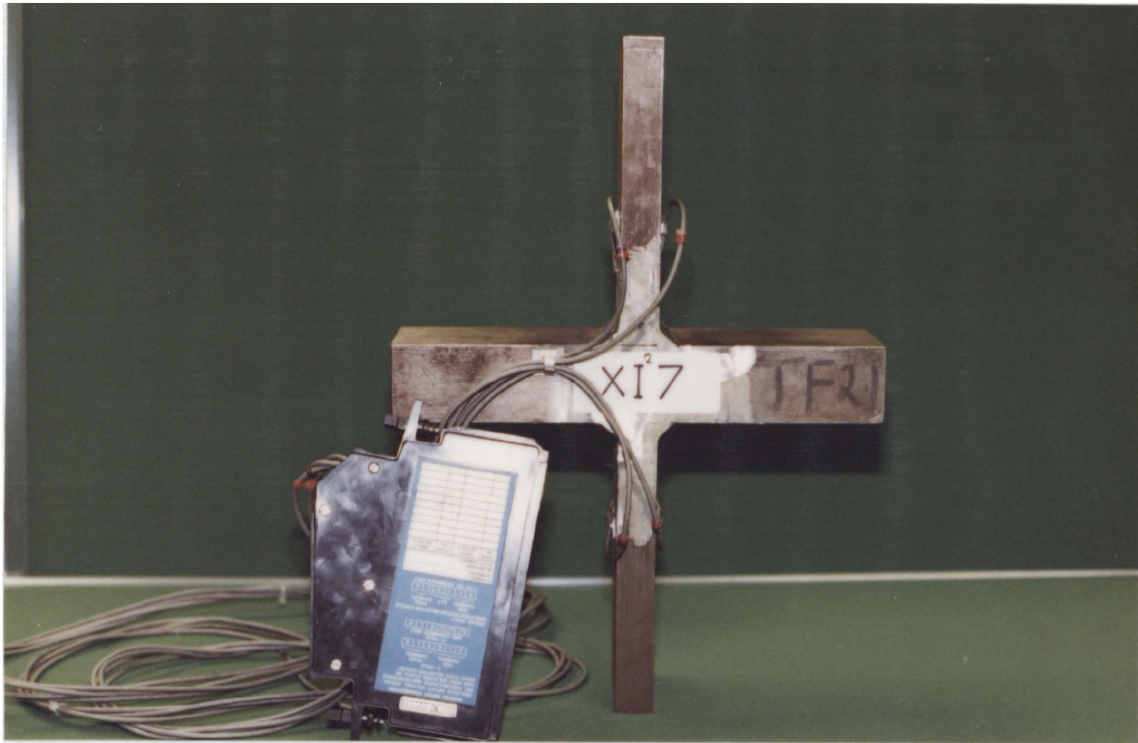


Fig. A1^o Instrumented Cruciform Fillet Welded Joint



Fig A2 Fatigued Specimen Test XI¹-4 showing the fatigue surface and the variations in the fillet weld root shape, attachment size 25mm.



Fig A3 Fatigued Specimen Test XI²₃ showing the fatigue surface attachment size = 12mm.



Fig A4 Fatigued Specimen Test XJ¹₁₂ showing the fatigue surface attachment size = 50mm.

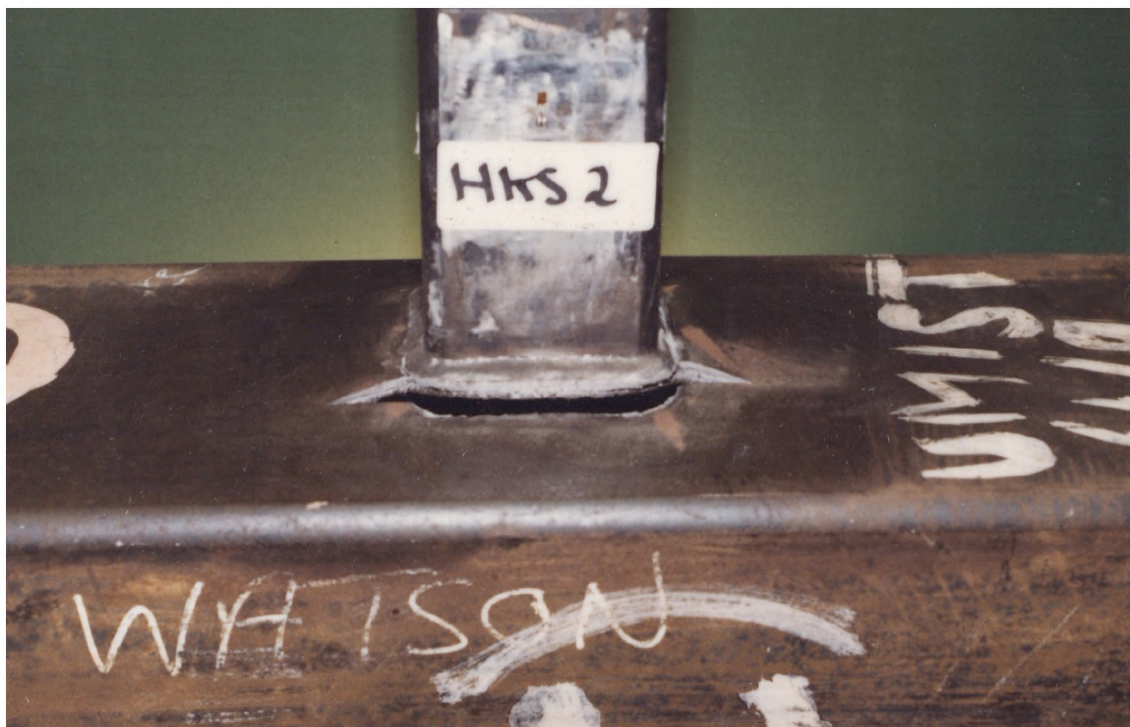
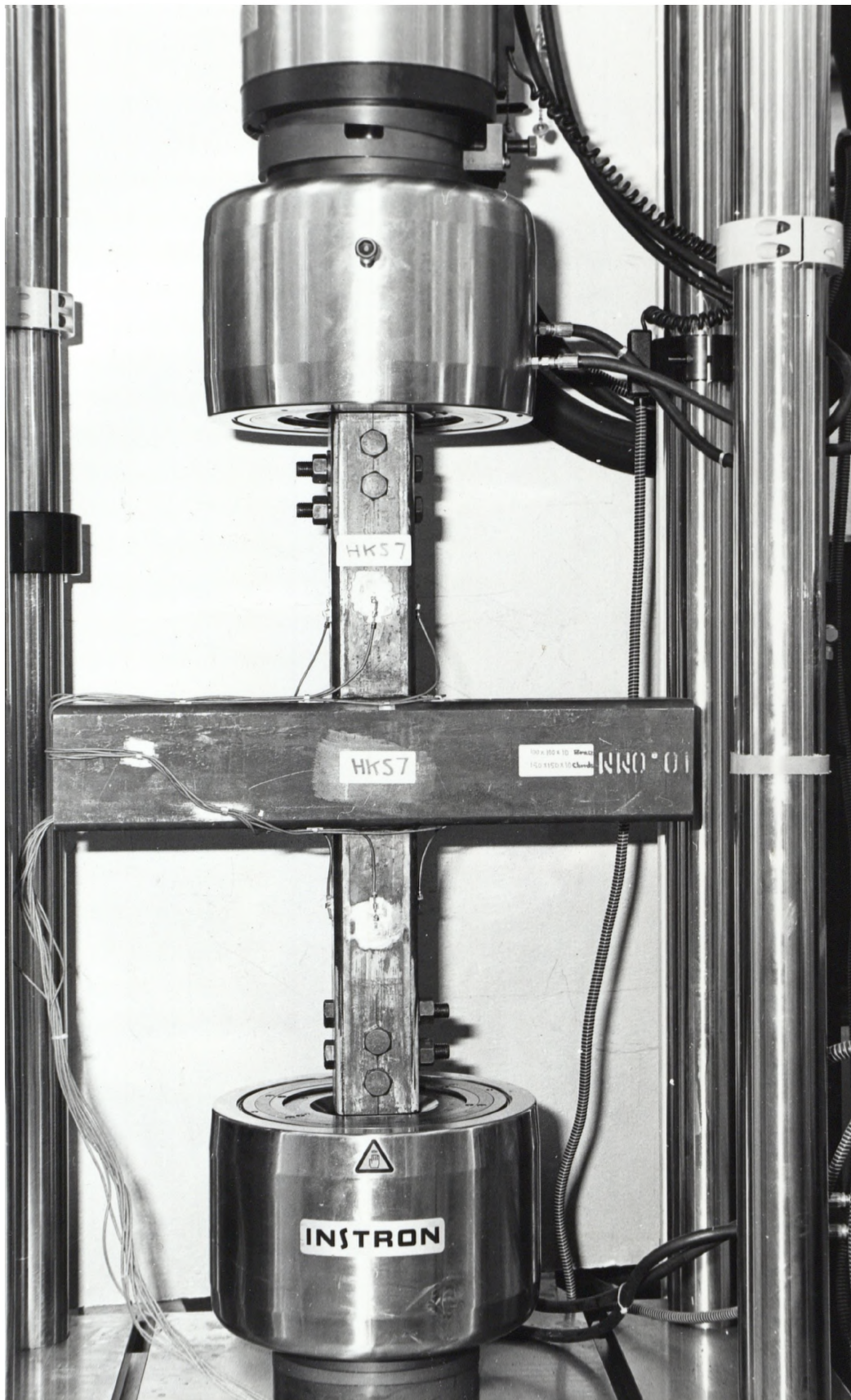


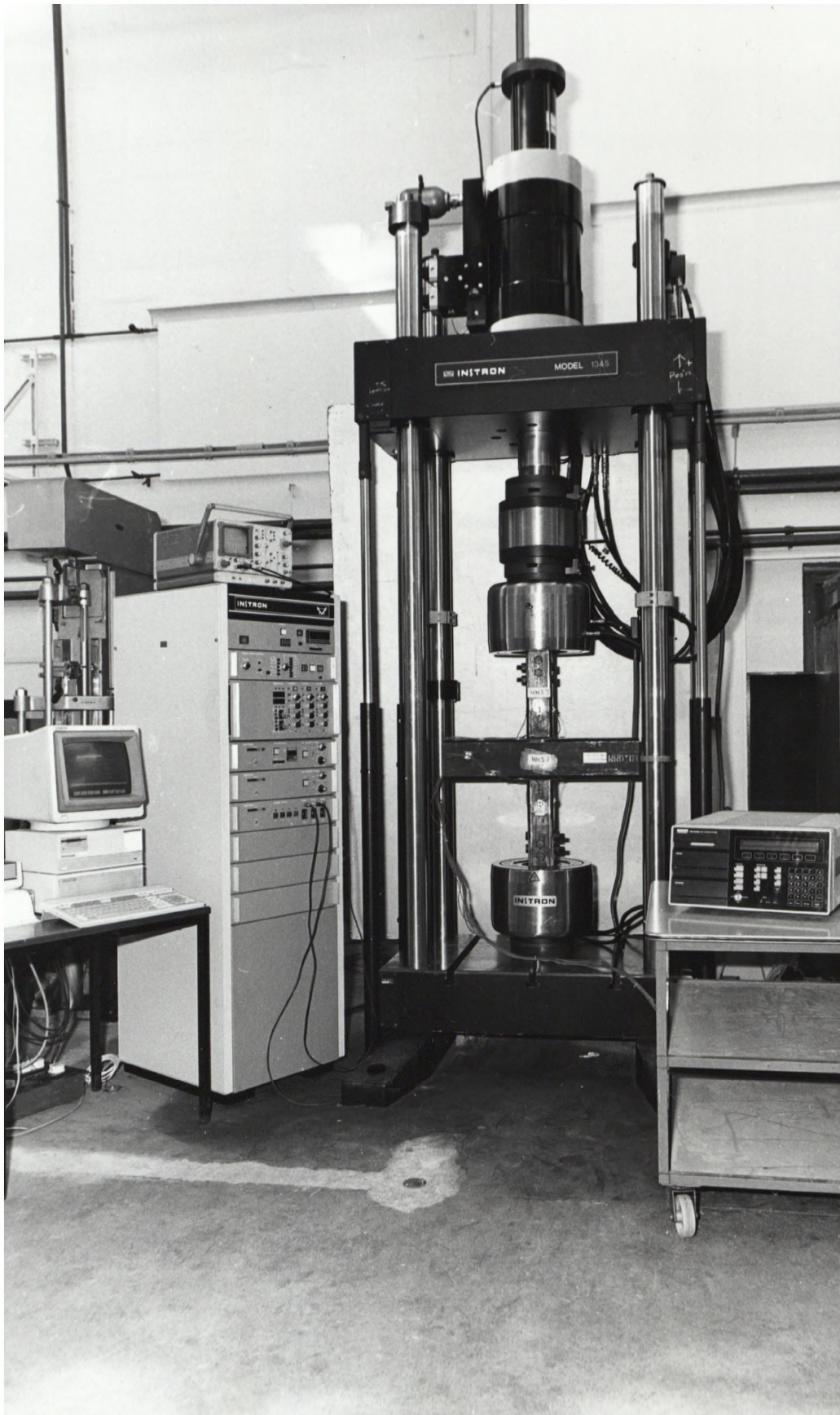
Fig A5 Toe Failure



Fig A6 Root Failure



A 7
Assembled SHS Joint in the Instron Testing Machine
192



Testing Arrangements for SHS Joints and Monitoring Equipment

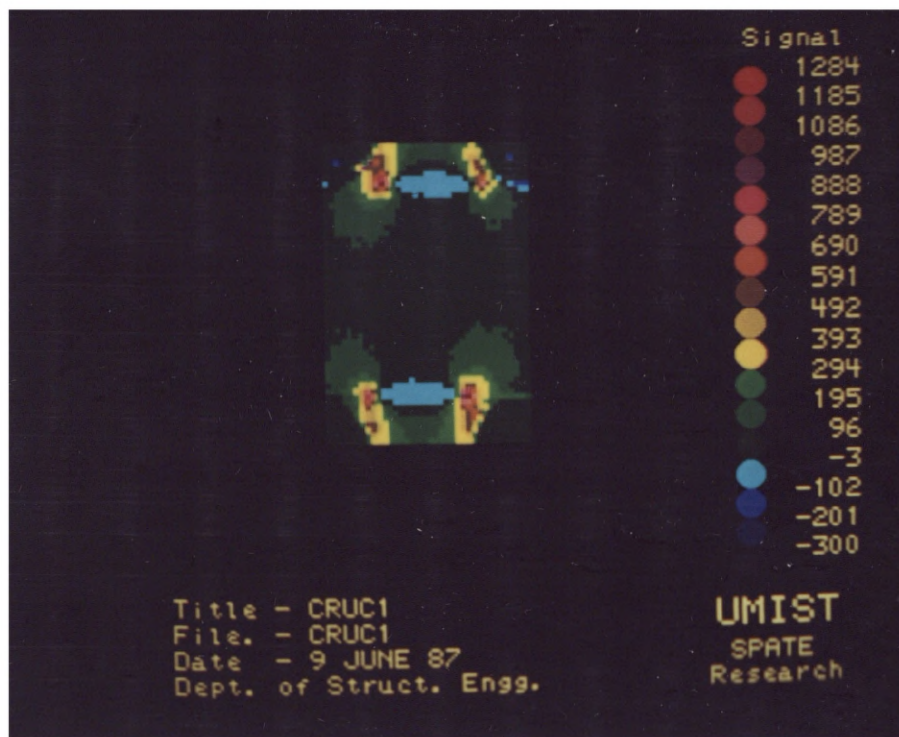


Fig A9 Plate Joint $A_{tt} = 12 \text{ mm}$

REFERENCES

1. BS5400: Steel, Concrete and Composite Bridges. Part 10, Code of Practice for Fatigue.
2. GURNEY, T. R., Welding Institute Rules for Fatigue Design, Welding Institute Research Bulletin, May 1976.
3. UK DEPARTMENT OF ENERGY, Offshore Installations, Guidance on Design and Construction.
4. DET NORSKE VERITAS Rules for the Design, Construction and Inspection of Fixed Offshore Structures, March 1982.
5. Design of Tubular Joints for Offshore Structures, UEG PUBLICATION, VR33, 1985, CIRIA, London.
6. WORDSWORTH, A.C., and SMEDLEY, G.P. Stress Concentrations at Unstiffened Tubular Joints. Paper 31, European Offshore Steel Research Seminar, Cambridge, 1978.
7. HALEEM, R., 'Some Aspects of SHS Welded Joint Behaviour'. CIDECT, 77/41.
8. WARDENIER, J., DAVIES, G 'The Strength of Predominantly Statically Loaded Joints with Square or Rectangular Hollow Section Chord', IIW Doc., XV-492-81.
9. WARDENIER, J., Hollow Section Joints', Delft University Press, 1982.
10. DAVIES, G., WARDENIER, J., STOLLE, P., 'The Effective Width of Branch Cross Walls for RR Cross-Joints in Tension. Steven Report 6-81-7.
11. PACKER, J. A and HALEEM, A. S, Ultimate Strength Formulae for Statically Loaded Welded HSS Joints in Lattice Girders with RHS Chords. CSCE Conference, 1981.
12. EASTWOOD, W. and WOOD, A. A., 'Welded Joints in Tubular Structures Involving Rectangular Hollow Sections' University of Sheffield.
13. SUB-COMMISSION XV-A (1976) Calculation of Welded Constructions subjected to Static Loading, Welding in the World, V14.

14. BS5950: 'Structural Use of Steelwork in Building', 1985.
15. BS639: Covered Electrodes for Manual Metal-Arc Welding of Carbon and Carbon Manganese Steels.
16. BS4360: Specification for Weldable Structural Steel, 1979.
17. CIDECT Monograph No. 6, draft, 1982.
18. AUSTEN, I. M., Factors Affecting Corrosion Fatigue Crack Growth in Steels, Select Seminar, European Offshore Steels Research, Preprints, Vol. 1, November 1978, Welding Institute, Abington Hall, Cambridge, Great Britain.
19. CIDECT Monograph No. 7, Constrado, April 1982.
20. WARDENIER, J. and KONING, C. H. M., The Fatigue Behaviour of N-Type Joints In Welded Lattice Girders, Delf University Reports 6-78-11 and 6-80-3.
21. NOORDHOE, H. C., WARDENIER, J. DUTTA, D. Fatigue Behaviour of Welded Joints of J Square Hollow Section, Part II: Analysis Stevin Report 6-80-4.
22. MARG, F., DUTTA, D., Fatigue Strength of Welded Joints of Hollow Sections, Symposium on Tubular Structures, Delft, October 1977.
23. MANG, F., Fatigue Strength of Welded HSS Joints, International Symposium of Hollow Structural Sections, CIDECT, Toronto, 1977.
24. GRIFFITH, A. A. (1921), The Phenomena of Rupture and Flow in Solids, Phil. Trans. R. Soc., London, A, 221, 163-97.
25. IRWIN, G. R. Analysis of Stress and Strains Near End of a Crack Transversing in a Plate. Trans ASME, J. App. Mech., 1957, 24, 361-364.
26. SIH, G. C. On the Westergaard Method of Crack Analysis. Int. J. Fracture, 1966, 2, 628-631.
27. Draft Revision of PD6493, Nov. 1987.

28. PARIS, P. C. ERDOGAN, F. International Basic Engineering, Trans. ASME, Series D85, 528 (1963).
29. GURNEY, T. R. 'Fatigue of Welded Structures, 2nd Edition? Cambridge University Press, 1979.
30. MADDOX, S. J. (1975). An Analysis of Fatigue Cracks in Fillets Welded Joints. International J. Fracture 11, 221-243.
31. MADDOX, S. J. Assessing the Significance of Flaws in Welds Subject to Fatigue. Welding Research Supplement, May 1974.
32. ABAQUS Theory Manual, UMRCC (Pub.)
33. FISHER, T. W. & FRANK, A. The Fatigue Strength of Fillet Welded Connections, Sept. 1979, Journal of the Structural Division.
34. RICE, J. R. (1968), A Path Independent Integral and the Approximate Analysis of Strain Concentrations by Notches and Cracks, Trans. ASME, J. Appl. Mech. 35, 379-86.
35. PARKS, D. M. A Stiffness Derivative Finite Element Technique for Determination of Crack Tip Stress Intensity Factors. International Journal of Fracture, Vol. 10, No. 4, 1974.
36. BYSTROV, E. (1970), 'The Calculation of Stress Intensity Factors Using the Finite Element Method with Cracked Elements', International J. Fracture Mechanic, 6, 159-67.
37. Muskhelishvili, N. I. (1953), Some Basic Problems of the Mathematical Theory of Elasticity, Noordhoff, Leiden.
38. American Welding Society, Stuctural Welding Code D1.1 and American Petroleum Institute Code API RP2A.
39. GURNEY, T. R., Theoretical Analysis of the Influence of Attachment Size on the Fatigue Strength of Transverse non-load Carrying Fillet Welds. Welding Institute Report 19/1979.

40. CHU, W. H., The Influence of Plate Thickness Geometry on Fatigue Strength of Fillet Welded Joints. M.Sc. Thesis, UMIST, 1984.
41. BURDEKIN, F. M., CHU, W. H., CHAN, W. T., MANTEGHI, S., Fracture Mechanics Abnalysis of Fatigue Crack Propagation in Tubular Joints, International Conf. on Fatigue and Crack Growth in Offshore Structures. Inst. of Mech. Eng., London, March 1986.
42. American Association of State Highway and Transportation Officials, Standard Specification for Highway Bridges, Twelfth Edition, Washington, D.C., 1977.
43. KUROBANE, Y. (1981). New Developments in Tubular Joints Design. IIW DOC. XIII-1004-81.
44. FEMGEN (Finite Element Generator) FEGS Ltd.
45. ABAQUS User Manual 1, UMRCC.
46. BS5135: Process of Arc Welding of Carbon and Carbon Manganese Steels. 1984.
47. MANG, F., BUCAK, O., Fatigue of Welded Tubular Joints Design Proposed and Background Information.
48. BURDEKIN, F. M., and MANTEGHI, S. 'Use of SPATE Technique on Welded Joints First International Conference: Stress Analysis by Thermo Elastic Techniques.
49. CORDEROY, D. J. H., FORD, P. R. The Fatigue of Dynamically Loaded Fillet Welds, Metal Structures Conference, 1981.
50. ABAQUS, HIBBITT, KARLSSON and SORENSEN INC.
51. RAJKOTIA, D. P., SCHNOBRICH, W. C. Technical Report of Research, University of Illinois, Dec. 1980.

ProQuest Number: 29223105

INFORMATION TO ALL USERS

The quality and completeness of this reproduction is dependent on the quality and completeness of the copy made available to ProQuest.



Distributed by ProQuest LLC (2022).

Copyright of the Dissertation is held by the Author unless otherwise noted.

This work may be used in accordance with the terms of the Creative Commons license or other rights statement, as indicated in the copyright statement or in the metadata associated with this work. Unless otherwise specified in the copyright statement or the metadata, all rights are reserved by the copyright holder.

This work is protected against unauthorized copying under Title 17,
United States Code and other applicable copyright laws.

Microform Edition where available © ProQuest LLC. No reproduction or digitization of the Microform Edition is authorized without permission of ProQuest LLC.

ProQuest LLC
789 East Eisenhower Parkway
P.O. Box 1346
Ann Arbor, MI 48106 - 1346 USA